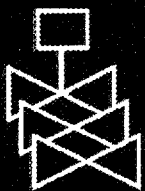
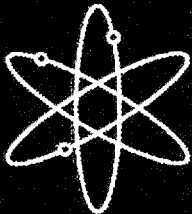
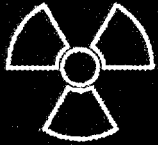
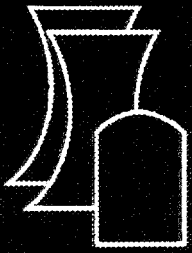


# Recommendations for Shielding Evaluations for Transport and Storage Packages

Oak Ridge National Laboratory

U.S. Nuclear Regulatory Commission  
Office of Nuclear Material Safety and Safeguards  
Washington, DC 20555-0001



## AVAILABILITY OF REFERENCE MATERIALS IN NRC PUBLICATIONS

### NRC Reference Material

As of November 1999, you may electronically access NUREG-series publications and other NRC records at NRC's Public Electronic Reading Room at <http://www.nrc.gov/reading-rm.html>. Publicly released records include, to name a few, NUREG-series publications; *Federal Register* notices; applicant, licensee, and vendor documents and correspondence; NRC correspondence and internal memoranda; bulletins and information notices; inspection and investigative reports; licensee event reports; and Commission papers and their attachments.

NRC publications in the NUREG series, NRC regulations, and *Title 10, Energy*, in the Code of *Federal Regulations* may also be purchased from one of these two sources.

1. The Superintendent of Documents  
U.S. Government Printing Office  
Mail Stop SSOP  
Washington, DC 20402-0001  
Internet: [bookstore.gpo.gov](mailto:bookstore.gpo.gov)  
Telephone: 202-512-1800  
Fax: 202-512-2250
2. The National Technical Information Service  
Springfield, VA 22161-0002  
[www.ntis.gov](http://www.ntis.gov)  
1-800-553-6847 or, locally, 703-605-6000

A single copy of each NRC draft report for comment is available free, to the extent of supply, upon written request as follows:

Address: Office of the Chief Information Officer,  
Reproduction and Distribution  
Services Section  
U.S. Nuclear Regulatory Commission  
Washington, DC 20555-0001  
E-mail: [DISTRIBUTION@nrc.gov](mailto:DISTRIBUTION@nrc.gov)  
Facsimile: 301-415-2289

Some publications in the NUREG series that are posted at NRC's Web site address <http://www.nrc.gov/reading-rm/doc/collections/nuregs> are updated periodically and may differ from the last printed version. Although references to material found on a Web site bear the date the material was accessed, the material available on the date cited may subsequently be removed from the site.

### Non-NRC Reference Material

Documents available from public and special technical libraries include all open literature items, such as books, journal articles, and transactions, *Federal Register* notices, Federal and State legislation, and congressional reports. Such documents as theses, dissertations, foreign reports and translations, and non-NRC conference proceedings may be purchased from their sponsoring organization.

Copies of industry codes and standards used in a substantive manner in the NRC regulatory process are maintained at—

The NRC Technical Library  
Two White Flint North  
11545 Rockville Pike  
Rockville, MD 20852-2738

These standards are available in the library for reference use by the public. Codes and standards are usually copyrighted and may be purchased from the originating organization or, if they are American National Standards, from—

American National Standards Institute  
11 West 42<sup>nd</sup> Street  
New York, NY 10036-8002  
[www.ansi.org](http://www.ansi.org)  
212-642-4900

Legally binding regulatory requirements are stated only in laws; NRC regulations; licenses, including technical specifications; or orders, not in NUREG-series publications. The views expressed in contractor-prepared publications in this series are not necessarily those of the NRC.

The NUREG series comprises (1) technical and administrative reports and books prepared by the staff (NUREG-XXXX) or agency contractors (NUREG/CR-XXXX), (2) proceedings of conferences (NUREG/CP-XXXX), (3) reports resulting from international agreements (NUREG/IA-XXXX), (4) brochures (NUREG/BR-XXXX), and (5) compilations of legal decisions and orders of the Commission and Atomic and Safety Licensing Boards and of Directors' decisions under Section 2.206 of NRC's regulations (NUREG-0750).

**DISCLAIMER:** This report was prepared as an account of work sponsored by an agency of the U.S. Government. Neither the U.S. Government nor any agency thereof, nor any employee, makes any warranty, expressed or implied, or assumes any legal liability or responsibility for any third party's use, or the results of such use, of any information, apparatus, product, or process disclosed in this publication, or represents that its use by such third party would not infringe privately owned rights.

# Recommendations for Shielding Evaluations for Transport and Storage Packages

---

---

Manuscript Completed: November 2002  
Date Published: May 2003

Prepared by  
B.L. Broadhead

Oak Ridge National Laboratory  
Managed by UT-Battelle, LLC  
Oak Ridge, TN 37831-6370

C. J. Withee, NRC Project Manager

Prepared for  
Spent Fuel Project Office  
Office of Nuclear Material Safety and Safeguards  
U.S. Nuclear Regulatory Commission  
Washington, DC 20555-0001  
NRC Job Code B0009





## **ABSTRACT**

This report provides recommendations on the approach to use in the preparation of radiation shielding evaluations for transportation and storage of packages containing radioactive material. The various methods, models, and processes relating to the source term, shielding and measurement portions of the submittals are described. The recommendations in this document are designed to address the regulatory requirements in 10 CFR Parts 71 and 72 and supplement the guidance in the standard review plans issued for transportation and dry cask storage.



# CONTENTS

	<u>Page</u>
ABSTRACT.....	iii
LIST OF FIGURES.....	vii
LIST OF TABLES.....	ix
ACKNOWLEDGMENTS.....	xi
1 INTRODUCTION.....	1
1.1 BACKGROUND.....	1
1.2 PURPOSE AND SCOPE.....	1
1.3 SUMMARY RECOMMENDATIONS.....	2
2 PACKAGE DESCRIPTION.....	3
3 SOURCE TERM GENERATION.....	5
3.1 POINT-DEPLETION METHODS AND CODES.....	5
3.1.1 SAS2H/ORIGEN-S.....	6
3.1.2 EPRI-CINDER.....	6
3.1.3 ORIGEN2.....	7
3.1.4 Characteristics Database.....	7
3.1.5 ORIGEN-ARP.....	7
3.1.6 Other Codes.....	8
3.2 SPENT FUEL ASSEMBLY MODELS.....	8
3.2.1 PWR Models.....	8
3.2.2 BWR Models.....	9
3.2.3 Plate-Type Fuels.....	10
3.3 PROCESSES.....	10
3.3.1 Active Spent Fuel Region Isotopics.....	11
3.3.2 Hardware Region Activation.....	12
3.3.3 Cross-Section Libraries.....	13
3.3.3.1 ORIGEN2 Library Selection.....	14
3.3.3.2 SCALE Library Selection.....	14
3.3.3.3 Group Structure Effects.....	14
3.3.3.4 Source Validation Studies.....	15
3.3.3.5 Source Term Components.....	15
3.3.4 Other Spent Fuel Types.....	16
3.3.5 Radioactive Material Sources.....	16
4 SHIELDING ANALYSES.....	19
4.1 METHODS.....	19
4.1.1 Point Kernel Method.....	19
4.1.2 Discrete-Ordinates Method.....	20
4.1.3 Monte Carlo Method.....	21
4.2 MODELING.....	22
4.3 DOSE RATE ESTIMATION.....	24

# CONTENTS (continued)

	<u>Page</u>
5 MEASUREMENTS.....	29
5.1 MEASUREMENT TECHNIQUES.....	29
5.1.1 Ionization Chamber.....	29
5.1.2 Proportional Counter.....	30
5.1.3 Geiger-Müller Tube.....	31
5.1.4 Scintillation Detectors.....	31
5.1.5 Semiconductor Radiation Detectors.....	31
5.1.6 Neutron Detectors.....	31
5.1.7 Bonner Spheres.....	31
5.2 MEASUREMENT ACCURACIES.....	32
5.3 MEASUREMENT LOCATIONS.....	32
5.4 MEASUREMENT CALIBRATION.....	34
6 SUMMARY.....	35
7 REFERENCES.....	37
APPENDIX A: DETAILS OF SAS2H MODELS.....	43
APPENDIX B: NUCLIDE IMPORTANCE AND PARAMETER SENSITIVITY STUDY FOR PWR/BWR SOURCE TERM GENERATION.....	51
APPENDIX C: EXAMPLE OF CALCULATIONAL MODELS AND RESULTS.....	61
C.1 DESCRIPTION OF THE SHIELDING DESIGN.....	63
C.1.1 Discussion and Results.....	63
C.2 SOURCE SPECIFICATION.....	64
C.2.1 Gamma Source.....	66
C.2.2 Neutron Source.....	67
C.3 MODEL SPECIFICATION.....	67
C.3.1 Description of the Shielding Configuration.....	67
C.3.2 Smearred Basket and Cavity Volume Fractions.....	71
C.4 SHIELDING EVALUATION.....	74
C.5 SOURCE AND SHIELDING INPUTS.....	77

# LIST OF FIGURES

<u>Figure</u>	<u>Page</u>
1 Sample loading curve as a function of burnup and cooling time .....	27
2 Pulse-height versus applied-voltage curves to illustrate ionization, proportional, and Geiger-Müller regions of operation .....	30
A.1 Graphical representation of SAS2H procedure for generating burnup-dependent cross-section libraries for the ORIGEN-S code .....	45
A.2 Flow chart for SAS2H procedures .....	46
A.3 Pin-cell model for representing the repeating lattice structure of a typical fuel assembly .....	47
A.4 Typical Path B models for PWR and BWR fuel, assuming cell-weighted cross-section material in the regions labeled "Fuel Zone" .....	48
B.1 Dose rate versus cooling time for carbon steel/resin cask, including fractional contribution due to primary gamma, neutrons, and secondary gamma particles .....	53
B.2 Fractional contribution to the total dose due to neutrons from decay of actinides for carbon steel/resin cask for 50 GWd/MTU burnup source .....	54
B.3 Fractional contribution to the total dose due to primary gammas from decay of fission products and activation products for carbon steel/resin cask for 50 GWd/MTU burnup source .....	55
B.4 Variation of key isotopes with specific power at fixed burnup .....	58
B.5 Variation of key isotopes with enrichment at fixed burnup .....	58
B.6 Variation of key isotopes with fuel density at fixed burnup .....	59
B.7 Variation of key isotopes with moderator density at fixed burnup .....	59
C.1 Shielding model – radial .....	68
C.2 Shielding model, axial .....	69
C.3 GBC-32 detailed basket model .....	70
C.4 Surface dose rate profiles along the side of GBC-32 cask .....	75
C.5 Dose rate profile at 2 m from the conveyance surface for GBC-32 cask .....	75
C.6 Dose rate profile along top surface of GBC-32 cask .....	78
C.7 Dose rate profile 2 m from top of GBC-32 cask .....	78

## LIST OF FIGURES (continued)

<u>Figure</u>	<u>Page</u>
C.8 Dose rate profiles at 1 m from side of GBC-32 cask under accident conditions .....	80
C.9 Dose rate profiles for 1 m from top of GBC-32 cask under accident conditions.....	80
C.10 ORIGEN-ARP source generation sample input.....	82
C.11 Sample SAS4 input for primary gamma calculation under normal conditions .....	85

# LIST OF TABLES

<u>Table</u>		<u>Page</u>
1	Comparison of scale factors .....	13
2	Example non-conformance actions .....	34
A.1	BWR moderator density versus burnup .....	49
B.1	Parameter ranges of variation .....	56
B.2	Power coefficients, $\rho_i$ for parameter variations, $x_i$ .....	60
C.1	Summary of dose rates for GBC-32.....	64
C.2	Description of Westinghouse fuel assembly.....	65
C.3	Fuel assembly hardware parts and materials .....	65
C.4	Westinghouse fuel assembly gamma spectrum .....	66
C.5	Westinghouse fuel assembly neutron spectrum.....	67
C.6	Source and shield material densities .....	72
C.7	SAS4 radial analysis results .....	76
C.8	SAS4 axial analysis results .....	79
C.9	SAS4 radial accident analysis results .....	81



## ACKNOWLEDGMENTS

The author is grateful to the staff of the U.S. Nuclear Regulatory Commission's Spent Fuel Project Office for their support of this work and their direction and review, which was key to its completion. In particular, gratitude is expressed to C. J. Withee of the NRC and S. M. Bowman of Oak Ridge National Laboratory for their preparation of the initial outline of this work and task management and A. H. Wells, a private consultant, who drafted most of the material in the sections on selection of measurement locations and measurement calibration. Appreciation is also expressed to the reviewers of this document, C. V. Parks, J. C. Wagner, and S. N. Cramer. The careful formatting of this document by W. C. Carter is also acknowledged.



# 1 INTRODUCTION

## 1.1 BACKGROUND

This document gives recommendations on the preparation of the shielding section of an application for a transportation or storage package containing radioactive material. This report was prepared in consultation with the staff of the Spent Fuel Project Office of the United States Nuclear Regulatory Commission (U.S. NRC).

Packages used to transport fissile and Type B quantities of radioactive material are designed and constructed to meet the performance criteria specified in Title 10 of the Code of Federal Regulations (CFR), *Part 71 – Packaging and Transportation of Radioactive Material* (10 CFR Part 71).<sup>1</sup> Similarly the storage requirements for spent nuclear fuel and high-level radioactive wastes are covered in *Part 72 – Licensing Requirements for the Independent Storage of Spent Nuclear Fuel and High-Level Radioactive Waste* (10 CFR Part 72).<sup>2</sup> Currently there are several documents that aid the applicant in the preparation of licensing applications. They include NRC Regulatory Guide 7.9, *Standard Format and Content of Part 71 Applications for Approval of Packaging for Radioactive Material*,<sup>3</sup> which contains suggested content and formatting for an application, and NUREG-1536, *Standard Review Plan for Dry Cask Storage Systems*.<sup>4</sup> Two documents are available that contain standard review plans for transportation packaging; they are NUREG-1609, *Standard Review Plan for Transportation Packages for Radioactive Material*,<sup>5</sup> and NUREG-1617, *Standard Review Plan for Transportation Packages for Spent Nuclear Fuel*.<sup>6</sup> This report is designed to supplement these documents in the preparation and review of packaging applications.

## 1.2 PURPOSE AND SCOPE

This report is designed to assist the preparer of the shielding section of a Safety Analysis Report for Packaging (SARP) for submittal to the NRC. While the term packaging is generally associated with transport, this document applies this term to both transport and storage applications. This assistance includes recommended procedures for performing the analyses, including detailed information about models, cross sections, methods, and analysis data. The sample calculations reported herein were performed with the SCALE system,<sup>7</sup> but no specific endorsements are made about the use of a particular code system.

This document assumes the reader is familiar with the Standard Format Guide and pertinent sections of the regulations contained in 10 CFR Parts 71 and 72. The recommendations provided in this document are intended to assist in the preparation of safety analyses in support of the applications for packaging. Section 2 of this report briefly describes the expected packaging descriptions in the submittal, followed by detailed recommendations for source term methods, models, and processes in Section 3. Section 4 gives specific and relevant information on shielding methods, models, and processes to be included in the supporting analyses of Chapter 5 of a submittal. Recommended techniques for dose rate measurements and instrument calibration are summarized in Section 5. These measurements are used to ensure regulatory dose limits are met prior to transport of qualified packages. Three appendices are included with this document. Appendix A gives detailed suggestions when using the SCALE/SAS2H procedure<sup>8</sup> for radiation source generation. Appendix B gives source term importance and sensitivity information for key nuclides and physical parameters. Included in Appendix C is an example application of the recommendations described in this report.

### **1.3 SUMMARY RECOMMENDATIONS**

A summary of the specific recommendations contained in the text of this report is presented here. Further explanation of each of these recommendations is provided in the main body of the report.

1. Provide a complete description of the packaging including physical dimensions, material compositions, and material densities. See Section 2 for more details.
2. Provide a description, including sketches with dimensions and materials, of the calculational models. Note differences between calculational models and actual package designs, and discuss how these differences affect the results of the calculations. See Section 4 for more details.
3. Fully describe the bounding source configuration, including why it is bounding including justification as to why the source configuration is bounding. Describe the parameters used to generate the source and indicate any sources omitted together with the rationale for their omission.
4. Provide a description of the codes(s), cross-section data, and flux-to-dose conversion factors used in the analysis, together with references that provide complete information. Discuss software capabilities and limitations. See Section 4 for more details.
5. Clearly present summary dose rate information for both normal and accident conditions, indicating the limiting locations.
6. Provide sufficient information in the application to support independent analyses without reference to external documents.

## 2 PACKAGE DESCRIPTION

This section describes the level of packaging description detail expected in the submittal for licensing of a transportation and/or storage package. The specific requirements in this section are taken from the various review guides<sup>4-6</sup> and are only repeated for completeness.

The general information chapter of the SARP should give the overall package design. A summary of the design features important for shielding purposes needs to be included in the shielding section with perhaps greater detail than that provided in the general information section. The design features important to radiation protection safety include, but are not limited to:

- dimensions, tolerances, compositions, and densities of materials for neutron and gamma shielding, including those of structural or thermal components considered in the shielding evaluation;
- concentration and composition of neutron absorbers;
- structural components that maintain the contents in a fixed position within the package; and
- dimensions of the conveyance (if applicable) that are considered in the shielding evaluation.

All information presented in the text, drawings, figures, and tables should be consistent with each other and with that used in the shielding evaluation. The information supplied should be described in sufficient detail to permit an independent review, with confirmatory calculations, of the package shielding design. Consistency with the important items in the shielding analysis (i.e., shield dimensions, material densities, fuel type and content along with burnup, enrichment, and cooling time) should be checked closely. If ranges of these items are specified, clearly state the range of each item and any assumed correlations with the ranges for the other items. Pay particular attention to adequately describe potential streaming paths.

If the package is designed for multiple types of contents, specify each of the assumed contents along with the supporting analysis that shows the limiting package contents for each of the locations specified in the applicable regulations.

The chapter should provide references to the results of the tests for both normal conditions of transport (if applicable) and hypothetical accident conditions. A clear description of the assumed package/cask conditions and the resulting models should be provided.

For storage applications (if applicable) the assumed storage array or other assumed configurations, as specified in the design criterion from Section 2 of the SARP, should be clearly presented.



### 3 SOURCE TERM GENERATION

The generation of a source term plays a key role in the overall shielding analysis for a radioactive material packaging evaluation. There are a number of options for determining these quantities. The primary tools used in source term studies are based on the point-depletion method and utilize either the matrix exponential or Bateman chain techniques, or both. The codes that implement these methods include ORIGEN<sup>9</sup> and CINDER<sup>10</sup> codes. The ORIGEN code is the industry standard; however, there are a number of differing techniques, which utilize this approach. These techniques include:

- the use of the ORIGEN2,<sup>11</sup> ORIGEN-S,<sup>12</sup> or ORIGEN-ARP<sup>13</sup> codes with built-in cross-section libraries;
- custom source term databases for specific reactor types based on ORIGEN-type calculations for a wide range of fuel-assembly conditions; and
- computational procedures using the SAS2H/ORIGEN-S<sup>8</sup> module to quantify source terms for arbitrary reactor models and conditions.

Recommended procedures for each of these options are given in this section.

#### 3.1 POINT-DEPLETION METHODS AND CODES

The standard technique for estimating source term information for spent nuclear fuel is the point-depletion method as implemented in the ORIGEN family of codes. The technique uses the following governing equation that represents both production and loss terms appropriately averaged over the given system. The general expression for the production and loss rate of a nuclide is

$$dN_i / dt = \sum_j \delta_{ij} \lambda_j N_j + \sum_k f_{ik} \sigma_k \Phi N_k - (\lambda_i + \sigma_i \Phi) N_i,$$

where

- $N_i$  = atom density of nuclide  $i$ ,
- $\lambda_i$  = radioactive decay constant of nuclide  $i$ ,
- $\sigma_i$  = spectrum-average neutron absorption cross section,
- $\delta_{ij}$  = fraction of radioactive decay from nuclide  $j$  to  $i$ ,
- $f_{ik}$  = fraction of neutron absorption by nuclide  $k$  and transmuted to isotope  $i$ , and
- $\Phi$  = space and energy-averaged neutron flux.

This can be written in matrix form as:

$$N' = A N \quad \text{with the solution of}$$

$$N = \exp(At) N(0).$$

The ORIGEN family of codes uses the above approach with a Taylor's series approximation of the matrix exponential solution supplemented by the Bateman equations.

For the Taylor series approximation, the time variable in these equations is treated in a step-wise mode, where the total time is broken up into time steps where the method is successively applied. These time steps are recommended to be no more than 100 days for a depletion case and a maximum of 100 days for the initial time step with subsequent time steps obeying the “rule-of-3’s” for decay. Under the rule-of-3’s, each decay step should be no more than a factor of 3 times the previous time step. Thus, the decay steps for a 10,000-year case should be entered as: 0.3, 1, 3, 10, 30, 100, 300, 1000, 3000, and 10,000 years. To prevent the necessity of very short time intervals, very short-lived nuclides are removed from the  $A$  matrix above and treated using the Bateman chain equations. The Bateman equations solve for specific mass chains and are thus more accurate for very short-lived nuclides.

The CINDER code uses the Bateman equations exclusively. Both codes make use of the point-depletion techniques where the flux and cross sections shown in the equations above are energy- and space-averaged over the entire system. Thus, these codes are based on the same underlying methods and thus tend to give very similar results if the input cross sections and decay constants are the same. The next section will review the major similarities and differences of the codes.

### 3.1.1 SAS2H/ORIGEN-S

The SCALE module SAS2H was developed to allow somewhat arbitrary light-water-reactor (LWR) fuel assembly isotopics and source terms to be quantified. The code sequence combines depletion calculations with the generation of case-specific cross-section libraries by use of a built-in neutronics capability (see Appendix A). The fuel-pin size and pitch, fuel/clad/moderator constituents and their densities, fuel/clad/moderator temperatures, specific power, power history, borated water concentration, assembly geometry and pitch are all input quantities. The assembly geometry is limited since the models are one-dimensional (1-D); however, a two-pass procedure allows for a wide variety of fuel types to be modeled (see Section 3.2 for a discussion of SAS2H models). The SAS2H code is relatively easy to use due to automatic setup, coupling, and execution of a series of individual codes. The SAS2H module is a big improvement over the stand-alone use of the ORIGEN-S code on which it is based. The ORIGEN-S code is not easy to use and has complete, but often confusing documentation. The SAS2H module and the ORIGEN-ARP code (see Section 3.1.5) were designed to utilize the power and flexibility of the ORIGEN-S code while improving the user interface.

Currently, pressurized-water reactors (PWRs) and boiling-water reactors (BWRs) are readily modeled and sample problems are included in the documentation. Recently, additional reactor types including plate-type fuels, RBMK, VVER, and CANDU reactors have been successfully modeled. The more complex assembly types (e.g., BWR with Gd-rods, pins splits, axially-varying moderator densities) present some difficulties for the SAS2H program, but prescriptions are included in the manual to mimic most of these complexities.

A useful feature of the SAS2H package is the ability to save the burnup-dependent cross-section libraries for any system modeled with SAS2H and apply to an identical analysis performed via ORIGEN-ARP. The ORIGEN-ARP capabilities are described further in Section 3.1.5.

### 3.1.2 EPRI-CINDER

There are a number of different versions of the CINDER code. These include the original CINDER code as well as CINDER-2, CINDER3, CINDER7, CINDER10, and EPRI-CINDER. Of these codes, only EPRI-CINDER is in the public domain. The basic library in the EPRI-CINDER code is intended only for typical LWR applications. There is a mechanism for generating other libraries through the EPRI-CELL code, but EPRI-CELL is not in the public domain. EPRI-CELL does not have the capability for estimation of structural material activation, and therefore its uses are limited. It also has only a limited number of publicly-available libraries. Therefore this report will concentrate on the ORIGEN family of codes.

### 3.1.3 ORIGEN2

This version of the ORIGEN code was redesigned from the original code and updated libraries for various reactor types were included. The original libraries included high-temperature-gas-cooled-reactor (HTGR), LWR, liquid-metal-fast-breeder-reactor (LMFBR), and molten-salt-breeder-reactor (MSBR) reactor types. The initial reactor models for LWRs were expanded to include specific PWR and BWR types operating with enriched uranium, uranium/plutonium, and depleted uranium/thorium fuel cycles. ORIGEN2-compatible reactor models for LMFBR and CANDU were also developed and documented. The latest set of updated libraries includes standard and extended cycles for BWR and PWR reactors corresponding to burnup values of 27.5 and 33 GWd/MTU for the standard cycles and burnup values of 40 and 50 GWd/MTU for the extended cycles, respectively.

This wide variety of libraries, along with the updated code interfaces, made the ORIGEN2 code a very popular package that is still used extensively worldwide. The generation of fuel-assembly hardware sources using ORIGEN2 is straightforward (see Section 3.3.2). There have been several attempts at linking the ORIGEN2 code to the multidimensional Monte Carlo code MCNP. The code MOCUP<sup>14</sup> allows the user to generate effective one-group cross sections using an arbitrary reactor model and then generate a library compatible with the ORIGEN2 code. This option is very powerful; however, its use is somewhat complicated.

Several limitations have hindered the continued development of the ORIGEN2 code. The first is the amount of effort and level of complexity associated with generating libraries for new reactor types and variations on existing libraries. The source algorithm in ORIGEN2 produces a gamma spectrum in a fixed group structure that should be manually rebinned into another group structure if a multigroup shielding calculation is desired. There is currently no groupwise neutron spectrum in the code output, which necessitates the user generating one by hand.

### 3.1.4 Characteristics Database (CDB)

The CDB<sup>15</sup> was envisioned as an automated, very efficient method for generating source terms for LWR reactor spent-fuel studies. The database consists of a compilation of source terms from a number of LWR spent fuel scenarios. These scenarios were quantified using the ORIGEN2 code at multiple burnups, enrichments and cooling times. The user specifies a small set of fuel parameters (fuel type, burnup, enrichment, cooling time) and the database automatically interpolates the collection of source term information to the desired spent fuel conditions. This method is still available, but is no longer being supported or developed; therefore, its usefulness is limited. Shortcomings of these data exist where the *changes* in the source term due to *changes* in burnup, enrichment, etc., produce inconsistencies due to the use of different libraries for differing burnup levels. For example, the predicted source term differences between 35 (generated using ORIGEN2 with a 33 GWd/MTU library) and 45 GWd/MTU (generated using ORIGEN with a 50 GWd/MTU library) burnups were incorrect because the base calculations were performed using differing underlying cross-section libraries.

### 3.1.5 ORIGEN-ARP

ORIGEN-ARP is a PC-based Windows GUI (graphical user interface) program that combines the production of a problem-dependent ORIGEN-S cross-section library with the ORIGEN-S calculation and post processing of the output for plotting purposes. The code is very easy to use relative to ORIGEN-S in stand-alone mode. The ARP (automatic rapid processing) program is designed to produce case-specific ORIGEN-S cross-section libraries from an input set of fuel depletion parameters by interpolating existing ORIGEN-ARP multi-burnup cross-section libraries that correspond to fixed fuel-type, burnup, enrichment, and moderator density combinations. The supplied libraries correspond to four assembly types;  $14 \times 14$

PWR, 15 × 15 PWR, 17 × 17 PWR, and 8 × 8 BWR. Additional libraries are planned with the release of SCALE 5. The depletion parameters specified can range from 0–60 GWd/MTU burnup, 1–5 wt % <sup>235</sup>U enrichment, and an arbitrary power history. These assembly types and parameter ranges correspond to the underlying ORIGEN-ARP multi-burnup cross-section libraries produced by the SCALE/SAS2H code and saved for use by ARP. Once ARP has produced the case-specific ORIGEN-S cross-section libraries that correspond to the specified power history, the ORIGEN-S code is called and executed automatically. A part of the Windows-GUI specifies the options for output by the ORIGEN-S code and the portions of the output that are desired for plotting. The user can select via the click of a button whether the full ORIGEN-S output or selected plots are viewed on the screen.

The results from an ORIGEN-ARP calculation are virtually identical with those of a corresponding SAS2H case. Therefore, the use of ORIGEN-ARP is very efficient for the reactor types and conditions that have already been modeled with SAS2H. ORIGEN-ARP can readily produce hardware region sources using the scale factor approach (Section 3.3.2). Although not currently available in SCALE, reactor types including VVER, RBMK, CANDU, and MTR have been successfully processed into ARP libraries.

### 3.1.6 Other Codes

Other codes that solve for spent-fuel isotopics and/or source terms include WIMS,<sup>16</sup> KORIGEN,<sup>17</sup> FISPIN,<sup>18</sup> HELIOS,<sup>19</sup> and SAS2D<sup>20</sup> (recently re-named TRITON). These codes, with the exception of SAS2D, were developed outside the United States and appear to be excellent implementations of source generation techniques. However, they will not be covered in detail in this report. The TRITON (formerly SAS2D) code is scheduled to be released with SCALE 5. TRITON uses capabilities similar to the SAS2H/ORIGEN techniques discussed in this document and additionally allows for multiple-pin depletions to be solved in a single case.

## 3.2 SPENT FUEL ASSEMBLY MODELS

For most of the source term generation techniques, the fuel assembly model is implicit in the cross-section library and thus the library is typically only used for fuel types that closely match that used to generate the library. Of the primary techniques discussed above, only the SAS2H technique has the capacity to specifically model various assembly types. The specific modeling options include:

- Single pin cell – a single fuel pin with white/reflected boundary conditions;
- Simple assembly – full assembly model, but with only limited modeling of heterogeneous assembly features; and
- Full assembly – detailed modeling of pin-by-pin characteristics and depletion are available.

Of these options only the first two are available in the publicly-released SAS2H module (see Appendix A for details on SAS2H inputs). Thus, the following discussion of the generation of assembly models will concentrate on the capabilities and limitations of the techniques in SAS2H.

### 3.2.1 PWR Models

Many PWR assemblies have a relatively simple design in that all of the fuel pins have the same enrichment and the only level of heterogeneity is due to the presence of water holes. Under these conditions, the use of a single pin-cell-only model is acceptable. If pin-cell-only models are used with assemblies containing water holes, it is recommended that the extra moderator be included in the pin-cell by modifying the pitch to maintain the correct moderator-to-fuel ratios.

Experience has shown that inclusion of the water holes explicitly by the simple assembly option does enhance the agreement with experimental isotopic measurements. The standard treatment of the water holes using the simple-assembly option is to first model the infinite pin cell to obtain cell-weighted cross sections for the pin cell, and then perform a second calculation with the water hole model explicitly surrounded by the homogenized cell-weighted material representing the remainder of the fuel assembly. In this case the preservation of moderator-to-fuel ratios necessitates that only a fraction of the remainder of the assembly be modeled. Under this option, the standard rule for  $N$  actual water holes in the assembly is that the water-hole calculation should model a  $1/N$  portion of the full assembly.

Capabilities also exist in SAS2H to treat the presence of burnable poison rods (BPRs). This situation is more complex; however, the standard procedure is the same as described above for the water hole, except the BPR is modeled inside the water hole. This treatment is only correct if *all* the waterholes are filled with BPRs, which is rarely the case. For cases in which the water holes are not all filled with BPRs, SAS2H has an option to correct the amount of BP material in a single hole (e.g., if 2 of 4 holes are empty the BP number densities are halved). SAS2H also has the capability to change the number of BPRs as a function of reactor cycle. This allows for the simulation of the removal of BPRs over the lifetime of an assembly.

A modeling difficulty that is unique to PWR assemblies is the inclusion of the boron letdown curve in the source term determination. This operational procedure is automatically handled by SAS2H in the following manner. The input value for the boron concentration in the water is recommended to be the average over the first cycle. If the average changes for other cycles, the boron fraction value (BFRACT) should be used to modify the input concentration. If multiple libraries per cycle are chosen, the code will automatically scale the average boron concentration up or down corresponding to the burnup of each segment. The cycle boron concentration is assumed to vary linearly with burnup from a high of two times the average at the beginning of cycle (BOC) to zero at the end of cycle (EOC).

The use of full assembly pin-by-pin depletion capabilities such as HELIOS and TRITON (see Section 3.1.6) are not needed for the accurate modeling of standard PWR assembly source terms. As PWR assemblies increase in complexity over time, the use of these more rigorous tools could become necessary.

### 3.2.2 BWR Models

The complexities of a BWR fuel assembly are numerous. They include the use of both axially and radially varying enrichments and moderator densities, use of partially inserted control blades, and integral burnable poison fuel rods. These complexities preclude the use of a pin-cell model for BWR source term analyses. The use of a simple assembly model is hampered by these complexities as well. However, the results of several studies<sup>21</sup> confirm the usefulness of the simple assembly model for BWR analyses. The recommended BWR assembly model consists of an explicit representation of a gadolinium fuel rod and associated channel moderator surrounded by layers of cell-weighted fuel (from the pin-cell calculation), assembly channel, and bypass moderator (higher-density water located outside the assembly channel). The key to these models is the conservation of the actual fuel-to-moderator ratios as was described above for PWR assemblies. For BWR assemblies, the fraction of the assembly to be modeled,  $1/M$ , corresponds to the number of gadolinium fuel rods,  $M$ . If water holes are present in the assembly, this extra water is placed just inside the assembly channel at the assumed channel moderator density.

In this recommended model, the fuel enrichment is assumed to be the average over the entire assembly (excluding natural uranium reflectors if present). The assumed average moderator density is determined based on a power density or burnup weighting of the moderator density axial distribution (see Table A.1 and corresponding text). There is a slight variation of the neutron source production due to the spectral shift for low-density moderation; however, a check of the calculations reported in Reference 21 reveals that the peak

generation of  $^{244}\text{Cm}$  occurs in the same axial node where the peak power occurs. Thus, the power or burnup weighting of the moderator density adequately captures the spectral variation.

The final issue is that of the influence of the control blades and their movement on the magnitude of the source terms for BWR fuel assemblies. This issue is currently unresolved and requires further study. In the interim; however, the use of the above conclusions can be used to speculate on the effects. The predominant effect on the generation of source terms is the integral power. The majority of the power from BWR assemblies under control blade cycling (the in-and-out movement of the blades over time) comes when the control blades are effectively removed. Thus, the influence of blade insertion on the total source is expected to be small. The influence of previous perturbations in the reactor configuration is generally seen to decrease over time; hence, the influence of control blade movements is expected to have little effect on the final sources if they occur early in the assembly lifetime.

### 3.2.3 Plate-Type Fuels

Plate-type fuels are seen largely in research reactors, not power reactors. There are, however, quite a large number of such facilities worldwide. The SAS2H capability for analyzing the source term for plate fuel is relatively new. As a result very little experience is available for this option. No known benchmark studies are available for this fuel type, and a known deficiency (see below) currently exists with the SAS2H software.

The procedure for modeling plate fuel is to specify the SYMMSLABCELL geometry option, which performs a "pin-cell" calculation on an infinite array of a typical plate. The cell-weighted cross-section library from this step is then used in a full assembly calculation using the same approach as the PWR and BWR calculations described above. The primary difference is that the parameter VOLFUELTOT should be specified for this option since the width of the plate is not available to the code. In a few cases, the assembly calculation can be performed on the full core if there are no repeated small units of plates in the core. An example of this is the High Flux Isotope Reactor (HFIR) at the Oak Ridge National Laboratory (ORNL), where the entire core is a single assembly consisting of two concentric rings of plate fuel. It should be noted in using this option that although fuel plates are modeled in the pin cell calculation, the full assembly calculation is assumed by the code to be a cylindrical assembly.

A known deficiency in the SAS2H procedure for plate-type fuel concerns the generation of the neutron source due to  $(\alpha, n)$ . The generation of neutrons due to the interaction of  $\alpha$  particles with a target material is treated in an automated manner in the SAS2H code. The code currently assumes a  $\text{UO}_2$  matrix for the production of neutrons due to  $\alpha$  particle interaction. In plate-type fuel, typically, the fuel is a uranium-aluminum alloy or a mixture of uranium oxide and metal-oxide powders. These fuel matrix scenarios require the separate execution of the ORIGEN-S or ORIGEN-ARP code in a stand-alone manner with the borosilicate glass option. This calculation is further complicated by the lack of a sophisticated algorithm for the  $(\alpha, n)$  production. The algorithm does not allow for the differentiation of the metal in the clad and the metal in the fuel matrix. Also, the borosilicate glass option in the ORIGEN-S code generates a neutron spectrum corresponding to the  $(\alpha, n)$  production in boron only, and does not accurately produce spectra for other materials. This deficiency will be removed beginning with version 5.0 of the SCALE system and version 2 of the ORIGEN-ARP package.

## 3.3 PROCESSES

Previous sections have dealt with the methods of source term generation and the recommended models for generation of the underlying libraries for the most popular code systems. This section presents a list of recommendations for the generation of source terms using the most popular methods and models. These recommendations are presented with specific application to uranium-fueled LWR spent fuel sources,

hardware activation sources, and cross-section libraries in the following sections. A brief summary of other fuel types is given at the end of this section.

### 3.3.1 Active Spent Fuel Region Isotopics

Depending on the method of source term generation chosen, different parameters are available for selection. This section will address the important parameters in the source generation procedures, give typical values for many parameters, and (where possible) give the magnitude of the effect.

The most important parameters, with respect to the spent fuel source terms, are burnup, enrichment, fissile loading, and cooling time. The relationship between source terms and the magnitude of some of these parameters is well known. For example, the magnitude of the neutron source strength is proportional to the burnup raised to the fourth power.<sup>22</sup> The gamma source is similarly directly proportional to the burnup values.<sup>22</sup> The neutron and gamma sources decay over time exponentially according to the half-life values of the principal isotopic constituents. The neutron source is also known to increase significantly with decreasing enrichment for fixed burnup levels (see explanation below). A series of calculations is reported in Appendix B that allows for further examination of the variability of the neutron and gamma source terms with the input parameters. The parameters studied therein are variations in the specific power, enrichment, fuel density, fuel temperature, moderator temperature, boron loading, and moderator density.

The results in Appendix B indicate the following trends for PWR and BWR applications at an assumed cooling time of 5 years (numerical values in parentheses are the power coefficients\* of the variations in the source due to variations in the specified parameter):

1. Neutron source (primarily <sup>244</sup>Cm for cooling times beyond 5 years, <sup>242</sup>Cm can be important for times less than 5 years) is most strongly influenced by burnup (4.12), enrichment (-1.98), fuel density (-2.83), and moderator density (-0.44).
2. Gamma-ray source terms are primarily influenced by burnup (1.00), fuel density (-0.96 for <sup>60</sup>Co), moderator density (-0.79 for <sup>154</sup>Eu), specific power variations (0.65 for <sup>144</sup>Pr), and enrichment (-0.57 for <sup>60</sup>Co).

The gamma-ray source sensitivities are expected to vary over decay time, since the various dominant isotopes vary over time. The contributions of the various fission product and light-element isotopes to the primary gamma doses over decay time are shown in Figure B.3 in Appendix B. From the graph, it can be seen that <sup>144</sup>Pr and <sup>134</sup>Cs are the dominant sources for cooling times less than 5 years, <sup>60</sup>Co and <sup>137</sup>Cs for 5–20 years, and <sup>137</sup>Cs for more than 20 years.

These results confirm the importance of the burnup, enrichment and fissile loading (fuel density). In addition they are useful in determining the effect on the neutron or gamma sources of uncertainties in the parameter values. The practice of specifying a maximum burnup along with a minimum enrichment (either a single pair or a series of burnup/enrichment limits) and a minimum cooling time is typically used to establish a practical upper bound for the source strengths.

The importance of the fissile loading enters into both the enrichment and the fuel density. A check of the effective density is recommended to ensure a reasonable value. The theoretical density of UO<sub>2</sub> is 10.96 g/cm<sup>3</sup> and a practical density value to assume is 95% of theoretical density or 10.41 g/cm<sup>3</sup>. If only

---

\* These power coefficients are defined such that the variation in the source,  $S$ , is related to the variation in a parameter  $x_i$  by a power coefficient  $p_i$  according to the following relationship  $S \propto \prod_i x_i^{p_i}$ .

the total mass is given, the mass is converted into a fuel density by dividing by the effective fuel volume. The specification of a minimum fuel density (see Figure B.6 for the variation in key source isotopes with fuel density) should be considered only when fuel assemblies with a large range of initial fuel density are possible, which is not the case for PWR and BWR applications.

The moderator density has an important effect on  $^{154}\text{Eu}$ , which can be an important contributor to the gamma-ray source term. A variation in the moderator density causes a spectral change in the neutron flux and thus, isotopes that result from resonance or thermal capture ( $^{153}\text{Eu}$  neutron captures to  $^{154}\text{Eu}$ ) are sensitive to changes in the moderator density. The enrichment and fuel density effects are largely due to the amount of fissile material present. For smaller amounts of fissile material under the same burnup and specific power conditions, the thermal fluxes must increase to meet the total burnup and power specification. This increase in thermal flux gives rise to enhanced production of capture-produced isotopes like  $^{60}\text{Co}$ ,  $^{244}\text{Cm}$ , and  $^{134}\text{Cs}$ . The variation of  $^{144}\text{Pr}$  with specific power arises due to the very short half-life (285 days) of the parent  $^{144}\text{Ce}$ . Because of the short half-life of  $^{144}\text{Ce}$ , the early production is decayed away by the end-of-cycle. Only the atoms produced near the end-of-irradiation remain, and their production is directly proportional to the specific power near the end-of-irradiation.

The axial-burnup profile is also an important effect to be accounted for in the shielding analysis for a package containing spent fuel. The source corresponding to the peak burnup can be conservatively used for the radial dose rate calculation and the source corresponding to the average axial burnup is conservative for the top or bottom dose rate calculations. However, the degree of conservatism can be lessened by the inclusion of the entire burnup profile. The use of a typical burnup profile for the given level of burnup should be sufficiently accurate for these purposes.

In BWR environments the axially-varying water density can also contribute to a significant variation in the neutron source. The magnitude of this variation is clearly shown in Appendix B by the change in the  $^{244}\text{Cm}$  concentration as a function of the moderator density. However, the value of the moderator density typically used in a BWR application is 0.4–0.5 g/cm<sup>3</sup> based on a power or burnup profile weighting of the actual moderator density profile. As seen in Figure B.7, the neutron source (due to  $^{244}\text{Cm}$ ) is only slightly higher for moderator densities of 0.2–0.3 than those at 0.4–0.5 g/cm<sup>3</sup>. Therefore, the burnup profile effect masks the moderator density effect due to the much larger variation in the neutron source with burnup, which also changes axially. This effect was confirmed by observing that the peak source occurs in the same axial zone as the peak power in a case where BWR axial fuel zones were separately depleted using a burnup profile to select each zone power.

### 3.3.2 Hardware Region Activation

The activation of the assembly hardware in a spent fuel assembly can be an important part of the overall source-term generation procedure. The primary contributor to the source term is from activation of the  $^{59}\text{Co}$  impurity in structural materials like steel and inconel. The quantity of the impurity is the most important parameter in determining whether the hardware contribution is significant. Impurity levels of 0.5 wt % in structural materials can dominate the gamma source term for shielding calculations. This fact has been recognized in most modern fuel assemblies and more recently the amount of impurity has been limited to 0.1 wt % or less. The general procedure for generation of the hardware region sources is to include the elements in the hardware materials in the fuel assembly source term calculation. Scaling factors that depend on the location of the hardware (i.e., the endfittings are outside the active fuel region, the grid spacers and thimble plugs are in the fuel region) are applied to account for variations in the activation rate relative to the active fuel region. A summary of previously published scale factors is provided in Table 1. The values exhibit large variations and the basis for selecting the scale factors should be addressed by the applicant. The newer values are generally much larger and can create design problems in some casks. There is reasonable agreement between the 1987 and 1989 values for the plenum spring and bottom endfitting regions, such that the 1989 values are recommended. If the 1978 or 1987 values are used, the applicant should justify their use.

Scale factors for components in the active fuel region (i.e., control blades, BPRs, and thimbles) should be assumed to be unity. Ex-core components not included in Table 1 should be quantified using techniques similar to those used to generate the quantities in Table 1.

**Table 1 Comparison of scale factors**

Component	Element	ORNL-6051	DOE/RW-0184	PNL-6906
		(1978) <sup>23</sup>	(1987) <sup>24</sup>	(1989) <sup>25</sup>
Top end-fitting	Ni	0.011	0.051	0.10
	Nb	0.011	0.018	0.10
	Co	0.0074	0.034	0.10
Plenum-spring region	Ni	0.042	0.556	0.20
	Nb	0.042	0.174	0.20
	Co	0.028	0.365	0.20
Bottom end-fitting	Ni	0.011	0.290	0.20
	Nb	0.011	0.107	0.20
	Co	0.0074	0.202	0.20

The procedure for estimating the hardware source term differs depending on the analysis method. The ORIGEN2 procedure uses the flux estimate from the active fuel calculation along with an input quantity of structural materials (typically a gram of material multiplied by the above scale factor). The ORIGEN-S, ORIGEN-ARP, and SAS2H calculations each use, in essence, the same procedure. The ORIGEN-S code has the capability of deleting all but selected elements. The ORIGEN-ARP code uses this capability to generate the source for the fuel and the hardware combined, and then selects only the isotopes in the hardware materials and applies a scale factor to produce a hardware source. The ORIGEN-S element deletion technique can also be used with SAS2H; however, a standard SAS2H case should be followed by a stand-alone execution of ORIGEN-S which specifies which elements are to be deleted. The CDB and EPRI-CINDER codes do not have the capability of producing hardware sources.

### 3.3.3 Cross-Section Libraries

In general, the use of evaluated nuclear data cross-section libraries based on the latest available evaluation is recommended. Validation studies<sup>26</sup> have shown that substantial improvements are seen with ENDF/B-V<sup>27</sup> over libraries based on ENDF/B-IV.<sup>28</sup> These same studies indicate that some improvements are also seen in ENDF/B-VI,<sup>29</sup> the latest set of U.S. evaluated data. SCALE libraries fully utilizing ENDF/B-VI data are not available at this time for use in source term studies. As additional libraries become available, their use is recommended. Recommendations for specific cross-section libraries used in characterization of spent fuel source terms are difficult due to the large variety of techniques available and the limited library selection for each code. Thus, specific comments will be made for each technique along with recommended libraries, if appropriate.

### 3.3.3.1 ORIGEN2 Library Selection

The most recent ORIGEN2 libraries (PWR-UE, BWR-UE, PWR-US, and BWR-US)<sup>30</sup> should be reliable for typical LWR applications. As LWR fuel assemblies become more and more complex, the need for additional LWR libraries will grow. Results using the non-LWR libraries should be viewed as preliminary due to their limited use and significant elapsed time since their generation. The source sensitivities shown in the previous section indicate that large variations in the predicted source terms can be expected if the assembly parameters assumed when generating the libraries are not typical for that assembly type.

The capability of the MOCUP code procedure to generate additional ORIGEN2 libraries is a method that should allow for many additional assembly types to be included in an ORIGEN2 analysis. However, due to the complexity of the technique, a validation similar to that performed in Ref. 26 should be performed or referenced.

### 3.3.3.2 SCALE Library Selection

The use of the SCALE 44GROUPNDF5 library<sup>31</sup> is recommended for source term generation via the SAS2H or ORIGEN-ARP methods. The core cross-section libraries that have been released for use with ORIGEN-ARP are based on this recommended library. Validation studies<sup>26</sup> have shown that the 44GROUPNDF5 library, based on ENDF/B-V with selected isotopes from ENDF/B-VI, performs much better than the 27BURNULIB library,<sup>31</sup> which is based on the ENDF/B-IV evaluation.

### 3.3.3.3 Group Structure Effects

The dose rate predictions due to spent fuel are, in general, fairly insensitive to the number of energy bins (groups) in the neutron or gamma-ray source description. The dose rates *are* sensitive to the *location* of the upper- and lower-energy bounds of the energy groups. The dose rates are also sensitive to the effective cross sections; however, the next section on shielding will discuss these effects. The dose response is largely a high-energy response (energies above 500 keV) and thus only 10–20 groups are required for the neutron and gamma group structures. The selection of the group structure for gamma calculations can, under limited circumstances, cause inaccuracies to arise in the dose rate solution. The 18-gamma-group structure utilized in both ORIGEN2 and SAS2H/ORIGEN-S is appropriate for the <sup>144</sup>Pr-gamma line. The primary energy of this isotope is 2.18 MeV, which is well represented in either group structure (2.0 to 2.5 MeV). However, the 20-gamma-group structure in the BUGLE series of libraries is not well representative of this gamma energy (2.0 to 3.0 MeV). This isotope is important in spent fuel analyses for cooling times of < 5 years.

The ideal gamma group structure is one where the most important gamma lines are centered within the energy bins. This is because the effective cross section for the energy bin is chosen for the energy at the center of the bin. The important gamma lines for spent fuel correspond to <sup>144</sup>Pr (2.18 MeV), <sup>134</sup>Cs (0.60 and 0.80 MeV), <sup>60</sup>Co (1.17 and 1.33 MeV), <sup>137</sup>Cs (0.66 MeV), and <sup>154</sup>Eu (1.27 MeV). It is also highly recommended that the gamma lines be directly binned into the group structure used to perform the shielding analysis, not placed in a standard bin and manually rebinned into the energy bins used in the shielding analysis. However, if one chooses to manually rebin, note the binning criterion in the following paragraph. The ORIGEN-S family of codes (SAS2H, ORIGEN-ARP) can bin the gamma lines sources into an arbitrary group structure, while the ORIGEN2 code bins into a fixed 18-gamma-group structure.

For discrete gamma lines, there is a one-to-one correspondence between the energy source (MeV/second) and the particle source (particles/second). However, once placed into the energy bin, approximations should be made to relate the number of particles and amount of energy. The standard procedure is to conserve the energy of the particles. Under this approximation the number of particles is adjusted by the ratio of the gamma energy to the average energy of the bin. This binning procedure is not rigorous, but is sufficiently accurate as long as the bins are not too large (a maximum factor of about 1.2 between the bottom and top

energy bounds are recommended) and the most important gamma lines are near the average energy of the bin (recommended minimum difference of < 5%). These recommendations are loosely based on the example shown in Table 9.20 of Ref. 22 where a 10% difference in the gamma line energy results in a 40% change in the calculated dose for a deep-penetration shield.

#### 3.3.3.4 Source Validation Studies

Validation of the neutron and gamma sources is a difficult task. The approach generally taken is a validation of the concentrations of the important isotopes relative to neutron and gamma source terms. Measurements have been published<sup>26,32</sup> for six of the seven isotopes discussed in Section 3.3.1. These isotopes (i.e., <sup>60</sup>Co, <sup>134</sup>Cs, <sup>137</sup>Cs, <sup>154</sup>Eu, <sup>144</sup>Pr, <sup>242</sup>Cm, and <sup>244</sup>Cm) are the major contributors to both neutron and gamma-ray sources. The only isotope not included in these measurements is <sup>144</sup>Pr, which is only important for short cooling times (i.e., < 5 years). Comparison of predicted isotopics with these measurements indicates that using the latest versions of the nuclear data files (ENDF/B-V and ENDF/B-VI) typically give agreements within 10%. Earlier nuclear data files showed differences of up to 40% for these same nuclides. The use of measurement benchmarks is encouraged for validation purposes.

The above conclusions regarding isotopic importances are largely based on comparisons with measured data that contain maximum burnups of about 40 GWd/MTU. However, additional studies<sup>33</sup> have recently become available that approach 50 GWd/MTU. Similar conclusions to those noted above are reached in this new study. Sensitivity studies have indicated that no significant change in the nature of the comparison is expected with burnups up to 75 GWd/MTU (Ref. 34). However, ultimately the validation of source terms for burnups approaching 75 GWd/MTU will need to be demonstrated via the use of assay measurements. As these enhanced burnup measurements become available, their results should be factored into future analyses.

#### 3.3.3.5 Source Term Components

The cross-section libraries available to the users of the ORIGEN family of codes also have built-in assumptions regarding the makeup of the neutron and gamma-ray source terms. The neutron source during decay is typically made up of spontaneous fission and ( $\alpha$ ,n) contributions. The default for the ORIGEN codes is production of ( $\alpha$ ,n) neutrons from a UO<sub>2</sub> matrix. If fuel other than uranium is present, the computation will correctly include the energies of the  $\alpha$  particles from these other actinides. However, if the fuel is not in an oxide matrix, one will be automatically assumed. Optionally, an explicit ( $\alpha$ ,n) capability is available for non-oxide fuels (see Section 3.2.3).

Similarly, the gamma-ray sources have two components during spent fuel decay after irradiation, the fission-product decay-gamma radiation and the radiation from bremsstrahlung due to slowing down of  $\beta$  particles in the fuel. The radiation from bremsstrahlung has a continuous energy spectrum from the energy of the  $\beta$  particle downward and can have a small effect on the predicted gamma dose rates. The built-in option in the ORIGEN codes assumes bremsstrahlung contribution due to a UO<sub>2</sub> matrix. It is possible to estimate bremsstrahlung from a water medium or omit the bremsstrahlung contribution by picking the appropriate alternative ORIGEN library. The three library names are maphuo2b (ft26f001), maphh20b (ft24f001), and maphnobr (ft23f001). A modification of the ORIGEN input is necessary to change the selected library unit from 26 to either 23 (no bremsstrahlung) or 24 (water bremsstrahlung). Alternately, the appropriate library can be copied to the ft26f001 file and the ORIGEN cases executed with standard inputs. This procedure is simplified with ORIGEN-ARP 2.0 where the choice of bremsstrahlung options is selected from a menu.

### 3.3.4 Other Spent Fuel Types

There are large numbers of other spent-fuel types that could be covered in this section. However, it is not necessary to cover them with the same level of detail as the LWR spent fuels. MOX fuels are expected to have the same general characteristics as high-burnup  $\text{UO}_2$  fuel with an enhanced contribution from neutrons due to initial presence of plutonium in the fuel assembly. However, there is little or no isotopic validation available for MOX fuels, thus additional studies need to be carried out to ensure the performance of current source procedures for these fuels.

A small class of fuels utilize thorium as a fertile blanket/target along with some form of fissile uranium as a driver. The use of thorium or  $^{233}\text{U}$  as fuel gives rise to the production of  $^{232}\text{U}$  that contains highly radioactive daughters, in particular  $^{208}\text{Tl}$ . Bounding concentrations of  $^{232}\text{U}$  should be justified for these fuels. Indeed, for unirradiated quantities of thorium, the presence of  $^{208}\text{Tl}$  needs to be considered, since it is one of the daughters of thorium decay.

Care should be used in the source generation for fuels in a matrix other than oxygen. Typically, the neutron source for oxide-based fuel is almost entirely spontaneous fission. The  $(\alpha, n)$  contribution to the neutron source from an oxide matrix is about two orders of magnitude below the spontaneous fission values. However, for other fuel matrices this may not be the case. Common materials that are significant producers of neutrons via  $(\alpha, n)$  are beryllium, boron, aluminum, and fluorine.

### 3.3.5 Radioactive Material Sources

Radioisotopic sources come in many sizes, shapes, and forms. Actinide-bearing sources generally are neutron-specific producers, either via spontaneous fission or  $(\alpha, n)$  when combined with various target materials. The spontaneous fission sources are generally rated based on the specific neutron source rate or by mass of the fissioning isotope. Typically, the source magnitude can be easily calculated if the mass is known. The source spectrum can also be calculated by hand from given spectrum formulae such as a Watt or Maxwellian curve and parameters specific for each nuclide (see Appendix H of Ref. 35). Alternately, these calculations are easily performed by the point-depletion codes, which generally have built-in spectra for the most important nuclides.

For radioactive sources that generate neutrons via the  $(\alpha, n)$  process, the neutron production rate can be estimated via standard point-depletion codes. However, the spectra are dependent on the target materials and are thus more complicated than the methodology in some of the standard codes. The SOURCES<sup>36</sup> code, version 5.0 or later of ORIGEN-S, and version 2.0 or later of ORIGEN-ARP can estimate both the number of neutrons per second and their energy spectrum under these circumstances. For situations where the  $(\alpha, n)$  contribution to the total source is significant, it is necessary to accurately quantify or establish bounding values for all impurities, especially light elements that are known to produce significant  $(\alpha, n)$  quantities.

Curies or grams usually specify the quantity of these radioactive sources. For isotopic sources with simple (one daughter product) parent-daughter decay schemes, the source magnitude and energy spectrum computation is straightforward. For these simple sources, the source magnitude can easily be calculated by hand. Gamma-line source data can then be used to estimate the spectrum or simply input the specific energy lines if a point-energy code is being used.

For radioisotopic sources with many daughters, care should be exercised in the conversion from curies or grams to source particles per second. The buildup of daughter products should be taken into account, either explicitly via a decay code calculation or approximately by inclusion of equilibrium daughter products. If the sources are calculated via an explicit calculation using a decay code, the quantity of interest is the peak dose due to the source, not the peak activity of the source. Typically, these peaks occur simultaneously;

however, knowledge of the dominant contributor to the dose and its gamma-line energy is useful in this determination.

It is necessary to decay the specified quantities of source material until the peak dose occurs. If the amount of primary source material at the time of peak dose has changed due to the decay, then it is necessary to renormalize the total quantity of primary source material to the initial values. Renormalization to the initial quantities of source material is necessary only when the time of peak dose rate is a significant fraction of the half-life for the parent source isotope.



## 4 SHIELDING ANALYSES

This section of the report will describe the various computational approaches to the solution of radiation protection problems, followed by factors to consider when deciding which methods and models are appropriate for a given application. The last portion of this section will address specific issues in the generation of shielding and dose rate solutions that will typically arise in preparation of a safety application for transport and storage packaging.

### 4.1 METHODS

Over the years a variety of shielding analysis methods have been utilized for radiation protection activities. These methods include a series of point and line source analytical solutions, the point kernel technique, various deterministic techniques like discrete ordinates and spherical harmonics, and more recently multidimensional Monte Carlo solutions. Transportation and storage casks containing radioactive materials fall into a class of shielding applications deemed deep-penetration problems. Deep-penetration problems can be loosely defined as 2-3 orders of magnitude attenuation due to the shielding materials. Under these conditions, the methods and data applied to the problem solution are extremely important for accurate analyses. This section will briefly describe the primary methods currently in use, the point kernel technique, discrete-ordinates methods, and Monte Carlo techniques along with their strengths, weaknesses, and recommended usage.

#### 4.1.1 Point Kernel Method

Point kernel techniques are extremely simple yet effective for a number of shielding applications for spent fuel packaging. The technique is based on an analytic point source solution where the unattenuated flux at any distance  $r$  from the source point is proportional to the source rate (particles/s) divided by  $4\pi r^2$ . Attenuation is treated in an approximate manner through the use of built-in attenuation coefficients and buildup factors. The point kernel technique breaks an arbitrary source volume into volume segments and assumes the total source in that volume is a point source at the center of the volume. The contributions to the detector flux/dose from all source volumes are summed to obtain the point kernel solution.

Point kernel techniques are best utilized when their shortcomings are clearly recognized and avoided. This discussion of potential inaccuracies of point kernel techniques is primarily aimed at the two most widely used programs (i.e., the ISOSHIELD/MICRO-SHIELD<sup>37</sup> and QAD<sup>38</sup> codes). Point kernel techniques should only be used when the primary source of radiation is due to gamma rays, since the current implementations do a poor job of characterizing neutron attenuation. In general the method should be able to handle practically any source geometry; however, the current most popular codes work best when the source geometry is rather simple. Homogeneous source bodies at the center of the configuration are the easiest source geometry to model. A thorough understanding of the code options is necessary to model more complicated source forms. The current versions of these codes also perform best when the shield body has only one primary gamma shielding material. The buildup factors that are built-in to the code are appropriate for only a single material gamma shield. If there is a multiple-layer shield, the QAD manual states that the buildup factors should correspond to the most significant outermost shield material. There are several other procedures for determining the effective material for a multiple-layer shield. Once an effective Z is known, the material with a Z value that most closely matches the effective Z is entered for the buildup factor calculations.

A final deficiency in the use of point kernel techniques is the oblique or grazing angle approximation. This inadequacy of the technique occurs when the path between the primary source point and detector point penetrates the shield body at a very large angle relative to the normal. A practical test for this effect is that

the height-to-diameter ratio of a cylinder should be less than about 30 for mid-plane doses on the side of the cylinder. Similarly the ratio of the source-to-detector lateral distance to the shield thickness should also be less than 30. These shortcomings should be of little practical importance for typical spent fuel packaging applications.

The technique is useful for geometry spot checks on a more complex geometry (e.g., the radial dose from a smeared cavity for checking a detailed basket configuration model). Another useful feature is the ease at which gamma group structure effects can be determined by using the source generation procedures to produce a very fine energy group source for comparison with a standard few group source. The SCALE system automates this procedure by allowing the point kernel code, QADS, to directly read the source from an ORIGEN-S/SAS2H/ORIGEN-ARP calculation. (See Appendix A for discussion of output format for sources produced by ORIGEN.)

Point kernel techniques are not recommended for void penetration studies or any streaming calculations, since the method uses a line-of-sight attenuation method that does not account for reflection from the sides of the streaming path. The point kernel method also produces the output dose rates in a useful format. The dose rate is tabulated for each *source* energy group. This allows the direct determination of the most important source energies or groups. This is a useful feature for determining the causes of differences between various calculations or even various methods. Non-kernel methods include gamma-ray energy degradation in the transport solutions; therefore the dose by source group is not available.

#### 4.1.2 Discrete-Ordinates Method

Discrete-ordinates codes provide a direct solution to the Boltzmann transport equation<sup>39</sup> and thus provide a more rigorous solution than the point kernel method. The method derives its name from the discretization of the angular variation in the particle flux into discrete angular directions. Existing codes are available with 1-D, two-dimensional (2-D), and three-dimensional (3-D) capabilities. The spatial variable in the Boltzmann equation is discretized into spatial meshes to enable the approximation of the spatial derivative as a finite difference. The energy variation in flux is similarly discretized by defining energy ranges or groups where effective cross sections have been defined. This discretization of the system unknowns makes the method more accurate as the spatial, energy, and angular segments are refined. The system angular representation can be characterized as the  $S_n$  quadrature order, and is recommended to be  $S_{16}$  for shielding calculations. The mesh size for the spatial discretization is material dependent; however, a rule-of-thumb is that the flux and/or dose rate should not change more than a factor of two between neighboring mesh intervals. Recommended mesh sizes for typical shielding materials are as follows:

1. for gamma radiation, mesh size of 0.3 cm (uranium), 0.5 cm (lead), 0.7 cm (iron), 1.0 cm (concrete);
2. for neutron radiation use 1.0 cm mesh for all materials; and
3. for source media and low-density materials mesh size can be 3–5 cm.

The use of discrete-ordinates methods is typically limited to the cavity and shield portions of the geometry. This limitation is due to both inefficiencies and inaccuracies in extending the solution through several meters of void or air. The recommended approach for these calculations is like that in XSDOSE (1-D)<sup>40</sup> and FALSTF (2-D and 3-D),<sup>41</sup> where the leakage from the shield is processed along with a last flight collision estimator to produce fast and accurate estimates of the flux and dose rates for external detectors.

The inclusion of neutron upscatter effects in a discrete-ordinates calculation can be quite problematic due to the increased difficulty in the convergence of problems with significant upscatter. Upscatter effects are only important for thermal neutrons where the velocity of the neutron is comparable to the velocities of target materials due to thermal energy. Under these conditions neutrons can gain energy in a collision with a target

nucleus. These effects are only important in shielding calculations when the production of secondary gammas are important (see Section 4.3), since the production of gammas is due in many cases to thermal neutron capture. In 1-D codes, the treatment of upscatter is generally accomplished by increasing the number of outer iterations to 20–40 or more for large systems. In 2-D and 3-D codes, computing time restraints can necessitate a change in the default iteration strategy. The approach is to break the problem into pieces, first the non-thermal groups, then thermal groups where upscatter is possible, then finally the secondary gamma calculations.

The convergence of the flux is key to obtaining an accurate solution using the method of discrete ordinates. The flux convergence criterion is usually set at  $10^{-4}$  and this value is generally sufficient. However, the user should verify that the convergence has been reached. Messages generated by the codes typically indicate when convergence has occurred, but the results are typically given whether the solution converges or not. For problems with significant fission occurring, the fission density should also be checked to ensure it has converged. The convergence criterion on the fission density is usually the same as that of the flux.

A general problem encountered in discrete-ordinates analyses is the occurrence of ray effects. Ray effects refer to unphysical peaks or rays in the solution due to the inability of the angular quadrature formula to approximate the scalar flux. Ray effects are generally observed in problems that have weakly scattering media and/or localized sources. The numerical solutions tend to be overestimates or underestimates of the correct solutions along fingers or rays emanating from the point source. The mitigation of ray effects is typically accomplished by an increase in the angular quadrature for the problem. As previously stated, the use of  $S_{16}$  for cask calculations is generally sufficient for shielding calculations. For situations in which the source is effectively a point and the desired dose rate locations are several hundred meters away, the use of a first-or-last collision code<sup>40</sup> could be necessary. Additionally, for void streaming problems, a higher angular quadrature or a tailored quadrature set is usually needed for accurate solutions.

Various discrete ordinate codes offer differing algorithms for the spatial finite difference approximation. They include step, linear, linear step, linear-zero, standard weighted, and theta weighted. The step and linear algorithms are sufficient for some problems, but the deep-penetration nature of spent fuel cask problems makes the use of one of the weighted differencing schemes necessary. The standard weighted-difference scheme is the most general and easy-to-use; however, for extremely difficult problems the theta-weighted technique may be necessary. The theta-weighted procedure is the most efficient; however, it does require user expertise in the selection of the optimal theta parameter. Deep-penetration problems are readily solved using discrete-ordinates codes, provided the spatial mesh is fine enough such that the flux or dose response does not change by more than a factor of two between adjacent spatial meshes. Validation of deep-penetration problems is important because cross-section errors of only a few percent can cause significant errors in calculated responses external to the shield (see Section 4.3).

### 4.1.3 Monte Carlo Method

The Monte Carlo method provides a stochastic solution to the Boltzmann transport equation. The solution for the energy-, angular-, and spatial-dependent flux density can be obtained using the integral form of the Boltzmann transport equation. In this form the flux at any location is the integral of contributions from all other locations within the system. The contributions from all other points in the system are quantified using a transport and a collision kernel. These kernels define the probabilities of a particle transferring from any point in phase space to any other point in phase space and the collisions that occur during that transfer. The Monte Carlo procedure uses the probabilities defined by these kernels to track a particle from its birth at a source to its loss via capture or leakage from the system. The transport kernel determines the particle's travel to a collision site. The collision kernel then determines its fate at the collision site. The Monte Carlo code is designed to generate a series of these particle histories in order to estimate the desired quantity (flux or dose rate). There are several techniques for estimating the flux at given locations. The first involves a point detector flux estimate in which the contribution from each collision site to the point detector is

estimated using the transport operator and then summed over all collision sites. The second is a boundary-crossing flux estimator in which the number of particle tracks crossing a given surface is tallied and the average flux along the surface is then generated. The final detector technique is a flux-within-a-volume estimator. This technique uses the collision density or track-length within the volume to estimate the volume-averaged flux.

Monte Carlo methods are very powerful in that they can accurately model the entire physical system in 3-D. However, for deep-penetration shielding problems, the use of biasing is required for realistic solution times. Using appropriate biasing, deep-penetration problems can be readily solved with accuracies primarily dependent on the cross-section accuracies. Similarly, void-streaming problems can be solved using Monte Carlo techniques, provided proper biasing is used. For a detailed discussion of biasing, the reader is referred to Refs. 42 and 43. The popularity of automated and/or user-friendly biasing techniques has increased, and codes using these methods are rapidly becoming the standard in shielding analysis techniques.

The prudent use of full 3-D geometry packages requires that a visualization tool be available. These tools allow the full geometry or selected portions to be viewed for correctness. If possible, the entire geometry should be checked as well as selected portions that are key to the correct problem solution, such as placement of thick gamma and neutron shields, location of source materials, and correct material placement in those locations. The correct starting locations for source particles should be verified, if possible, along with the correct placement of selected detectors. As with any Monte Carlo code, the solution will have statistical variations. It is essential to examine these uncertainties to ensure the reliability of the reported solutions.

The estimation of the dose rates at selected locations can be determined using either point, surface, or volume detectors. For dose profile generation, surface detectors are generally much more efficient than point detectors, but can be more difficult to use. The point detectors do not function as well on the outermost surface of a shield, and the use of surface detectors is recommended there. External to the shield either method is acceptable. If surface detectors are chosen, the use of detector segments is recommended in order to give an estimate of the spatial variation. These detector segments should be chosen small enough to show the variation, but large enough to produce good statistics. The recommended detector statistics are less than 5–10% standard deviation for a point, surface, or volume detector.

A unique advantage of the Monte Carlo method is the ability to efficiently utilize point cross sections. The use of essentially continuous energy nuclear data is useful in that a number of cross-section processing steps are omitted, primarily the group averaging and resonance processing procedures. While validation of methods utilizing point cross sections is still desirable, the level of effort is expected to be somewhat less than applications using multi-group cross sections. It is recommended that, if applications using multi-group data are submitted, spot checks be made of the same systems with point cross-section data (see Ref. 35). Obviously, if measurement data are available, either method can be validated using those data. A sample validation study is given in Ref. 44. See Section 4.3 for further discussion of these validation studies.

## 4.2 MODELING

The development of models for shielding applications is a very important part of the overall analysis. There are extremes on either side of the modeling decisions, a full bolt-by-bolt description of the package geometry versus a simplified 1-D concentric cylindrical geometry. Rarely is the full geometric description necessary or even desirable for shielding applications. For example, the modeling of a full pin-by-pin geometry for a fuel assembly typically produces the same answer as a smeared assembly model to within the combined statistics of the two solutions. At the opposite extreme, a 1-D model is a useful calculation; however, it needs to be benchmarked against more realistic models. For the point kernel and Monte Carlo options, a full 3-D model is the norm. However, the degree of detail needed in the model is highly variable, depending on the geometric complexity and experience of the users.

An assumption that drastically simplifies the model is the smearing of the source and/or materials in the packaging cavity. Under this approximation the active fuel materials are smeared over the cavity radius and the hardware/endfitting materials are also smeared over the cavity radius, but in a separate region. This procedure is conservative (see exception noted in next paragraphs) if the source is smeared over the cavity radius, not just the effective source material radius, and the actual thickness of any structural material located outside of the fuel assemblies or source material is included on the inner surface of the cavity. For example, if a ½-inch steel wrapper surrounds the entire assembly arrangement, a ½-inch steel layer should be placed on the inside of the cavity in the model. Any other basket material should be smeared with the fuel or ignored for conservatism. If there is a solid insert in the cavity region surrounding all of the fuel assemblies, the minimum thickness of the insert should be modeled. For dry cavities, the smearing of the cask materials is accomplished by multiplying the respective volume fractions and material densities together.

For a wet cavity, a cell-weighted homogenization should be performed since the neutron source multiplication in the cavity region should be treated as accurately as possible. For the dry case, a smearing of the cavity without cell-weighting will result in a few percent error in the system multiplication factor; however, the system multiplication factor is so low (typically 0.3–0.4) that the error in the multiplication of the source is insignificant. This neutron source multiplication is typically approximated as  $1/(1-k_{eff})$  for systems that are far subcritical. However, most modern codes optionally include the source multiplication in the shielding solution.

The above discussion assumes the active length is approximately the same as the cavity height. For short assemblies stacked on top of each other with supports or spacers separating them, smearing over the cavity height is not recommended. Under these circumstances, the separate smeared assembly axial regions should be modeled explicitly.

If the azimuthal variation in dose rates around the cask is desired, the recommended approach is to model the actual basket geometry while smearing each assembly within its separate enclosure/or basket location. Under this assumption, many of the detailed elements of the basket can either be smeared along with the assembly or omitted for conservatism. This procedure is quite powerful and allows for a detailed model of the basket without the unnecessary complication of modeling the fuel assemblies pin-by-pin. Under this assumption, the fuel hardware/endfitting materials are also smeared and placed on the top/bottom of the smeared fuel assemblies.

For discrete-ordinates solution techniques,<sup>41,45</sup> the options of 1-D, 2-D, or 3-D representation of the system geometry are available. For 1-D models, the simulation of the radial variation in cylindrical geometry is considered the most accurate approximation (of course the cavity should be smeared in this case). A 1-D slab, or Cartesian geometry option for the top or bottom of a cylindrical application, is also useful where the leakage from the radial direction is treated approximately via buckling factors that are built into the codes. An accurate model should support this option since conservatism is dependent on the choice of buckling values. In 2-D, cylindrical bodies can be accurately solved using RZ geometry. This method allows the radial and axial calculations to be performed simultaneously. Either a homogeneous source region or a series of concentric cylindrical source regions should be used to approximate the cavity model under these circumstances. An XY model is available but is not typically useful for cask shielding applications. The 3-D options consist of XYZ or RΘZ geometries that are typically not used for cylindrical cask applications. The RΘZ option can be used to model non-azimuthally symmetric geometries, but these calculations are quite difficult since the flat surfaces in the cavity region should be modeled as a series of arcs. Similarly, the XYZ geometry option is useful in the description of the square-lattice structure of the cavity basket materials, but difficult when modeling the cylindrical shield bodies.

The presence of fins in the outer cask body gives rise to computational and modeling difficulties. Their treatment is problem dependent due to the large variation seen in fin designs. The most prudent approach is to quantify the expected effects using a computational tool based on the particular situation. There are

several techniques that have proven useful in this regard. Several examples include the use of a discrete-ordinates  $R\Theta$  (or similar model using 3-D Monte Carlo) model for estimating the streaming effects of an axial fin. For radial fins, an RZ model should concisely capture the streaming effects. For both 2-D discrete ordinate and 3-D Monte Carlo, the problem is greatly simplified by using the fin symmetry to estimate the overall fin effect. Using symmetry, along with reflected boundary conditions, it is only necessary to model a single fin and, hence, greatly reduce the computational difficulty. In these models a smeared basket is reasonable even if the full analysis treats the basket in explicit detail.

Fins with void material between them can be safely ignored in the shielding analysis; however, their removal may give rise to a large conservatism. For fins with interstitial neutron moderator material, the omission of the fins (and replacement with neutron moderator material) is still conservative provided the gamma radiation is the dominant contributor to the regulatory dose rates. If neutrons are a significant portion of the doses, the replacement of the fin material with neutron moderator material is nonconservative and should be avoided.

Estimation of radiation streaming through void penetrations and local doses from trunnion placement are additional shielding issues that require thought and innovative solutions. The computational tools suggested for the estimation of fin effects also apply for these problems. An RZ model could be used to predict the streaming through a straight radial penetration or quantify the dose profile around a complicated trunnion model. For large cask irregularities like a trunnion, it is possible to use a series of 1-D slices that are weighted by their respective areas to obtain an average dose rate. However, caution is advised using these models since they tend to only give correct values for the large portions of the geometry and can give incorrect values for small, but important portions (e.g., gaps and low-density materials) of the geometry. Monte Carlo solutions for these situations again require the prudent use of geometrical approximations, such as the reduction of the effective cask height or radius (only the neighboring 20–30 cm needs to be modeled) for penetrations of the package. For these cases, special biasing is typically needed to efficiently solve these problems.

An additional area that can give rise to computational difficulties is radial streaming due to the presence of largely differing geometries in the axial direction of the cavity region. Geometric complexities can arise due to horizontal disks placed in the cavity region for support of the basket or separators between short assemblies stacked end-to-end in the cavity region. The presence of these complex geometries can challenge biasing techniques, and the presence of computational difficulties should be evaluated.

Impact limiters are constructed of low-density materials designed to absorb the impact forces and reduce damage to the package during the required drop tests. As such, they are of little consequence to the shielding design, although wooden impact limiters can impact the neutron dose rates. Their inclusion in the shielding analysis is optional since their omission should, in all cases, be conservative. Many times the impact limiters are omitted, but the surface and 2 m locations reflect their presence. If they are included in the accident calculations, the accident analysis should show that they remain on the package and intact.

### 4.3 DOSE RATE ESTIMATION

The quantification of dose rate information for submittal of a licensing application involves a number of processes using the models and methods discussed above. This section describes a number of different subjects that are necessary for the accurate generation of dose rate information.

A formal validation of the shielding portion of the SARP submittal is not requested. The use of reasonable procedures and well-established computer codes is expected to produce acceptable results. The NRC review phase will decide the quality of the procedures and typically conduct confirmatory calculations as well. Comparison to measured values for similar applications should only enhance this process. The series of

assay measurements<sup>26,32</sup> performed for spent fuel on select isotopes can be used to characterize the reliability of the source predictions. These analyses allow for the determination of acceptable source quantity predictions on a nuclide-by-nuclide basis. As stated in Section 3.3.3, such a study indicated that the latest SCALE burnup library predictions for the major source isotopes are acceptable since they agree with measurements to within 10%. Similar studies have been performed for loaded spent fuel casks.<sup>44</sup> The results of these studies show neutron dose predictions are generally within 30% of the measurements, the hardware gamma doses are well predicted if the quantities of <sup>59</sup>Co impurity levels are known, and the gamma doses from the active fuel region are overpredicted by about 40%. The report compared several major shielding codes in these analyses including SAS4/MORSE,<sup>46</sup> MCNP,<sup>35</sup> DORT,<sup>41</sup> and MARMER,<sup>47</sup> which is a point kernel code. The conclusion was that all these codes gave results that were in general agreement with each other. Another study<sup>48</sup> sponsored by the Organization for Economic Cooperation and Development (OECD) gave similar results and conclusions although the predictions for gamma doses from the active fuel region were closer to measured values than those of Ref. 44. The spent fuel cooling time considered in the OECD study was approximately 6 months, whereas spent fuel planned for cask loading in the U.S. has typical cool times > 5 y. While each of these studies is limited, they provide a basis for confidence in the major code packages used for spent fuel source term and cask shielding.

The selection of flux-to-dose conversion factors is an important part of the overall shielding analysis. The accepted values for use in dose rate studies for cask shielding qualification are the ANSI/ANS 6.1.1-1977 (Ref. 49) values or their equivalent. The use of the latest version of this standard<sup>50</sup> is not recommended since it predicts dose rates that are, in some instances, substantially lower than those of the 1977 standard and the NRC has not adopted the approach embodied in the 1991 updated standard.

An understanding of the general trends in shield design for particular casks is a key in the design and review of cask applications. For many radioisotope sources only the gamma doses are of importance, since the primary radioactive mechanism is decay gamma rays. For neutron sources like <sup>252</sup>Cf and plutonium-beryllium, the primary particle production is due to neutrons, but primary and secondary (or capture) gamma rays are also present. Another situation that occurs in many transportation scenarios is the backscatter of radiation from the ground or from surrounding packages. While present, this effect is usually ignored due to the variability of the backscatter configuration.

In spent fuel applications, the contact dose rates, due to gamma rays for an unshielded assembly, are about five orders of magnitude higher than those for neutrons. Therefore, the gamma shield is the most important design aspect until sufficient gamma shielding is added to make the neutron and gamma contributions about equal. At that point, both neutron and gamma shielding should be added to further decrease the dose rates. These trends will change for higher burnup fuel, since the neutron dose increases exponentially with burnup, while the gamma dose only increases linearly. Typically, secondary gamma dose rates from a cask are a small fraction of the neutron dose rates. An exception to this behavior is a concrete shield, where neutron and secondary gamma dose rates are nearly equal.

A situation that occurs, if shields are not designed properly, is the production of secondary gamma rays due to neutron capture in the shield itself. This may necessitate placing a gamma shield outside a concrete shield to shield the gamma rays produced within the shield. Also, the addition of a neutron shield without a strong absorber material present (i.e., a water shield without dissolved boron) can allow for the neutrons to be thermalized, then produce secondary gamma rays in the neutron shield or backscatter to generate secondary particles near the outside of the gamma shield, where little further shielding is present.

There are a number of approaches to the shielding analysis for spent fuel storage arrays. The analyst can simply analyze a single cask and quantify the surface dose rates along with doses at postulated site boundary locations. Cask dose rates from 20 to 400 mrem/h have been accepted in previous 10 CFR Part 72 evaluations. The specific approval of such a cask is therefore dependent upon its actual placement at a site-specific location. Other approaches quantify the dose rate for an assumed array of storage casks with an

assumed minimum site boundary (typically 100 m from the casks). This dose rate should be a fraction of the limiting 25 mrem/year since other neighboring contributors should also be taken into account. Under both approaches, a cask array calculation ultimately has to be performed. These calculations are quite complex and can challenge even the most modern codes and computer hardware. The treatment of cask array calculations will be briefly summarized for two shielding codes, MCNP and SKYSHINE.<sup>51</sup> These codes have very different approaches for solving cask arrays, the former is a rigorous Monte Carlo code, and the latter uses a series of approximations including point kernel techniques for dose attenuation and air transmission factors for air scattering. The MCNP code can use several techniques to simulate cask arrays. The first technique uses a single cask model with appropriate reflected boundary conditions to model a pair, a single infinite row, or two infinite rows depending on the reflected boundary conditions. The second technique inserts the single cask model into an  $N \times N$  array model with the actual array dimensions. This second technique uses the so-called array geometry or repeated structures capability. These computations can be quite time-consuming, but are possible with today's computers. These calculations are very rigorous and are considered the current state-of-the-art.

The SKYSHINE code uses a simple, box geometry model for each cask. The thickness of the four walls of the box is specified as well as the dimensions of the array of box units. The shielding of a cask by other casks in the array is treated by an approximate technique. The geometry is crude but the techniques are applicable to cask array calculations. The computational algorithms in SKYSHINE are quite crude and there have been reported errors in the code;<sup>52</sup> thus, sufficient expertise in using the code is needed to get meaningful results. The latest version of this code, SKYSHINE-III,<sup>52</sup> has corrected many of these problems and has been benchmarked against rigorous codes and measurements.

The typical approach for a cask shielding submittal is the calculation of dose rates from either a single limiting condition (specific burnup/enrichment/cooling time) or a series of limiting conditions that produces equivalent (or less than) dose results to that of the single bounding condition. Each of the specific conditions in the series has a maximum burnup, minimum enrichment, and minimum cooling time. Under the series approach, a curve like the one shown in Figure 1 is produced. Each of the burnup points shown in the plot has an associated minimum enrichment level. A minimum enrichment specification is necessary because the predicted dose rates increase with decreasing enrichments at a fixed burnup, thus the values for each burnup would be bounded. This approach offers much more flexibility than the single limiting condition, since any assembly that lies above the line shown in the graph could be loaded into the cask.

An alternate licensing approach for transport applications is to back calculate the contact dose rates or specific source terms for each item to be loaded into the cask such that the regulatory dose limit on the exterior of the cask is precisely met. This allows for the establishment of a limiting dose rate or source specification for items placed into the cask. At loading, each item is measured or numerically compared to the individual item limits. An approach using measurements is typically not used since measurement of individual items is time consuming and hence expensive. To properly use this alternate technique, the limiting dose rates or source levels for items loaded into the cask should be separately evaluated for neutron and gamma doses. This approach first assumes that all of the dose is due to gamma and arrives at a limiting dose rate of  $G$  rem/h for each item, then assumes that the entire regulatory limiting dose rate is due to neutrons and arrives at a limiting dose rate for each item of  $N$  rem/h. The measured or calculated neutron and gamma dose rates for each item can be normalized by  $N$  and  $G$ , respectively, and the contributions combined and compared to unity as a loading condition. Under this approach, a widely varying set of radiation items could be loaded, each of which should be measured or calculated prior to loading and the entire cask measured after loading.

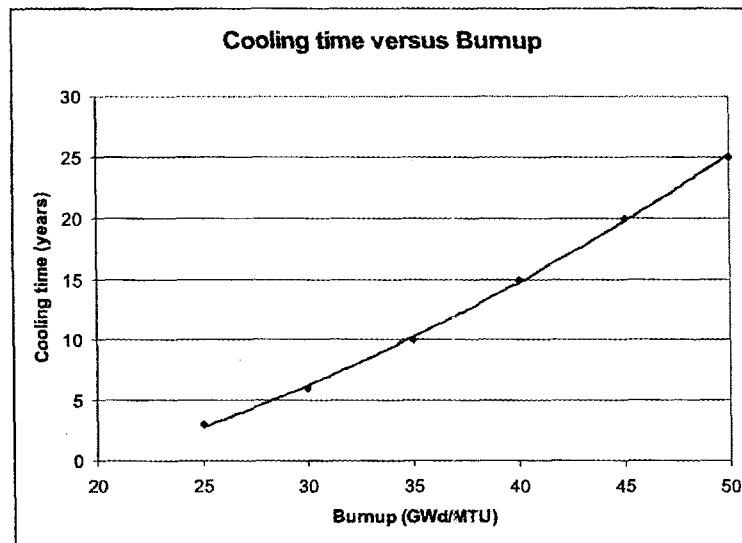


**Figure 1 Sample loading curve as a function of burnup and cooling time**

Since the alternate approach using individual item measurements is almost entirely measurement based, it is recommended that a single sample calculation be supplied in the submittal. This calculation should be for a bounding loading. This sample calculation is designed to allow for the confirmation of the series of analyses on which the submittal is based, and also give reasonable assurance that the desired contents will indeed meet the loading criterion. The following conditions should always be met:

1. An application should show compliance with the regulations, normal and accident conditions (i.e., sole reliance on a measurement is not permitted).
2. The method should consider the energy of the radiation and the actual shielding materials.



## 5 MEASUREMENTS

Dose rate measurements are used in practice to provide a final verification that the loadings for each specific package do not cause the regulatory limits to be exceeded. As such, these measurements are an important component of safety that need to be examined critically for adherence to acceptable standards. This section summarizes the various techniques available for dose rate measurements and their expected accuracies, along with standard calibration schemes and their effects on the overall system if calibration errors are present. Additionally, recommendations are provided for the number and location of expected measurements as well as a plan of action in the event that the cask loading does not meet the regulatory limits.

### 5.1 MEASUREMENT TECHNIQUES

The primary measurement mode for particle radiation is by the quantification of the ionization produced inside the detector by the passage of various charged particles. Primary techniques that measure the amount of ionization present include ionization chambers, proportional counters, Geiger-Müller counters, scintillation counters, and semi-conductor detectors. Each of these detectors can directly determine the number of charged particles present. The first three techniques employ a gas-filled chamber, each with unique properties corresponding to the magnitude of the applied voltage across the detector (see Figure 2). In Figure 2, the ionization chambers operate in Region II, the proportional counters in Region III, and the Geiger-Müller counters in Region IV.

For uncharged particles (e.g., neutrons and gamma rays), the production of secondary charged particles is necessary for detection. These processes include Compton scattering for gamma rays where the photon collides with an electron, freeing it from the atom and transferring energy to it. Neutrons can interact with target materials such as boron and the resulting alpha particle can be detected to imply the neutron population in the region.

Detectors can operate in either pulse or current modes. In the pulse mode, the detectors produce outputs for each particle that interacts within the detector volume; while in the current mode, the detector output is an average over a large number of events. Certain techniques are better suited for pulse mode, such as the proportional and Geiger-Müller counters. These techniques produce enough ions per particle that the pulse mode is possible. For ionization chambers, pulse mode is possible if the number of ions per particle is sufficiently large to overcome the noise in the electronic signals. The increase in ions per particle for the proportional and Geiger-Müller regions is due to gas multiplication, where the ions have sufficient energy due to the additional applied voltage to produce secondary ions as they travel to the collection point. In the ionization and proportional regions, differentiation of various particles is possible due to the varying pulse heights for differing particles (note the differences in ions produced per particle for alpha and beta particles in Figure 2).

#### 5.1.1 Ionization Chamber

The concept of an ionization chamber is that the radiation entering the device produces ionization in the filling gas material which can be directly measured either as an electric current or total amount of charge released inside the chamber over time. The electric current type is used for dose rate measurements while the charge type is used for total dose measurements since both the current and total charge released can be easily related to the energy deposited in surrounding materials.

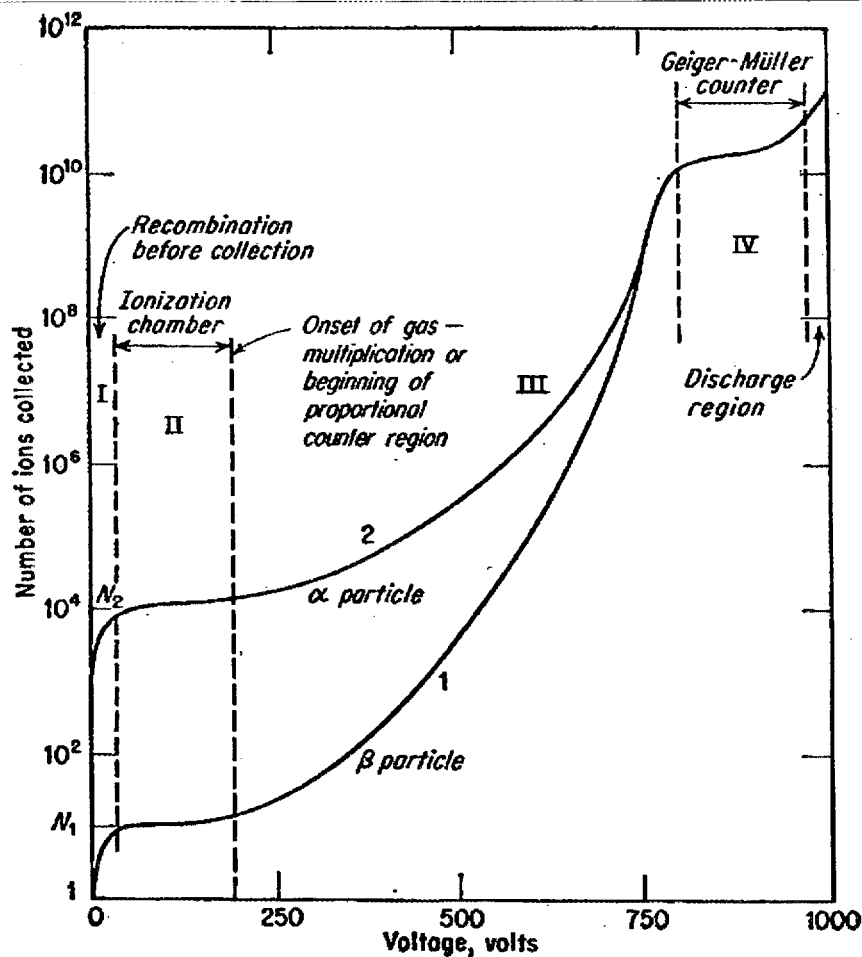


Figure 2 Pulse-height versus applied-voltage curves to illustrate ionization, proportional, and Geiger-Müller regions of operation [Source: Ref. 53 (Reprinted from C. G. Montgomery and D. D. Montgomery, *J. Franklin Inst.*, 231: 447 (1941). Reprinted with permission from Elsevier.)]

The basis for these measurements is the Bragg-Gray<sup>53</sup> principle that states that the amount of ionization produced in a gas cavity serves as a measure of the energy dissipated in the surrounding material. This procedure assumes that the particle flux in the gas cavity is the same as in the surrounding material.

### 5.1.2 Proportional Counter

The proportional counter is operated in Region III, as shown in Figure 2, where gas multiplication becomes important. The increase in the number of ions produced per particle makes the electronic amplification requirements less demanding and hence the accompanying electronic equipment is simplified. Most proportional counters operate in pulsed mode in order to allow the discrimination of the particle types due to the difference in specific ionization. Since multiple particle types can be differentiated by their pulse sizes, proportional counters are very useful for combined neutron and gamma dose measurements.

### 5.1.3 Geiger-Müller Tube

Geiger-Müller tubes are very useful since they can handle a very high output count rate, and can measure any type of particle with high sensitivity. However, they do not differentiate the particle type and thus are of limited use in multiple-particle fields. The high sensitivity is due to their operation in Region IV shown in Figure 2, where the gas multiplication is at its peak value. Their use is quite flexible in that they can be made into practically any size and shape at a reasonable cost.

### 5.1.4 Scintillation Detectors

Scintillation devices operate under a property whereby certain crystal substances emit light or scintillations when exposed to ionizing particles. The magnitude of these bursts of light is proportional to the amount of energy deposited in these crystals. Therefore, as with proportional counters and pulsed ionization chambers, these detectors can be used to measure the energy dependence of various atomic particles as well as differentiate between them. The light emitted by these devices is typically detected and converted to an electric current by a photomultiplier tube.

### 5.1.5 Semiconductor Radiation Detectors

The placement of an electric field across a semiconducting material allows the material to act as a charged particle detector in a manner analogous to the various ionization detectors previously discussed. The passing of a charged particle through the semiconductor produces electron-hole pairs that are separated and collected, resulting in an electric signal, which can be measured. This class of detectors is very important for general detection of a wide variety of particles. Some semiconductor detectors (e.g., intrinsic germanium, germanium/lithium, or intrinsic silicon) require cryogenic cooling, while others (e.g., variants of cadmium telluride) function at room temperature. TLDs (thermoluminescent detectors) function at room temperature, but the dose reading is performed in a laboratory, so the measurement is not real-time and is not useful for a cask survey.

### 5.1.6 Neutron Detectors

Since neutrons are neutral particles, they must interact with additional materials to produce particles that can be detected. The typical neutron detector uses neutron-induced reactions such as  $(n,\alpha)$ ,  $(n,p)$ ,  $(n,\gamma)$ , and  $(n,\text{fission})$  to estimate the neutron population in the detector. As a result, the standard ionization chamber, proportional counter, Geiger-Müller tube, scintillation, and semi-conductor techniques previously discussed can then be used to measure neutrons when an interacting material is added. Due to the small range of particles, these reaction-producing materials are normally either part of the filling gas or in thin shells surrounding the detectors.

Many times when neutron emissions are desired, gamma rays are also present; therefore, it is necessary to discriminate between these particle types. This is not typically possible using ionization chambers, but is readily accomplished using proportional counters. A technique, which is useful for practically any measurement technique, is the use of two chambers, one sensitive to neutrons and gamma rays, and the other only sensitive to gamma rays. The difference between the two measurements is that attributed only to neutrons for a mixed radiation field.

### 5.1.7 Bonner Spheres

Bonner Spheres are concentric spherical layers of polyethylene (or other hydrogenous material) that can be placed over a neutron detector to adjust the sensitivity of the instrument to the neutron spectrum. Neutron detectors actually measure charged particles, generally recoil protons produced by collisions with hydrogen.

A well-thermalized spectrum, such as that found outside a reactor vessel that requires a moderator to function, can be detected directly by an instrument such as a  $\text{BF}_3$  counter with a good efficiency. A fast spectrum, such as that found outside a fast or intermediate spectrum reactor vessel or a spent fuel transportation cask, will cause the neutrons to pass through the detector without many interactions with the boron (low efficiency). The addition of one or more Bonner Spheres to a detector thermalizes the neutron spectrum allowing more interactions to take place within the detector, thus increasing the detector efficiency. Detectors that do not include hydrogenous thermalizing layers are very inefficient for neutron measurements outside a spent fuel cask, especially at two meters from the package boundary where the total dose rate (neutron plus gamma) should be  $< 10$  mrem/hour. Sequentially adding thicknesses of Bonner Spheres also allows a rough estimate of the spectrum outside a cask.

## 5.2 MEASUREMENT ACCURACIES

Measurement accuracies, for gamma and neutron dose rates outside a spent fuel transportation cask, are generally about ten percent for the gamma field but are difficult to quantify for the neutron because knowledge of the neutron spectrum is required. Gamma measurements can be quite precise if desired, but hand-held survey meters are typically accurate to ten percent, and the actual accuracy of a particular detector can be determined by a proper calibration. Neutron detectors can be calibrated with reasonable accuracy (10–20%) but the spectral dependence of the detector efficiency curve requires knowledge of the spectrum for the field being measured.

Accuracy of a measurement includes the effects of the accuracies of the detector calibration and the accuracy of the positioning of the detector. Positioning errors are not large at the ends and sides of a spent fuel cask if a distance measurement is made, because the field gradient in these locations is not very pronounced. Areas near valves and trunnions, which alter the cask shielding locally, have larger gradients and precise positioning becomes very important. When large gradients are present, care must be taken to ensure proper detector size in estimating peak dose rates.

Typically the difference between measurements and calculated dose rates also includes the effect of tolerances in shielding thicknesses. Calculations may be performed with nominal thicknesses and material densities plus a sensitivity calculation to determine the effects of tolerances, or they may be performed using conservative values for all parameters. If the first approach is used, then tolerances will have an effect on the comparison of measured and calculated dose rates. In the second approach, all calculated values for gamma dose rates should exceed measurements, although the greater uncertainties in neutron dose rate measurements may produce a measurement greater than the calculated value in some instances. Often the differences between calculations and measurements are primarily due to the uncertainties of source calculations.

## 5.3 MEASUREMENT LOCATIONS

The locations at which measurements are made should depend upon the design of the shipping cask. The minimum number of measurement locations should be chosen to describe important parts of the radiation field, plus enough other locations to develop trends or profiles to aid in locating any “hot spots”. An example of a “hot spot” would be the cask side surface adjacent to the stellite balls at the upper end of a BWR fuel channel.

Measurements should be made for at least each of four azimuthal quadrants at the axial mid-plane and nominally  $\pm 1$  m from the mid-plane along the cask side surface and at the cask ends. In addition, measurements should be made at locations of penetrations such as valve ports, vent ports, and streaming paths where cask features such as trunnions penetrate or cutaway the neutron shield. The dose rates at two meters from the cask side (edge of the conveyance for exclusive use) establish the potential exposure to the

public, while the dose rates on the cask surface govern the exposure to radiation workers involved in operations such as loading or cleaning a cask prior to shipment. Cask maintenance would not normally be performed with a loaded cask, and dose rates are normally quite low during maintenance.

Failure to satisfy regulatory dose limits can be caused by weaknesses in the confirmatory measurement program, but only in cases for which the dose rates are higher than expected from calculations. Unexpectedly high dose rates are due to higher than planned source strengths either for the entire fuel assembly or for a portion of a fuel assembly. Potential problems to avoid with the confirmatory measurement include:

- Failure to perform a confirmatory measurement prior to shipment,
- Failure to use properly calibrated detectors (see Section 5.4),
- Failure to properly locate dose points for measurement, and
- Failure to properly operate a detector.

Shipments that contain high burnup fuel assemblies, or that contain unusual “hot spots,” pose the greatest radiological risks. High burnup fuel assemblies are a concern because of the exponential dependence of neutron source on burnup, which becomes important above 40–45 GWd/MTU. Alternatively, a moderate-burnup fuel assembly can exceed planned dose rates if the time of shipping is substantially less than the minimum approved cooling time.

Shipments that contain “hot spots” are also a concern for regulatory compliance. The example of stellite balls at the top end of a BWR assembly channel shipped with an assembly is instructive because it causes a greater risk to radiation workers than to the public. The increased risk is only seen at the cask surface because the highly localized high radiation area becomes geometrically diffused at two meters from the cask package boundary. Nevertheless, the potential exists to exceed regulatory limits at two meters in this case. Another potential concern, which is possible but not as likely, is the shipment of a startup source within a fuel assembly. The high neutron source present in the startup source could overwhelm the neutron shielding effectiveness of a cask in a zone near its axial position in the fuel assembly. A properly calibrated and operated detector measurement can always prevent such a failure to meet regulatory limits. If excessively high dose rates are found, corrective actions can be made to ensure that the radiation sources are less than the certificate limits or that localized “hot spots” are compensated for by the addition of auxiliary shielding. Note that the use of auxiliary shielding is only acceptable if the shielding stays in place during normal conditions of transport and dose rates during hypothetical accident conditions, without the auxiliary shielding, are less than the regulatory limits. In the event of failure of the measurements to verify conformance with the regulatory limits, steps should be outlined similar to those shown in Table 2.

**Table 2 Example non-conformance actions**

Condition	Required action	Completion time
A. Package average surface dose rate limits not met (2 m limits not met for transport)	A.1 Administratively verify correct fuel loading	24 hours
	<b>AND</b> A.2 Perform written evaluations to verify compliance with the ISFSI offsite radiation protection requirements of 10 CFR Part 20 and 10 CFR Part 72 (storage casks only)	48 hours
B. Required action and associated completion time not met	B.1 Remove all fuel assemblies from the package	30 days

## 5.4 MEASUREMENT CALIBRATION

Calibrations are typically performed using National Institute of Standards and Technology (NIST)-traceable gamma sources or neutron sources, so that the actual source intensity at the time of calibration is well known. Quality assurance programs require periodic re-calibrations of detectors to account for instrument drift and to ensure that the batteries, which power survey detectors, are properly charged. The re-calibration procedures specify the frequency of re-calibration and establish goals for the determination of detector efficiency, accuracy, systematic deviations, and uncertainties.

Generally, a failure to perform a measurement correctly, or the use of an improperly calibrated survey instrument, will not be expected to result in an unsafe condition due to conservatism in calculated source values and shielding effectiveness. However, caution should be exercised if neutron doses are a significant portion of the total dose. The effect of an uncalibrated gamma detector may not cause a major effect for gamma rays, because gamma detectors tend to work well or not at all. Due to the strong change in quality factor with neutron energy, proper calibration of neutron detectors to the incident neutron spectrum is important for accurate dose rate measurements. The use of an improperly calibrated neutron detector can cause a measurement error on the order of a factor of ten, especially due to spectral effects.

A more serious potential problem arises if a detector designed solely for use in a well-thermalized neutron field is used for measurements of a spent fuel cask. Even though spent-fuel-shipping casks often include substantial neutron shielding thicknesses at the sides and ends of the casks, these shields are not effective enough to establish a thermal neutron spectrum. The moderately fast spectrum that typically results contains a predominance of neutrons with sufficient energy to pass through the detector without losing enough energy to interact with the boron (or other neutron capture material), which produces the charged particle that would be counted. In such a circumstance, a dose rate of essentially zero could be reported even in the presence of fields approaching or exceeding the regulatory limits. The use of Bonner spheres or a detector efficiency curve vs. average energy is recommended under these circumstances.

## 6 SUMMARY

This report gives recommendations on the information to be included and methods to be incorporated into the preparation of the shielding chapter of an application for approval of a transportation or storage package containing radioactive material. This information is designed to supplement the various regulatory guides and standard review plans available.

Section 2 discusses the level of detail needed to adequately describe the packaging design and the specific features important to shielding evaluations. The format and content of a SARP application are also summarized in the various formatting guides and standard review plans issued by the NRC.

Section 3 describes the methods and codes applicable to source generation for spent fuel and radioactive materials. Details of modeling and data specifics for the characterization of typical spent fuels and radioactive sources are described.

Section 4 describes various computational methods and recommended modeling approaches for the shielding analyses that support the SARP application. Recommendations specific to dose rate estimation are also given along with references to detailed studies.

Section 5 gives background information on the various measurement techniques to quantify both neutron and gamma dose rates. Recommendations are given on the number and location of cask measurements as well as techniques for measurement calibration.



## 7 REFERENCES

1. Code of Federal Regulations, *Title 10, Energy*, Part 71, "Packaging and Transportation of Radioactive Material," 1998.
2. Code of Federal Regulations, *Title 10, Energy*, Part 72, "Licensing Requirements for the Independent Storage of Spent Nuclear Fuel and High-Level Radioactive Waste," 1998.
3. "Standard Format and Content of Part 71, Applications for Approval of Packaging for Radioactive Material," Regulatory Guide 7.9 (Proposed Revision 2), U.S. Nuclear Regulatory Commission, Washington, DC (May 1986).
4. *Standard Review Plan for Dry Cask Storage Systems*, U.S. Nuclear Regulatory Commission, NUREG-1536, February 1996.
5. *Standard Review Plan for Transportation Packages for Radioactive Material*, U.S. Nuclear Regulatory Commission, NUREG-1609, May 1999.
6. *Standard Review Plan for Transportation Packages for Spent Nuclear Fuel*, U.S. Nuclear Regulatory Commission, NUREG-1617, March 2000.
7. *SCALE: A Modular Code System for Performing Standardized Computer Analyses for Licensing Evaluations*, NUREG/CR-0200, Rev. 6 (ORNL/NUREG/CSD-2/R6), Vols. I, II, III, May 2000. Available from Radiation Safety Information Computational Center at Oak Ridge National Laboratory as CCC-545.
8. O. W. Hermann and C. V. Parks, "SAS2H: A Coupled One-Dimensional Depletion and Shielding Analysis Module," Vol. I, Sect. S2 of *SCALE: A Modular Code System for Performing Standardized Computer Analyses for Licensing Evaluations*, NUREG/CR-0200, Rev. 6 (ORNL/NUREG/CSD-2/R6), Vols. I, II, III, May 2000. Available from Radiation Safety Information Computational Center at Oak Ridge National Laboratory as CCC-545.
9. M. J. Bell, *ORIGEN – The ORNL Isotope Generation and Depletion Code*, ORNL-4628, Union Carbide Corporation (Nuclear Division), Oak Ridge National Laboratory, 1973.
10. T. R. England, W. B. Wilson, and M. G. Stamatelatos, *Fission Product Data for Thermal Reactors, Part 2: Users Manual for EPRI-CINDER Code and Data*, EPRI NP-356 Part 2 (LA-6747-MS), Electric Power Research Institute, December 1976.
11. A. G. Croff, *ORIGEN2 – A Revised and Updated Version of the Oak Ridge Isotope Generation and Depletion Code*, ORNL-5621, Union Carbide Corporation (Nuclear Division), Oak Ridge National Laboratory, July 1980.
12. O. W. Hermann and R. M. Westfall, "ORIGEN-S: SCALE System Module to Calculate Fuel Depletion, Actinide Transmutation, Fission Product Buildup and Decay, and Associated Radiation Source Terms," Vol. II, Sect. F7 of *SCALE: A Modular Code System for Performing Standardized Computer Analyses for Licensing Evaluation*, NUREG/CR-0200, Rev. 6 (ORNL/NUREG/CSD-2/R6), Vols. I, II, and III, May 2000. Available from Radiation Safety Information Computational Center at Oak Ridge National Laboratory as CCC-545.

13. S. M. Bowman and L. C. Leal, "ORIGEN-ARP: Automatic Rapid Process for Spent Fuel Depletion, Decay, and Source Term Analysis," Vol. I, Sect. D1 of *SCALE: A Modular Code System for Performing Standardized Computer Analyses for Licensing Evaluation*, NUREG/CR-0200, Rev. 6 (ORNL/NUREG/CSD-2/R6), Vols. I, II, and III, May 2000. Available from Radiation Safety Information Computational Center at Oak Ridge National Laboratory as CCC-545.
14. R. L. Moore, B. G. Schnitzler, C. A. Wemple, R. S. Babcock, and D. E. Wessol, *MOCUP: MCNP-ORIGEN2 Coupled Utility Program*, INEL-95/0523, September 1995.
15. *Characteristics of Potential Repository Wastes*, DOE/RW-0184-R1, Martin Marietta Energy Systems, Inc., Oak Ridge National Laboratory, July 1992.
16. C. J. Taubman and J. H. Lawrence, "WIMSD4 -- Version 100 and Cataloged Procedure," AEEW-M-1832, Atomic Energy Establishment, Winfrith, Dorchester, February 1981.
17. U. Fischer and H. W. Wiese, *Improved and Consistent Determination of the Nuclear Inventory of Spent PWR Fuel on the Basis of Cell-Burnup Methods Using KORIGEN*, KFK-3014 (ORNL/TR-5043), January 1983.
18. R. F. Burstall, *FISPIN A Computer Code for Nuclide Inventory Calculations*, ND-R-328(R), UKAEA/Risley Nuclear Power Development Establishment, Warrington, England, October 1979.
19. J. J. Casal, R. J. J. Stamm'ler, E. A. Villarino, and A. A. Ferri, "HELIOS: Geometric Capabilities of a New Fuel-Assembly Program," *Intl. Topical Meeting on Advances in Mathematics, Computations, and Reactor Physics*, Pittsburgh, Pennsylvania, April 28–May 2, 1991, Vol. 2, 1991.
20. M. D. DeHart, "SAS2D – A Two-Dimensional Depletion Sequence for Characterization of Spent Nuclear Fuel," 35583.pdf in *Proc. of 2001 ANS Embedded Topical Meeting on Practical Implementation of Nuclear Criticality Safety*, November 11–15, 2001, Reno, NV [ANS Order No.: 700284; ISBN: 0-89448-659-4].
21. J. C. Wagner, M. D. DeHart, and B. L. Broadhead, *Investigation of Burnup Credit Modeling Issues Associated with BWR Fuel*, ORNL/TM-1999/193, UT-Battelle, LLC, Oak Ridge National Laboratory, October 2000.
22. L. B. Shappert (ed.), *The Radioactive Materials Packaging Handbook*, ORNL/M-5003, Oak Ridge National Laboratory, Oak Ridge, Tennessee (1998).
23. A. G. Croff, M. A. Bjerke, G. W. Morrison, and L. M. Petrie, *Revised Uranium-Plutonium Cycle PWR and BWR Models for the ORIGEN Computer Code*, ORNL/TM-6051, Union Carbide Corporation (Nuclear Division), Oak Ridge National Laboratory (1978).
24. "Characteristics of Spent Fuel, High Level Waste, and Other Radioactive Wastes Which Require Long-Term Isolation," DOE/RW-0184, Office of Civilian Radioactive Waste Management, Washington, DC (1987).
25. A. Luksic, "Spent Fuel Assembly Hardware: Characterization and 10 CFR 61 Classification for Waste Disposal," PNL-6906, Vol. 1, Pacific Northwest Laboratory, Richland, Washington (1989).
26. O. W. Hermann, S. M. Bowman, M. C. Brady, and C. V. Parks, *Validation of the SCALE System for PWR Spent Fuel Isotopic Composition Analyses*, ORNL/TM-12667, Martin Marietta Energy Systems, Inc., Oak Ridge National Laboratory, March 1995.

27. R. Kinsey, comp., *ENDF/B Summary Documentation*, BNL-NCS-17541 (ENDF-201), 3<sup>rd</sup>. Ed., Brookhaven National Laboratory (ENDF/B-V) (1979).
28. R. Kinsey, comp., *ENDF/B Summary Documentation*, BNL-NCS-17541 (ENDF-201), 2<sup>nd</sup>. Ed., Brookhaven National Laboratory (ENDF/B-IV) (1973).
29. V. McLane, comp., *ENDF/B Summary Documentation*, BNL-NCS-17541 (ENDF-201), 4<sup>th</sup>. Ed., Brookhaven National Laboratory (ENDF/B-VI) (1996).
30. S. B. Ludwig and J. P. Renier, "Standard- and Extended Burnup PWR and BWR Reactor Models for the ORIGEN2 Computer Code," ORNL/TM-11018, Martin Marietta Energy Systems, Inc., Oak Ridge National Laboratory, December 1989.
31. W. C. Jordan and S. M. Bowman, "SCALE Cross-Section Libraries," Vol. III, Sect. M4 of *SCALE: A Modular Code System for Performing Standardized Computer Analyses for Licensing Evaluations*, NUREG/CR-0200, Rev. 6 (ORNL/NUREG/CSD-2/R6), Vols. I, II, and III, May 2000. Available from Radiation Safety Information Computational Center at Oak Ridge National Laboratory as CCC-545.
32. M. D. DeHart and O. W. Hermann, *An Extension of the Validation of SCALE (SAS2H) Isotopic Prediction for PWR Spent Fuel*, ORNL/TM-13317, Lockheed Martin Energy Research Corp., Oak Ridge National Laboratory, September 1996.
33. C. E. Sanders and I. C. Gauld, *Isotopic Analysis of High-Burnup PWR Spent Fuel Samples From the Takahama-3 Reactor*, NUREG/CR-6798 (ORNL/TM-2001/259), U.S. Nuclear Regulatory Commission, Oak Ridge National Laboratory, January 2003.
34. I. C. Gauld and C. V. Parks, *Review of Technical Issues Related to Predicting Isotopic Composition of Source Terms for High-Burnup LWR Fuel*, NUREG/CR-6701 (ORNL/TM-2000/277), U.S. Nuclear Regulatory Commission, Oak Ridge National Laboratory, January 2001.
35. J. F. Briesmeister (ed.), "MCNP – A General Monte Carlo Code for Neutron and Photon Transport," LA-7396-M, Rev. 2, Los Alamos National Laboratory (1986).
36. W. B. Wilson et al., "Sources-4A: Code System For Calculating ( $\alpha$ ,n), Spontaneous Fission, and Delayed Neutron Sources and Spectra," LA-13639, Los Alamos National Laboratory (September 1999).
37. R. L. Engle, J. Greenberg, and M. M. Hendrickson, *ISOSHLD – A Computer Code for General Purpose Isotope Shielding Analysis*, BNWL-236, Brookhaven National Laboratory (June 1966) and Supplement (March 1967).
38. *QAD-CGGP: A Combinatorial Geometry Version of QAD-P5A, A Point Kernel Code System for Neutron and Gamma-Ray Shielding Calculations Using the GP Buildup Factor*. Updated version available from Radiation Safety Information Computational Center as CCC-645/QAD-CGGP-A.
39. G. I. Bell and S. Glasstone, *Nuclear Reactor Theory*, Van Nostrand Reinhold, New York, 1970.
40. J. A. Bucholz, "XSDOSE: A Module for Calculating Fluxes and Dose Rates at Points Outside a Shield," Vol. II, Sect. F4 of *SCALE: A Modular Code System for Performing Standardized Computer Analyses for Licensing Evaluations*, NUREG/CR-0200, Rev. 6 (ORNL/NUREG/CSD-2/R6), Vols. I,

- II, and III, May 2000. Available from Radiation Safety Information Computational Center at Oak Ridge National Laboratory as CCC-545.
41. DOORS3.2: One-, Two- and Three-Dimensional Discrete Ordinates Neutron/Photon Transport Code System is a collection of computer codes packaged in RSICC as CCC-650.
  42. J. C. Wagner and A. Haghghat, "Automated Variance Reduction of Monte Carlo Shielding Calculations Using the Discrete Ordinates Adjoint Function," *Nucl. Sci. Eng.*, **128**, 186-208 (1998).
  43. J. S. Tang, C. V. Parks, and O. W. Hermann, "Automated Shielding Analysis Sequences for Spent Fuel Casks," Vol. 2, pp. 549-558 in *Proc. of Theory and Practices in Radiation Protection and Shielding*, April 22-24, 1987, Knoxville, Tennessee, 1987.
  44. B. L. Broadhead, J. S. Tang, R. L. Childs, C. V. Parks, and H. Taniuchi, *Evaluation of Shielding Analysis Methods in Spent Fuel Cask Environments*, EPRI TR-104329, Electric Power Research Institute, May 1995.
  45. R. E. Alcouffe, R. S. Baker, F. W. Brinkley, D. R. Marr, R. D. O'Dell, and W. F. Walters, *DANTSYS: A Diffusion Accelerated Neutral Particle Transport Code System*, LA-12969-M (June 1995).
  46. J. S. Tang and M. B. Emmett, "SAS4: A Monte Carlo Cask Shielding Analysis Module Using An Automated Baising Procedure, Vol. I, Sect. S4 of *SCALE: A Modular Code System for Performing Standardized Computer Analyses for Licensing Evaluations*, NUREG/CR-0200, Rev. 6 (ORNL/NUREG/CSD-2/R6), Vols. I, II, III, May 2000. Available from Radiation Safety Information Computational Center at Oak Ridge National Laboratory as CCC-545.
  47. J. L. Kloosterman, "MARMER, A Flexible Point-Kernel Shielding Code, User's Manual," IRI-131-89-03/2 (June 1990).
  48. H. F. Locke, *Summary of the Results of the Comparison of Calculations and Measurements for the TN 12 Flask Carried Out Under the NEACRP Intercomparison of Shielding Codes*, NEACRP-L-339, Nuclear Energy Agency, Paris, France, 1992.
  49. American National Standard, "Neutron and Gamma-Ray Flux-to-Dose-Rate Factors," ANSI/ANS-6.1.1-1977, American Nuclear Society, LaGrange Park, IL, 1977. (See also "Protection Against Neutron Radiation," NCRP-38, National Council on Radiation Protection and Measurements, Washington, D.C. (1971).)
  50. American National Standard, "Neutron and Gamma-Ray Fluence-to-Dose Factors," ANSI/ANS 6.1.1 1991, American Nuclear Society, LaGrange Park, IL, 1991. (See also "Data for Use in Protection Against External Radiation," ICRP-51, Pergamon Press, Oxford, U.K. (1987).)
  51. C. M. Lampley, M. C. Andrews and M. B. Wells, "The SKYSHINE-III Procedure: Calculation of the Effects of Structure Design on Neutron, Primary Gamma-Ray and Secondary Gamma-Ray Dose Rates in Air," RRA-T8209A (June 1982, revised September 1988).
  52. N. E. Hertel, D. G. Napolitano, and M. W. Granus, "Benchmarking and Application of SKYSHINE-III on Dry Storage Casks," in *Proceedings of ANS Radiation Protection and Shielding Division Topical*, April 19-23, 1998, Nashville, Tennessee.
  53. *Nuclear Radiation Detection*, William J. Price, McGraw-Hill Book Company, 1964.

54. B. L. Broadhead, *K-Infinite Trends with Burnup, Enrichment, and Cooling Time for BWR Fuel Assemblies*, ORNL/M-6155, Lockheed Martin Energy Research Corp., Oak Ridge National Laboratory, August 1998.
55. O. W. Hermann and M. D. DeHart, *Validation of SCALE (SAS2H) Isotopic Predictions for BWR Spent Fuel*, ORNL/TM-13315, Lockheed Martin Energy Research Corp., Oak Ridge National Laboratory, September 1998.
56. B. L. Broadhead, M. D. DeHart, J. C. Ryman, J. S. Tang, and C. V. Parks, *Investigation of Nuclide Importance to Functional Requirements Related to Transport and Long-Term Storage of LWR Spent Fuel*, ORNL/TM-12742, Lockheed Martin Energy Research Corp., Oak Ridge National Laboratory, June 1995.
57. J. C. Wagner, *Computational Benchmark for Estimation of Reactivity Margin from Fission Products and Minor Actinides in PWR Burnup Credit*, NUREG/CR-6747 (ORNL/TM-2000/306), U.S. Nuclear Regulatory Commission, Oak Ridge National Laboratory, September 2001.



**APPENDIX A**  
**DETAILS OF SAS2H MODELS**



# APPENDIX A

## DETAILS OF SAS2H MODELS

The SAS2H module of the SCALE system<sup>8</sup> is designed to allow for simple, but effective models for predicting the depletion/decay and source terms for spent fuel from LWR nuclear reactors. The simple models have one-dimensional (1-D) geometry and use 1-D radiation transport theory, but capture the essential elements of LWR fuel assembly geometry. Depletion and decay calculations are performed using the ORIGEN-S code, which is based on the point depletion method using matrix exponential solution techniques. Under the point depletion method, the nuclear reaction cross sections for a large number of isotopes (typically about 1600 for most ORIGEN libraries) are averaged over space and energy for a fuel assembly. These effective one-energy-group, one-spatial-point cross sections are then used along with a specific fuel loading and power history to predict the isotopic inventory over time and the source term characteristics after shutdown of the reactor.

The neutron transport analysis of the reactor fuel assembly is basically a two-part procedure in which two separate lattice-cell calculations are performed; one of which corresponds to an array of like pins, followed by a full assembly model. These transport calculations determine the neutron spectrum for the full assembly and, subsequently, the effective cross sections for the depletion analysis. At specified times during the irradiation, the cross sections are updated using resonance processing codes and 1-D transport analysis. These updated cross sections are then used in a depletion analysis to produce the time-dependent fuel composition to be used for the next cross-section update. This sequence is repeated over the operating history of the reactor. This procedure is shown graphically in Figure A.1 for a typical three-cycle case.

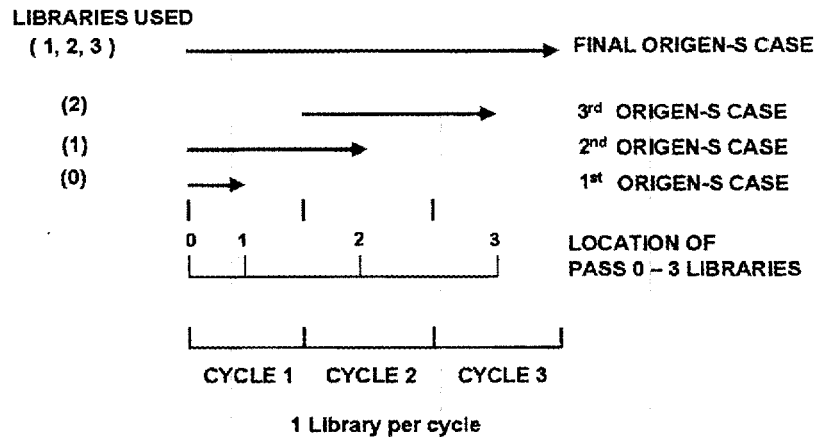


**Figure A.1** Graphical representation of SAS2H procedure for generating burnup-dependent cross-section libraries for the ORIGEN-S code

For a three-cycle case as shown, a total of four burnup-dependent cross-section sets are produced by SAS2H. These libraries correspond to fresh fuel, then the midpoint for each cycle. Once the required libraries are produced, a final ORIGEN-S case is executed using each of the burnup-dependent libraries. The isotopic concentrations and ending source terms are determined from this final ORIGEN-S calculation. The SAS2H code follows the flow shown in Figure A.2 for each library generation step. The sources generated by the final ORIGEN-S case are saved at the end-of-irradiation time and at the end of the final decay period specified in the user input.

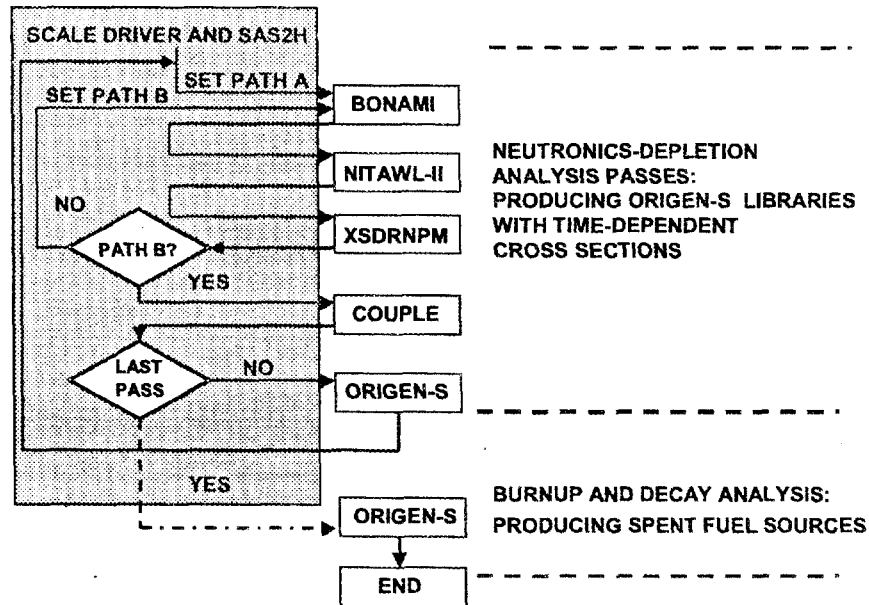


Figure A.2 Flow chart for SAS2H procedures

The five codes shown are executed in the order shown at each of the library generation steps. Each of these codes and their purpose is summarized below (references are given to sections in the SCALE manual<sup>7</sup> that describe the codes in detail).

BONAMI applies the Bondarenko method of resonance self-shielding for nuclides that have Bondarenko data included with their cross sections. BONAMI is described in Section F1, and the Bondarenko methods and applicability are discussed in Sections M7.2 and M7.A of Ref. 7.

NITAWL-II performs the Nordheim resonance self-shielding corrections for nuclides that have resonance parameters included with their cross sections. NITAWL-II is described in Section F2, and the Nordheim Integral Treatment is also discussed in Sections M7.2 and M7.A of Ref. 7.

XSDRNPM performs a 1-D discrete-ordinates transport calculation based on various specified geometries requested in the data supplied for SAS2H. The code, as applied by SAS2H, has the primary function to produce cell-weighted cross sections for fuel depletion calculations; XSDRNPM is described in Section F3. Also, the automatic quadrature generator, the unit-cell mesh generator, and convergence criteria applied by the code are presented in Section M7.2.5 of Ref. 7.

COUPLE updates the cross-section constants included on an ORIGEN-S nuclear data library with data from the cell-weighted cross-section library produced by XSDRNPM. Also, the weighting spectrum computed by XSDRNPM is applied to update all nuclides in the ORIGEN-S library that were not specified in the XSDRNPM analysis. COUPLE is described in Section F6 of Ref. 7.

ORIGEN-S performs both nuclide generation and depletion calculations for the specified reactor fuel history. Also, the code computes the neutron and gamma sources generated by the fuel assembly. ORIGEN-S is described in Section F7 of Ref. 7.

Each of these codes are executed twice for each library generation step, once for a Path A model and once for a Path B model. The Path A model is a simple pin-cell corresponding to an assembly lattice structure (see Figure A.3).

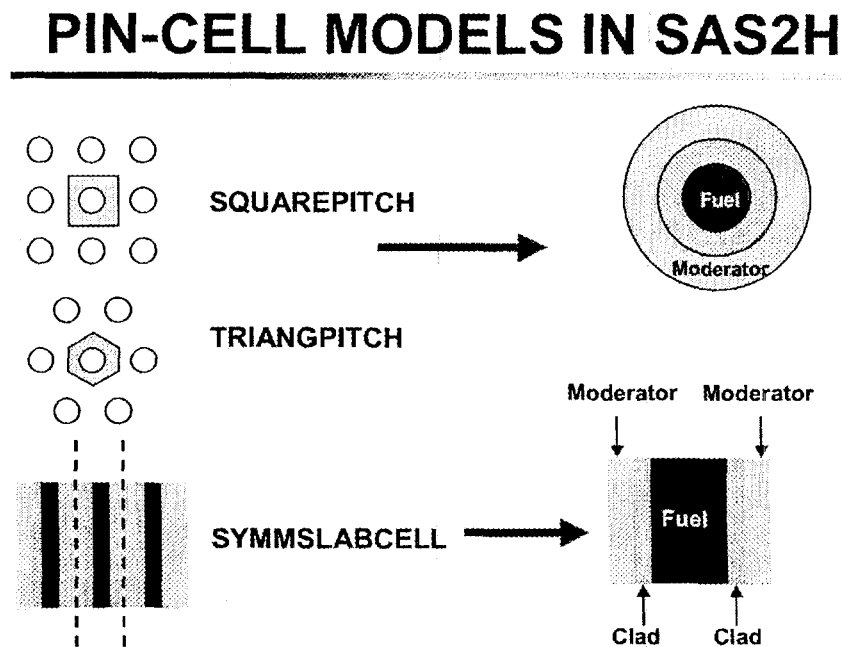
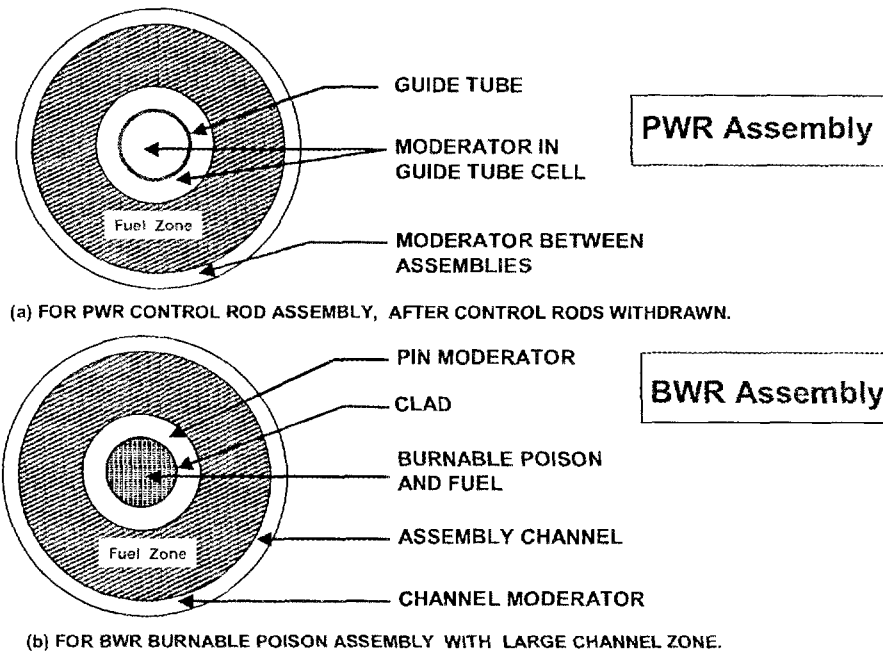


Figure A.3 Pin-cell model for representing the repeating lattice structure of a typical fuel assembly

These simple 1-D cylindrical models (for square and triangular pitched pins) and slab models (for plate-type fuel) along with reflected or white boundary conditions allow for the cell-averaged cross sections corresponding to the regular lattice portions of the fuel assembly to be quantified. In a second 1-D calculation, the Path B model is then executed to determine the average assembly spectrum and thus obtain spatial and energy-averaged cross sections for the entire fuel assembly. Typical Path B models for PWR and BWR fuel assemblies are shown in Figure A.4.



**Figure A.4 Typical Path B models for PWR and BWR fuel, assuming cell-weighted cross-section material in the regions labeled “Fuel Zone”**

This Path B model is designed to approximate the non-regular portions of the assembly lattice structure, i.e., the PWR fuel assembly model represents a portion of the assembly as surrounding a central water hole/guide tube arrangement. In order to conserve the moderator-to-fuel ratios, the amount of fuel and between-assembly-moderator that surrounds the central water hole is scaled by one over the total number of water holes in the full assembly.

The Path B model for a typical BWR assembly is similar; however, the central region consists of a typical gadolinium fuel rod, clad and moderator, surrounded by a fraction of the remainder of the full assembly. Again this fraction is determined by the ratio of one over the actual number of gadolinium rods in the full assembly. For a BWR assembly, this fraction is carried over to the fuel zone, assembly channel, and channel moderator regions as shown in Figure A.4. The use of variable enrichments (pin splits) radially across a BWR fuel assembly requires an additional modeling approximation. The standard technique is the averaging of the enrichments over all pins in the fuel assembly. Validation results confirmed the viability of this approach.<sup>55</sup> The moderator in a BWR application typically has variable densities inside the channel, with a near constant density outside the assembly channel. These radial density effects can be modeled using these prescriptions, although the axial density variations must be averaged for a single execution of SAS2H. The most appropriate method for averaging the axial moderator density is to weight the densities by the axial power or burnup profiles. An example of such a calculation is shown in Table A.1. These data were taken from an ORNL internal report,<sup>54</sup> but such data should be readily available from BWR utilities

Table A.1 BWR moderator density versus burnup<sup>a</sup>

Burnup (GWd/MTU)	Moderator density (g/cm <sup>3</sup> )
7.478	0.754
26.2	0.749
34.113	0.732
37.818	0.699
39.287	0.655
39.88	0.608
39.093	0.562
40.453	0.52
41.559	0.482
41.569	0.449
41.372	0.419
41.027	0.393
40.592	0.37
40.071	0.35
39.425	0.332
38.563	0.316
37.199	0.302
35.792	0.289
34.0	0.277
31.05	0.267
27.376	0.258
22.546	0.25
9.904	0.246
5.632	0.243

<sup>a</sup>Average moderator density from weighted burnup data is 0.444 g/cm<sup>3</sup>, all axial segments in the table have equal heights

Many modern BWR and PWR fuel assemblies contain axial reflector regions with natural uranium instead of enriched uranium fuel. These axial regions are typically of little consequence to a shielding analysis, since the source terms are proportional to the burnups, which are much smaller than those from the enriched regions. This can be seen in Table A.1 where the first (bottom of assembly) and last two segments (top of the assembly) correspond to natural uranium reflectors. The burnups are seen to be at least a factor of two smaller than those of the remaining regions.

The most widely used models for SAS2H currently correspond to PWR and BWR assemblies. Many other assembly types can be easily treated as well. The general rules are to construct the repeated portion of the assembly (currently SQUAREPITCH rods, TRIANGPITCH rods, and SYMMSLABCELL for plates are supported) using the Path A modeling, followed by a Path B assembly model which treats the heterogeneous portions of the geometry while conserving the moderator-to-fuel ratios for the full assembly. Keep in mind the following rules when constructing models for new assembly types:

1. Except for BWR fuel assembly models, do not begin the Path B model with fuel (mixture 500) in the first zone. It is necessary to place a small void pinhole in zone 1 if the first zone normally contains fuel. This is because the code expects fuel to be in zone 1 for a BWR model only.
2. Fuel assemblies can only contain one type of fuel, thus ensure all occurrences of fuel are identical.
3. Enter the quantities of non-fuel assembly hardware into the light element array. The code attempts to determine the quantity of cladding, but can fail depending on the method used to describe the cladding materials (e.g., Zirc2 or Zirc4 specifications for Zircaloy-2 and Zircaloy-4 will not work since the code can not determine the loading for each individual isotope in the mixture).
4. For non-PWR or BWR fuels it is recommended to include *all* the isotopes in the cross section library as trace quantities in the fuel (see Section M4 of the SCALE manual for lists of isotopes for each cross section library). This ensures that all isotopes are updated to the spectrum of the new assembly type. This has already been automatically performed for LWR fuel assemblies.

**APPENDIX B**

**NUCLIDE IMPORTANCE AND PARAMETER  
SENSITIVITY STUDY FOR PWR/BWR  
SOURCE TERM GENERATION**



## APPENDIX B

# NUCLIDE IMPORTANCE AND PARAMETER SENSITIVITY STUDY FOR PWR/BWR SOURCE TERM GENERATION

The determination of which nuclides are most important to the individual neutron and gamma-ray sources is difficult because their concentrations vary drastically over time. Indeed the most important nuclides for gamma rays at 6 months of cooling time are most likely decayed away at 10 years of cooling time. Thus, it is necessary to select a range of cooling times in order to determine the nuclide importance. Once the most important nuclides are known, it is possible to formulate the parameter sensitivities to the concentrations of those particular isotopes.

A previous study<sup>56</sup> analyzed the nuclide importance to neutron and gamma dose responses over decay times from 2 to 10,000 years. Three cask types selected for study included carbon steel/resin (27/13 cm shield thickness), lead/resin (13/13 cm shield thickness), and concrete shields (50 cm shield thickness). The study also selected sources corresponding to two different burnups, 20 and 50 GWd/MTU. Figure B.1 is taken from that study and indicates the relative contributions of neutron, primary gamma, and secondary gamma doses to the total dose rate on the carbon steel cask surface.

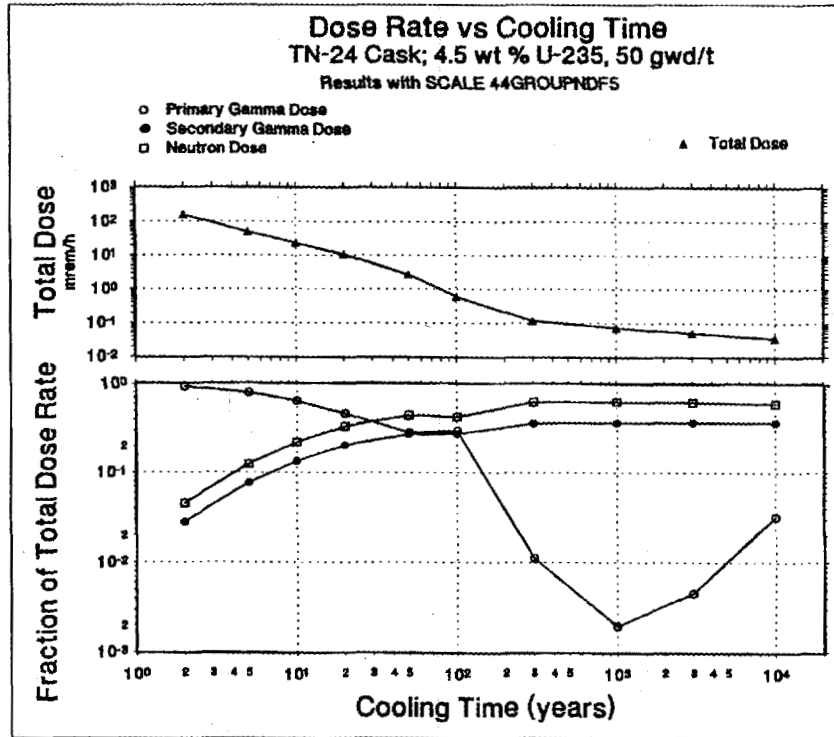


Figure B.1 Dose rate versus cooling time for carbon steel/resin cask, including fractional contribution due to primary gamma, neutrons, and secondary gamma particles

Cooling times of 5 to 20 years are typical for spent fuel transport issues. Over this range of cooling times, the primary gamma contribution dominates the total dose. However, at 50 GWd/MTU burnup, the neutron dose contribution equals the primary gamma contribution at about a 30-year cooling time for a carbon-steel cask. For the simple casks analyzed in the study, this cross over of importance from primary gamma to neutron contributions occurs at 20 years and 200 years, respectively for the lead/resin and concrete casks. The secondary gamma contribution to the total dose ranges from a factor of 2 to 10 lower than the neutron dose contribution, except for the concrete cask where they are about equal.

In order to understand the important isotopic contributors to the total dose, it is necessary to study each dose component separately. For the first 100 years of cooling time, the neutron dose is almost entirely due to the decay of <sup>244</sup>Cm as seen in Figure B.2. Only for decay times less than 2 years (by extrapolation of the data shown in the plot) does <sup>242</sup>Cm become important relative to <sup>244</sup>Cm. A plot for the secondary gamma contribution is not shown since it has the same features as Figure B.2. The secondary gamma particles arise from neutron capture; thus the general trends in their importance are virtually identical to those of the neutrons.

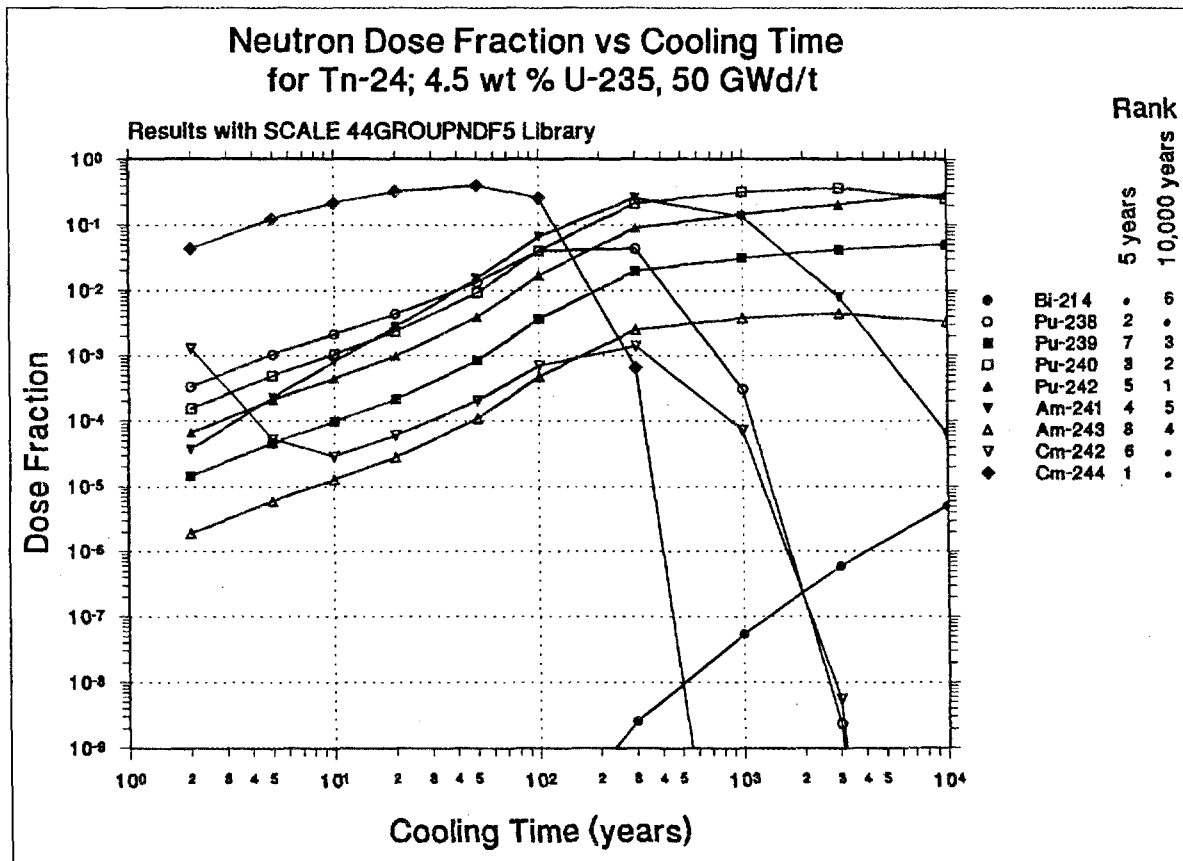


Figure B.2 Fractional contribution to the total dose due to neutrons from decay of actinides for carbon steel/resin cask for 50 GWd/MTU burnup source

The importance of fission product and activation isotopes with respect to the primary gamma doses is shown in Figure B.3. Clearly the range of cooling times plays an important part in the ranking of important contributors to the primary gamma doses (although only contributions to the primary gamma dose are shown, the dose fraction plotted is based on the total dose). At two years of cooling time the primary isotopes are <sup>144</sup>Pr, <sup>60</sup>Co, <sup>134</sup>Cs, and <sup>106</sup>Rh. For a cooling time of 10 years, <sup>60</sup>Co and <sup>154</sup>Eu are the dominant contributors. For 20 years cooling and beyond <sup>137</sup>Cs becomes an important contributor to the primary gamma dose. Thus, over the range of cooling times from 5–20 years the primary contributors to the primary gamma dose are <sup>144</sup>Pr, <sup>134</sup>Cs, <sup>60</sup>Co, <sup>137</sup>Cs, and <sup>154</sup>Eu.

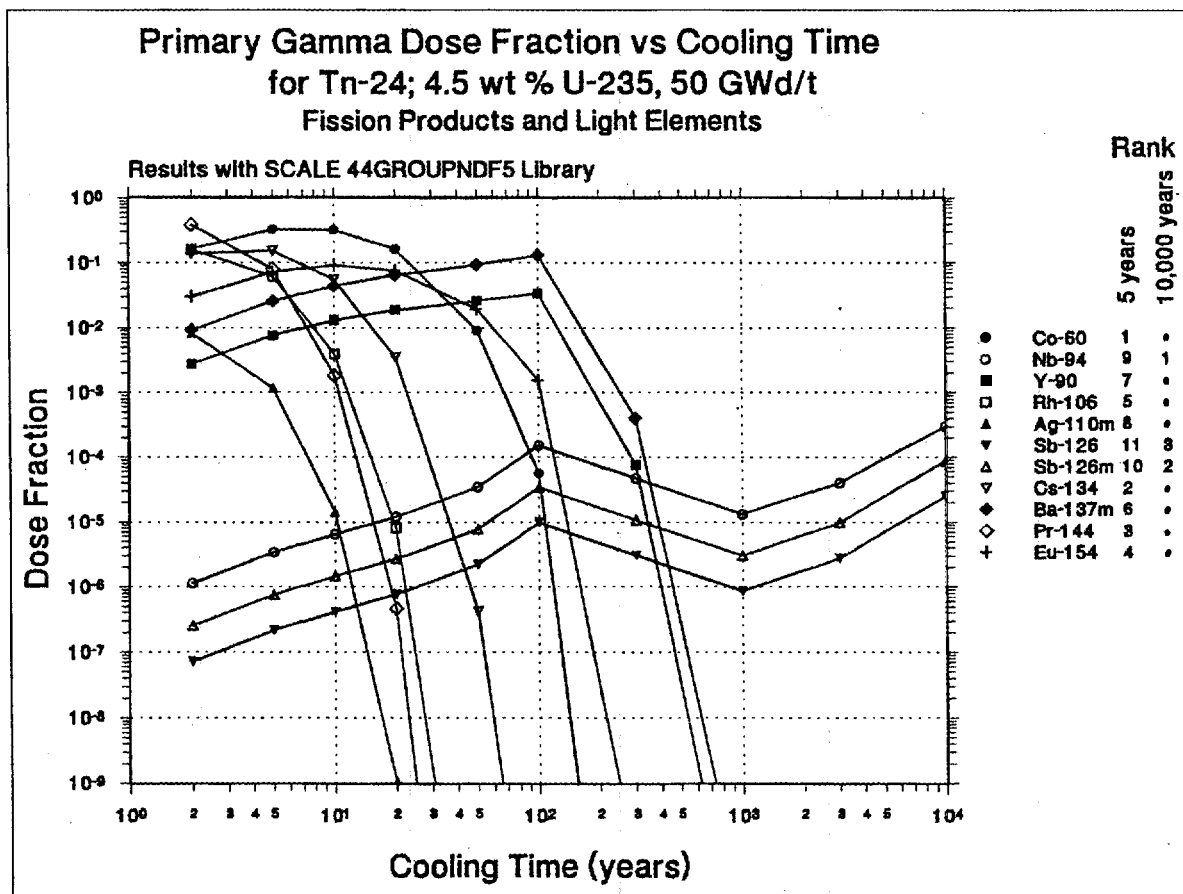


Figure B.3 Fractional contribution to the total dose due to primary gammas from decay of fission products and activation products for carbon steel/resin cask for 50 GWd/MTU burnup source

The remainder of this appendix presents the results of a series of calculations designed to determine the most important input parameters with respect to both the neutron and gamma-ray source generation for spent fuel applications. The isotopes selected are those determined above to be the most important contributors to the neutron and primary gamma dose contributions. The model for these calculations corresponds to a  $17 \times 17$  PWR fuel assembly; however, the parameter variations are large enough to incorporate typical BWR models as well. These models correspond to the SAS2H code with variations in the following input parameters: specific power, enrichment, fuel density, fuel temperature, moderator temperature, moderator density, and boron loading. The ranges of the parameter variations and the reference parameters are given in Table B.1. The broadness of these ranges is not physical, but the specific values were chosen such that the typical values should be in the middle of these ranges.

**Table B.1 Parameter ranges of variation**

Parameter	Range of values (Reference value <sup>a</sup> )
Specific power	10–50 (37.9) GWd/MTU
Enrichment	2.0 – 4.0 <sup>b</sup> (3.2) wt %
Fuel density	9.00 – 10.75 (9.88) g/cm <sup>3</sup>
Fuel temperature	500 – 1300 (811) K
Moderator density	0.2 – 1.0 (0.733) g/cm <sup>3</sup>
Boron loadings	0.0 – 1100 (550) ppm

<sup>a</sup> Reference burnup was 33 GWd/MTU, 880 days uptime, 5-years cooling time

<sup>b</sup> Enrichments of up to 5 wt % are now typical.

For each SAS2H calculation for the parameter variations shown in Table B.1, the relative masses of the six important isotopes (also including <sup>90</sup>Sr) were tabulated and plotted. Shown in Figures B.4 – B.7 are the variations in the concentrations of each of the six isotopes for the four most important parameter variations from Table B.1; specific power, enrichment, fuel density, and moderator density. The masses are presented as ratios to the isotopic mass corresponding to the smallest parameter value.

The significant effect of the specific power parameter on the concentration of <sup>144</sup>Pr is shown in Figure B.4. The specific power parameter has little effect on the remaining isotopes. This effect arises from the short half-life of the parent, <sup>144</sup>Ce (284 days). This half-life is short compared to the full irradiation time (880 days), thus the ending concentration is primarily the equilibrium concentration arising from the power levels near the assembly end-of-life.

The sensitivity of the various isotopes to the enrichment and fuel density variations is shown in Figures B.5 and B.6. It is obvious from these plots that these effects are related, since the orderings of the isotopes are the same, only the magnitudes are different. This effect can be explained by the increase in the thermal flux that accompanies the removal of fissile material at constant burnup. The enhanced thermal flux causes increased production for those isotopes that result primarily from activation, <sup>244</sup>Cm, <sup>60</sup>Co, and <sup>134</sup>Cs. The effect is more pronounced for <sup>244</sup>Cm since it is the result of several captures.

The results for the moderator density effect seen in Figure B.7 are perhaps the most interesting due to the rapid variations seen. The decrease in concentration seen for  $^{244}\text{Cm}$  and  $^{154}\text{Eu}$  at higher moderator densities is due to the presence of capture resonances in the vicinity of 1 eV. For these low-lying capture resonances a softer spectrum due to increased moderation can decrease the amount of activation. The scenario with  $^{60}\text{Co}$  is similar in that there is a resonance at about 100 eV in  $^{59}\text{Co}$ ; however, there is also a strong  $1/v$  tail, which increases the thermal capture to the point that the curve turns over around a moderator density of 0.6 g/cc.

The complete set of sensitivity results is shown in Table B.2. In each case, the value given in the table is the power coefficient,  $p_i$ , which relates the source,  $S$ , to each parameter,  $x_i$ , by the equation:

$$S \propto \prod_i x_i^{p_i} .$$

These coefficients are generated as power fits to the curves shown in Figures B4–B7. They are also useful for converting sources that use a given parameter value to the expected source using a modified parameter value; e.g., the neutron source at a moderator density of 0.4 can be scaled up to a moderator density of 0.6 via the formula  $(0.6/0.4)^{-0.44}$ . This scaling assumes the neutron source is entirely due to  $^{244}\text{Cm}$ . These coefficients are based on fits to the endpoints of the curves shown in Figures B4–B7, therefore caution on their use is recommended where inflection points are present in the data. In addition, for gamma rays multiple isotopes contribute to the gamma source, therefore scaling must be performed on each isotope and its effect on the total source and spectrum estimated.

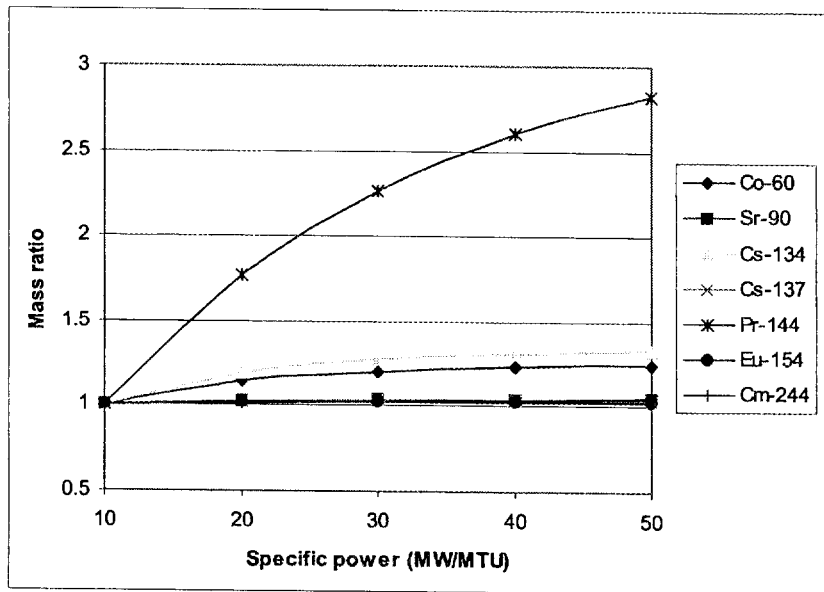


Figure B.4 Variation of key isotopes with specific power at fixed burnup

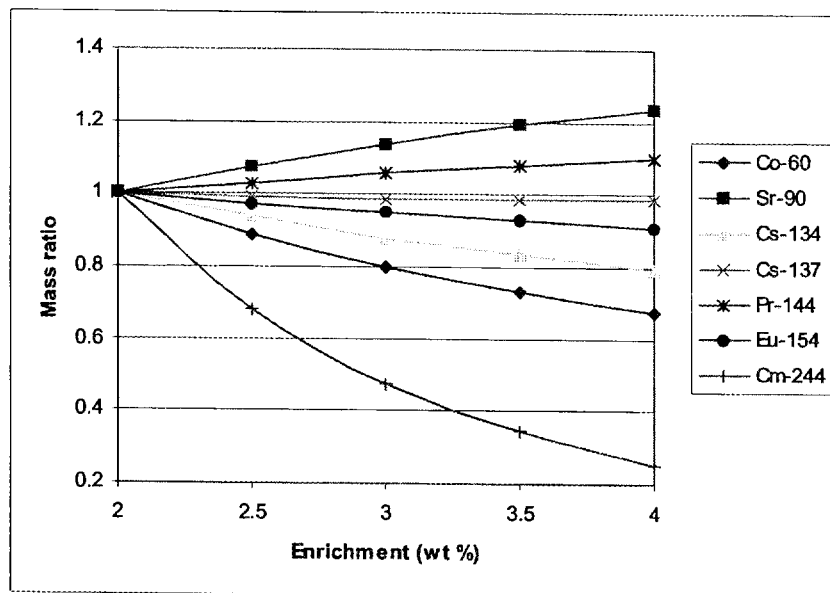


Figure B.5 Variation of key isotopes with enrichment at fixed burnup

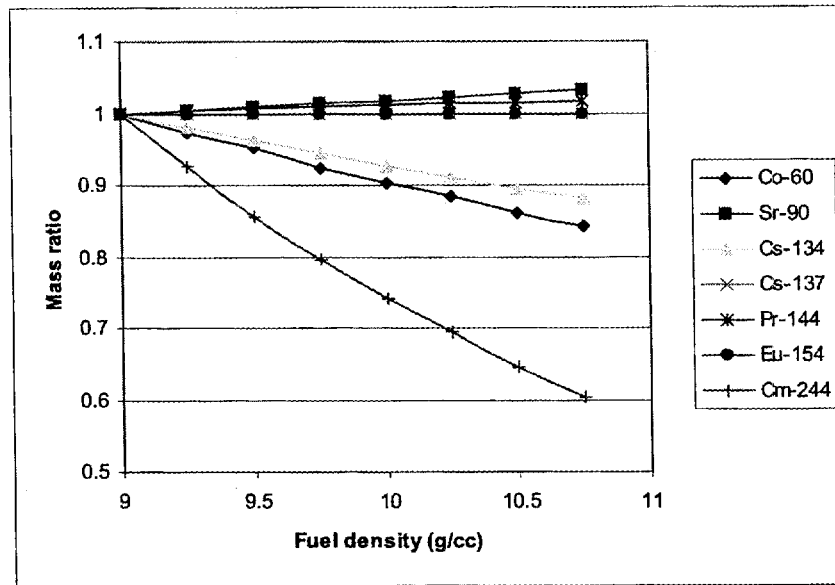


Figure B.6 Variation of key isotopes with fuel density at fixed burnup

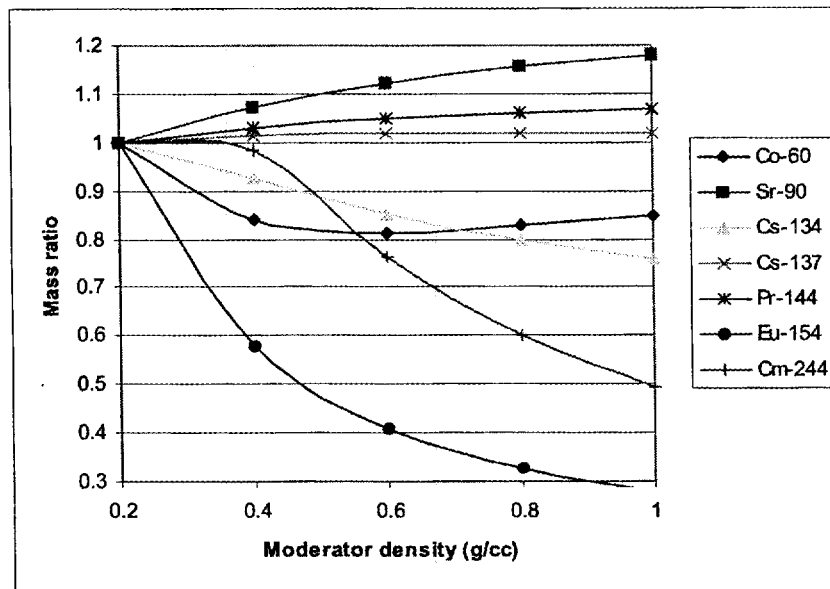


Figure B.7 Variation of key isotopes with moderator density at fixed burnup

**Table B.2 Power coefficients,  $p_b$  for parameter variations,  $x_i$  (see text)**

Parameter	Co-60	Sr-90	Cs-134	Cs-137	Pr-144	Eu-154	Cm-244
Specific power	0.14	0.03	0.18	0.03	0.65	0.02	0.03
Enrichment	-0.57	0.30	-0.33	-0.02	0.14	-0.14	-1.98
Moderator temp	-0.09	-0.03	-0.01	0.00	-0.01	-0.04	0.36
Fuel density	-0.96	0.18	-0.71	-0.01	0.10	-0.01	-2.83
Fuel temp	-0.03	-0.01	-0.04	0.00	0.01	0.01	-0.01
Moderator density	-0.10	0.10	-0.17	0.01	0.04	-0.79	-0.44
Boron loading	-0.01	-0.01	0.02	0.00	0.00	0.05	0.07

**APPENDIX C**  
**EXAMPLE OF CALCULATIONAL MODELS**  
**AND RESULTS**



# APPENDIX C

## EXAMPLE OF CALCULATIONAL MODELS AND RESULTS

This appendix gives an illustrative example of the information needed for submittal in the shielding chapter of a safety analysis report for packaging (SARP). The example presented is fictitious in nature and combines the information contained in several actual submittals along with an artificial model. The cask is designated Generic Burnup Credit cask with 32 elements (GBC-32) and was generated for use in burnup-credit criticality studies.<sup>57</sup> The cask shield body was modified from a single steel component to have the attributes of a realistic storage or transportation cask.

### C.1 DESCRIPTION OF THE SHIELDING DESIGN (EXAMPLE)

An evaluation of the shielding performance of the GBC-32 is performed to demonstrate compliance with the dose rate limits of 10CFR71.47 for normal conditions and 10CFR71.51(a)(2) for accident conditions. A detailed description of the packaging is normally provided in Chapter 1.0 of the SARP.

The shielding design feature of the GBC-32 cask is the cask body consisting of an inner shell of stainless steel surrounded by an outer shell of resin. The lid and the bottom of the cask provide shielding in the axial direction. The impact limiters, which consist of wood in stainless steel cases, were ignored for conservatism in the shielding analysis (only the location of the outer surface of the cask considers the impact limiter). The stainless steel basket liners were included in the model; however, the boral panels were conservatively omitted from the shielding analysis.

#### C.1.1 Discussion and Results

The spent fuel source terms used in this document were generated using the SCALE SAS2H<sup>8</sup> module for a typical Westinghouse  $17 \times 17$  fuel assembly. The cross-section library utilized in the source generation was the 44GROUPNDF5 neutron library,<sup>31</sup> which is based on ENDF/B-V with selected nuclides from ENDF/B-VI. The shielding calculations were performed with the SAS4 module,<sup>46</sup> which utilizes the MORSE-SGC/S three-dimensional (3-D) Monte Carlo code. The cross sections used in the shielding portion of this work was the 27N-18COUPLE library<sup>31</sup> which is a coupled 27-neutron and 18-gamma group library based on ENDF/B-IV data. The flux-to-dose conversion factors were based on the ANSI/ANS-6.1.1 (1977) standard.<sup>49</sup>

The dose rates calculated with SAS4 are summarized in Table C.1. The limiting surface dose rates on the cask top and bottom are 0.44 mSv/h (44 mrem/h) which are about a factor of 5 below the regulatory limit of 2 mSv/h (200 mrem/h). The limiting dose rates at the 2 m location are 0.082 mSv/h (8.2 mrem/h), also along the cask top and bottom. These dose rates are near the regulatory limits of 0.10 mSv/h (10 mrem/h); however, the impact limiter material was omitted from the analysis and the bounding axial-burnup profile was used in the analysis. The Monte Carlo statistics for these results are generally within 5%.

The accident analysis assumed both the impact limiter and resin neutron shields were removed. The limiting dose rate for the hypothetical accident is 2.93 mSv/h (293 mrem/h), about a factor of 3 below the regulatory limit of 10 mSv/h (1000 mrem/h).

**Table C.1 Summary of dose rates for GBC-32**

Normal conditions	Package surface <sup>a</sup> mSv/h (mrem/h)			2 Meter from vehicle <sup>a</sup> mSv/h (mrem/h)		
	Top	Side	Bottom	Top	Side	Bottom
Gamma	0.002 (0.2)	0.14 (14)	0.002 (0.2)	0.001 (0.1)	0.029 (2.9)	0.001 (0.1)
Neutron	0.440 (44)	0.21 (21)	0.440 (44)	0.081 (8.1)	0.049 (4.9)	0.081 (8.1)
Total	0.442 (44)	0.35 (35)	0.442 (44)	0.082 (8.2)	0.078 (7.8)	0.082 (8.2)
Limit	2 (200)	2 (200)	2 (200)	0.1 (10)	0.1 (10)	0.1 (10)

Hypothetical accident conditions	1 Meter from package surface <sup>a</sup> mSv/h (mrem/h)		
	Top	Side	Bottom
Gamma	0.002 (0.2)	0.14 (14)	0.002 (0.2)
Neutron	0.435 (43.5)	2.79 (279)	0.435 (43.5)
Total	0.437 (43.7)	2.93 (293)	0.437 (43.7)
Limit	10 (1000)	10 (1000)	10 (1000)

<sup>a</sup> Conservative dose rates calculated for top also used for bottom.

## C.2 SOURCE SPECIFICATION

The calculation of sources for spent fuel assemblies is performed for two regions, sources from the active fuel region and from the upper/lower hardware regions. These sources can be further broken into neutron and gamma-ray components. The active fuel region contains both components, while the hardware region contains only gamma sources due to the activation of <sup>59</sup>Co, an impurity in the steel and inconel structural materials.

Sources due to the active fuel region were generated via the ORIGEN-ARP code,<sup>13</sup> which is functionally equivalent to the SAS2H code. The assembly details for the assumed Westinghouse 17 × 17 fuel assembly are given in Table C.2. The quantities of material present in the top, plenum, and bottom hardware regions are given in Table C.3. From these masses, the curies of cobalt per kg of material values from Ref. 44 were used to determine the curie loadings of the top endfitting plus plenum (24.1 Ci <sup>60</sup>Co) and bottom endfittings (58.9 Ci <sup>60</sup>Co). The curies of cobalt per kg values from Ref. 44 are 10 Ci/kg stainless steel in the bottom nozzle, 2.5 Ci/kg stainless steel in the top nozzle, and 4.6 Ci/kg of steel or Inconel in the plenum region. These curies per kg of material values were determined from an average of measurements taken for six assemblies, with the lowest values omitted from the average. For

conservatism, the sources corresponding to the bottom endfitting activities were placed into the top endfitting location.

**Table C.2 Description of Westinghouse fuel assembly**

Assembly type/class	W 17 × 17
Active fuel length (cm)	365.76
No. of fuel rods	264
Rod pitch (cm)	1.260
Cladding material	Zircaloy-2
Rod diameter (cm)	0.950
Cladding thickness (cm)	0.057
Pellet diameter (cm)	0.819
Pellet material	UO <sub>2</sub>
Pellet density (g/cm <sup>3</sup> )	10.357 (94.5% theoretical)
Enrichment (wt % <sup>235</sup> U)	4.0
Burnup (MWd/MTU)	45,000
Cooling time (years)	10
Specific power (MW/MTU)	40
Weight of UO <sub>2</sub> (kg)	525.8
Weight of U (kg)	463.4

**Table C.3 Fuel assembly hardware parts and materials**

Part name	Weight (kg)/ assembly	Zone	Material name
Bottom nozzle	5.897	Bottom	Stainless steel 304
Holddown spring	0.960	Top	Inconel 718
Spacer – plenum	0.885	Gas plenum	Inconel 718
Top nozzle	6.890	Top	Stainless steel 304
Grid sleeve	0.091	Gas plenum	Stainless steel 304

### C.2.1 Gamma Source

The gamma sources for active fuel and from the assembly hardware are given in Table C.4. The active fuel sources are given in units of per MTU and per assembly (assm) for a cooling time of 10 years. The endfitting sources were generated assuming 58.9 Ci of  $^{60}\text{Co}$  were present in the top endfitting region. The endfitting and active fuel region sources include the effects of bremsstrahlung via interactions in an assumed  $\text{UO}_2$  fuel matrix.

**Table C.4 Westinghouse fuel assembly gamma spectrum**

Group no.	Energy (MeV)	Active fuel (photons/MTU-sec)	Active fuel (photons/assm-sec)	Top endfitting (photons/assm-sec)
1	8.00 – 10.0	3.40E+05	1.58E+05	0
2	6.50 – 8.00	1.60E+06	7.41E+05	0
3	5.00 – 6.50	8.16E+06	3.78E+06	0
4	4.00 – 5.00	2.03E+07	9.41E+06	0
5	3.00 – 4.00	8.30E+08	3.85E+08	0
6	2.50 – 3.00	6.63E+09	3.07E+09	3.57E+04
7	2.00 – 2.50	1.07E+11	4.96E+10	2.30E+07
8	1.66 – 2.00	2.70E+11	1.25E+11	0
9	1.33 – 1.66	1.36E+13	6.30E+12	9.71E+11
10	1.00 – 1.33	1.00E+14	4.63E+13	3.44E+12
11	0.80 – 1.00	1.80E+14	8.34E+13	1.53E+08
12	0.60 – 0.80	3.79E+15	1.76E+15	4.06E+06
13	0.40 – 0.60	3.41E+14	1.58E+14	1.17E+07
14	0.30 – 0.40	8.00E+13	3.71E+13	1.85E+08
15	0.20 – 0.30	1.23E+14	5.70E+13	1.41E+08
16	0.10 – 0.20	4.17E+14	1.93E+14	2.84E+09
17	0.05 – 0.10	5.72E+14	2.65E+14	1.17E+10
18	0.01 – 0.05	2.05E+15	9.50E+14	5.91E+10
Totals		7.76E+15	3.55E+15	4.48E+12

### C.2.2 Neutron Source

The neutron source spectra generated via the ORIGEN-ARP code is shown in Table C.5. The spectrum is shown for the first 7 of 27 groups in the SCALE 27 neutron group structure. All other groups are zero. This source corresponds to a cooling time of 10 years.

**Table C.5 Westinghouse fuel assembly neutron spectrum**

Group no.	Energy (MeV)	Neutrons/ MTU-sec	Neutrons/ assm-sec
1	6.43 – 20.0	1.170E+7	5.422E+6
2	3.00 – 6.43	1.238E+8	5.737E+7
3	1.85 – 3.00	1.368E+8	6.339E+7
4	1.40 – 1.85	7.294E+7	3.380E+7
5	0.90 – 1.40	9.109E+7	4.221E+7
6	0.40 – 0.90	9.112E+7	4.223E+7
7	0.10 – 0.40	4.178E+7	1.936E+7
8	0.02 – 0.10	6.158E+6	2.854E+6
Totals		5.754E+8	2.666E+8

## C.3 MODEL SPECIFICATION

The model described in this section corresponds to the normal conditions of transport. For the accident case, the resin neutron shield was removed from the analysis.

### C.3.1 Description of the Shielding Configuration

The GBC-32 cask was analyzed using the SCALE SAS4 module. The actual 3-D model is shown in Figures C.1 (x-y view) and C.2 (x-z view). The fuel assemblies were homogenized into the basket areas, with an explicit basket modeled as shown in Figure C.3. The gaps between assembly cells actually contain boral panels, but they were conservatively omitted from these models. The entire model is symmetric about the cavity midplane (a requirement of SAS4) and only the top cask geometry is modeled. This model is conservative since the top geometry has more space for radial streaming than the bottom geometry and the larger bottom endfitting source is placed into the top geometry model.

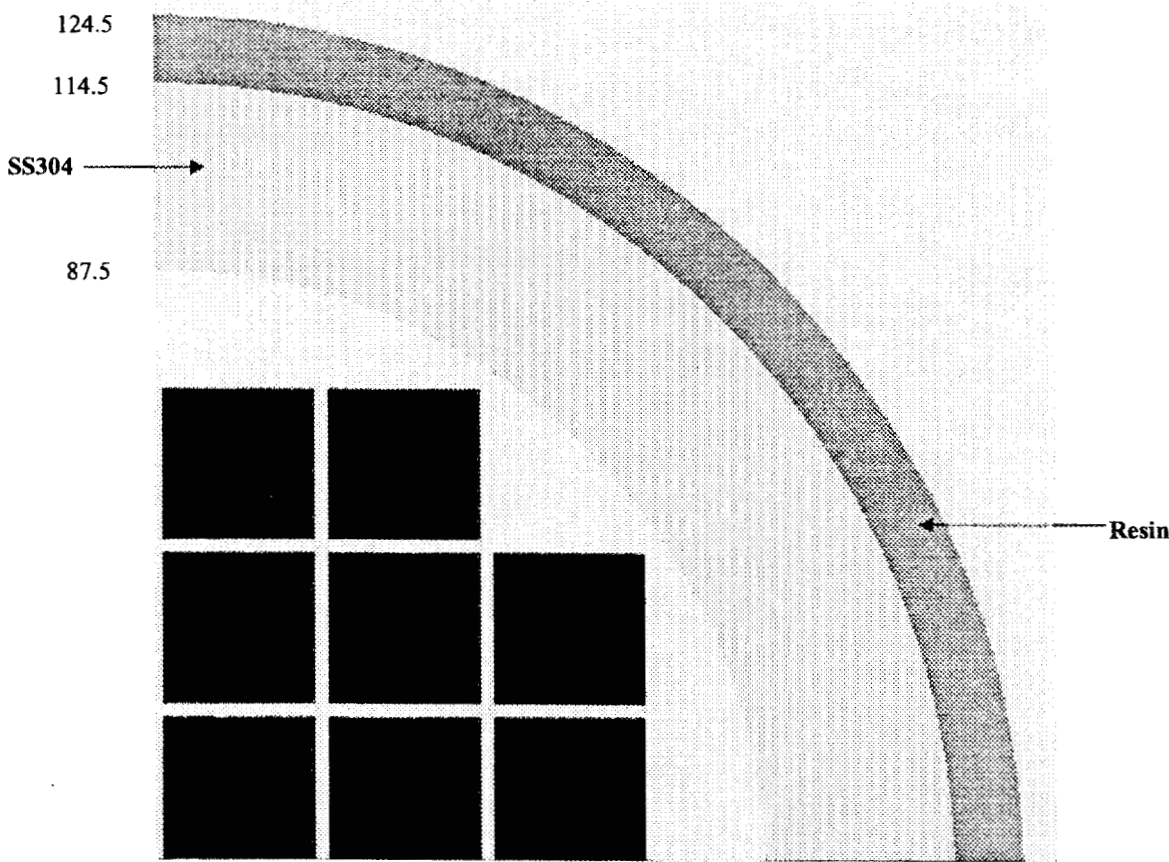


Figure C.1 Shielding model – radial (radii in cm)

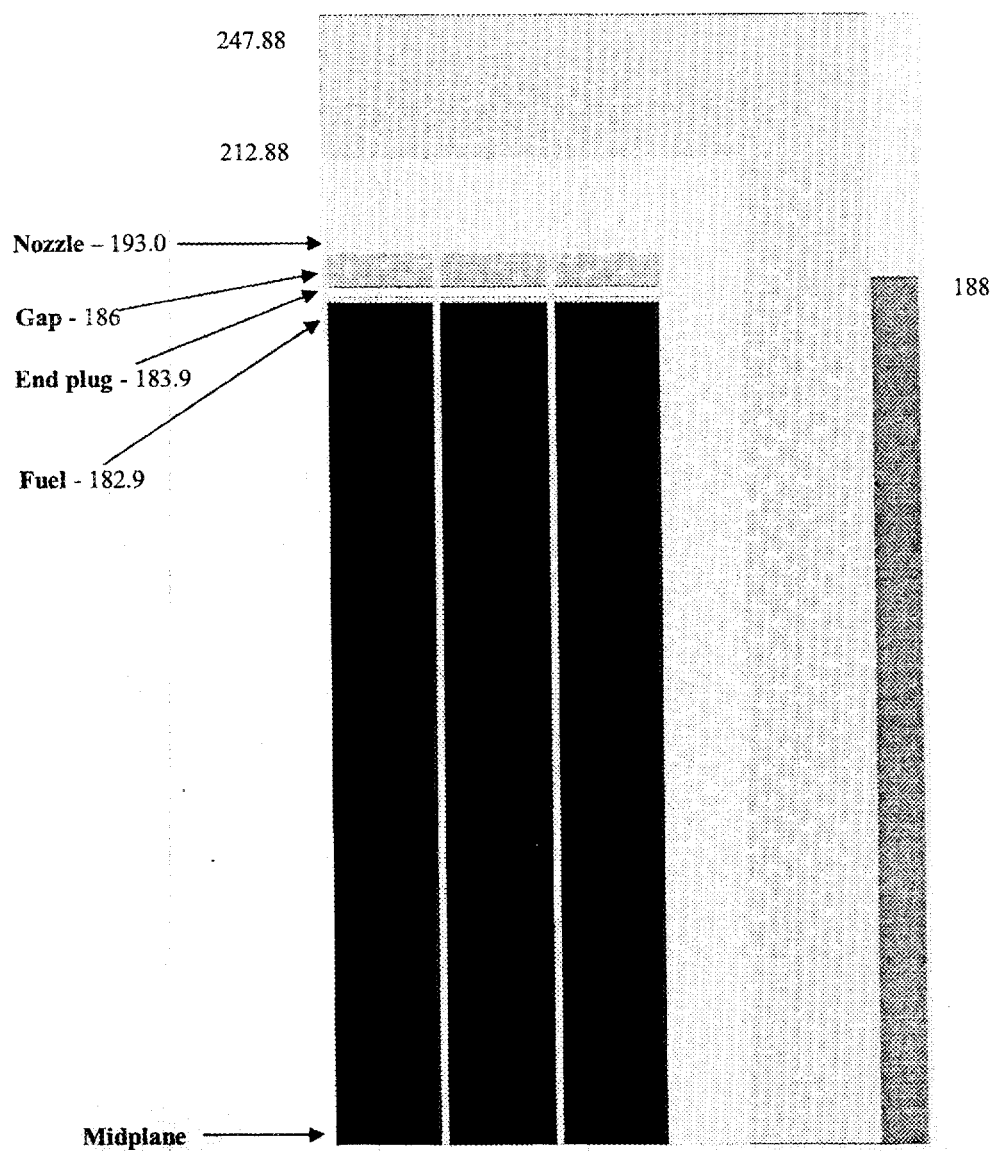


Figure C.2 Shielding model, axial (heights in cm from midplane)

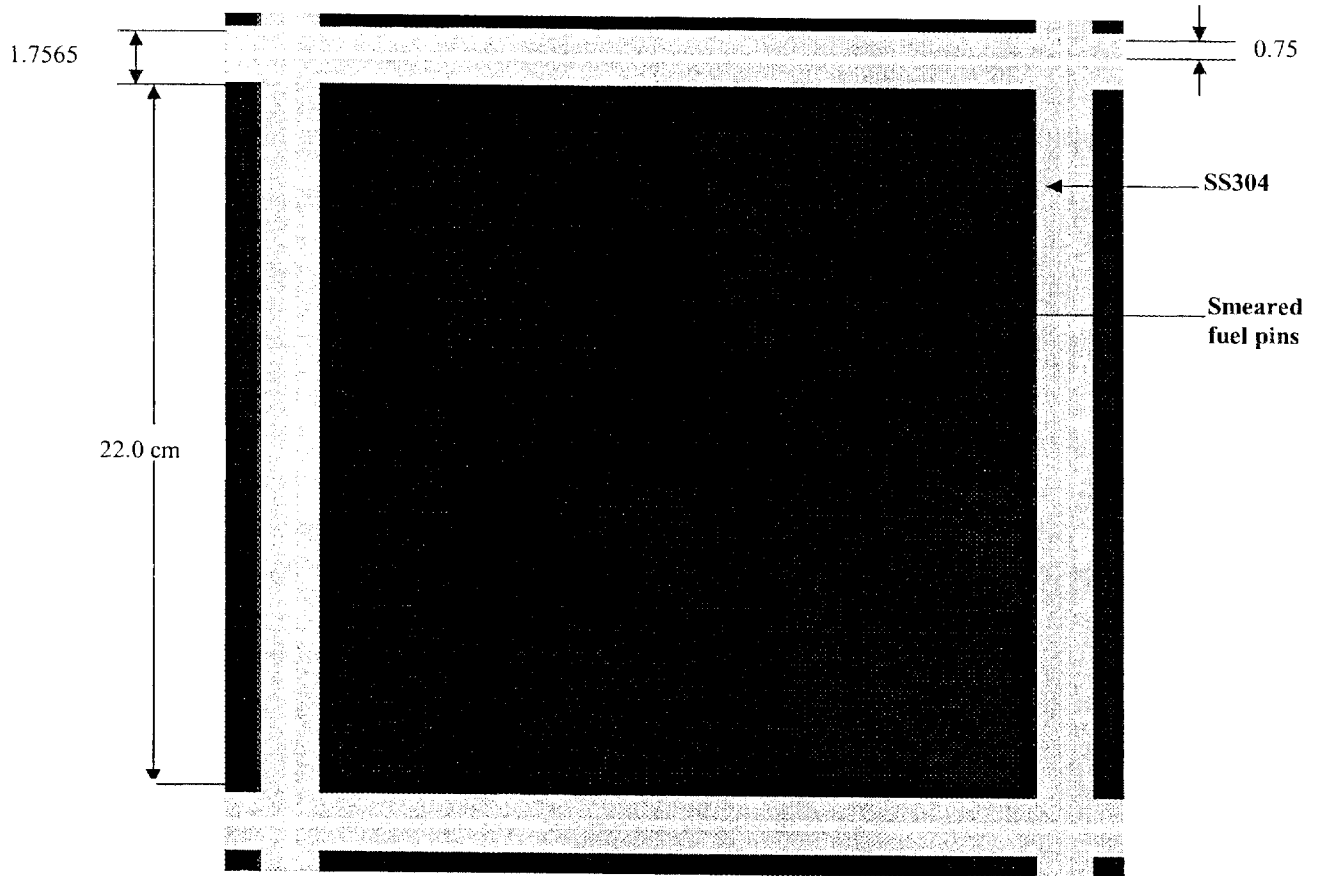


Figure C.3 GBC-32 detailed basket model (in cm)

The following dimensions are assumed for the GBC-32 cask body:

	Radius (cm)	Height (cm)
Cavity:	87.5	425.76
Stainless steel shell	114.5	495.76
Resin neutron shield:	124.5	376.00

### C.3.2 Smearred Basket and Cavity Volume Fractions

The fuel pins were not modeled explicitly in the basket region. The fuel pins were smeared over the basket, while the basket itself was modeled explicitly. The fuel and cladding volume fractions used to smear the fuel pins over the basket area are described below.

$$\text{Fuel Area} = 0.25\pi (0.819^2) \times 264 = 139.08 \text{ cm}^2$$

$$\text{Cladding Area} = 0.25\pi (0.95^2 - 0.836^2) \times 289 = 46.21 \text{ cm}^2$$

$$\text{Basket Cell Area} = 22^2 = 484 \text{ cm}^2$$

$$\text{Fuel Volume Fraction} = 139.08 \times 0.945 / 484 = 0.272$$

$$\rho_{\text{UO}_2} = 0.272 \times 10.96 = 2.981 \text{ g/cm}^3$$

$$\text{Cladding Volume Fraction} = 46.21 / 484 = 0.0955$$

$$\rho_{\text{clad}} = 0.0955 \times 6.56 = 0.626 \text{ g/cm}^3$$

For the 1-D adjoint calculation, the fuel and clad are further smeared over the entire cavity. The basket-to-cavity volume fraction is obtained from:

$$\text{Basket-to-cavity Volume Fraction} = 22^2 \times 32 / (\pi \times 87.5^2) = 0.6439$$

$$\rho_{\text{UO}_2\text{-Cavity}} = 2.981 \times 0.6439 = 1.9195 \text{ g/cm}^3 \quad (10.96 \times 0.1751)$$

$$\rho_{\text{clad-Cavity}} = 0.626 \times 0.6439 = 0.4031 \text{ g/cm}^3 \quad (6.56 \times 0.0615)$$

The hardware regions of the fuel assembly are also smeared into the basket area. The masses given in Table C.3 are used along with the effective volumes to arrive at volume fractions for each of three regions; the end plugs, guide tubes in the gap, and the bottom nozzle.

$$\text{End Plug Volume Fraction} = 0.25\pi \times 0.95^2 \times 289 / (22)^2 = 0.42$$

$$\text{Guide Tubes Volume Fraction} = 0.25\pi \times (0.95^2 - 0.835^2) \times 25 / (22)^2 = 0.008$$

$$\text{Bottom Nozzle Volume Fraction} = 5897 / [(22)^2 \times 7 \times 7.92] = 0.22$$

The shielding model densities are summarized in Table C.6.

**Table C.6 Source and shield material densities**

Mixture no.	Material	Density	
		(g/cm <sup>3</sup> )	(atoms/b-cm)
1 – UO <sub>2</sub>		2.982	
	U-235 (0.5)		2.693E-4
	U-238 (11.4)		6.382E-3
	Oxygen (88.1)		1.330E-2
1 – Zirc2		0.626	
	Zirconium (98.25)		4.064E-3
	Tin (1.45)		4.609E-5
	Iron (0.135)		9.120E-6
	Chromium (0.1)		7.256E-6
	Nickel (0.055)		3.536E-6
	Hafnium (0.01)		2.114E-7
2,4 – SS304		7.92	
	Iron (69.5)		5.936E-2
	Nickel (9.5)		7.720E-3
	Chromium (19)		1.743E-2
	Manganese (2)		1.740E-3
5 – Al	Aluminum (100)	2.699	6.020E-2
6 – Resin		1.580	
	Hydrogen (5.05)		4.768E-2
	Carbon (35.13)		2.786E-2
	Oxygen (41.73)		2.483E-2
	B-10 (0.19)		1.826E-4
	B-11 (0.86)		7.414E-4
	Aluminum (14.93)		5.265E-3
	Copper (2.11)		3.159E-4

Table C.6 (continued)

Mixture no.	Material	Density	
		(g/cm <sup>3</sup> )	(atoms/b-cm)
7 – Zircalloy	Zircalloy	2.6174	1.728E-2
8 – Zircalloy	Zircalloy	0.059	3.898E-4
9 – SS304		1.677	
	Iron (69.5)		1.239E-2
	Nickel (9.5)		1.639E-3
	Chromium (19)		3.699E-3
	Manganese (2)		3.685E-4
10 – SS304		2.614	
	Iron (69.5)		1.932E-2
	Nickel (9.5)		2.554E-3
	Chromium (19)		5.766E-3
	Manganese (2)		5.744E-4
10 – Inconel		0.282	
	Nickel (73)		2.114E-3
	Chromium (15)		4.903E-4
	Iron (7)		2.130E-4
	Titanium (2.5)		8.874E-5
	Silicon (2.5)		7.131E-4
11 – SS304		0.455	
	Iron (69.5)		3.366E-3
	Nickel (9.5)		4.451E-4
	Chromium (19)		1.005E-3
	Manganese (2)		1.001E-4
11 – Zircalloy	Zircalloy (100)	0.630	4.162E-3

Table C.6 (continued)

Mixture no.	Material	Density	
		(g/cm <sup>3</sup> )	(atoms/b-cm)
12 – UO <sub>2</sub>		1.920	
	U-235 (0.5)		3.082E-5
	U-238 (11.4)		4.249E-3
	Oxygen (88.1)		8.560E-3
12 – Zirc2		0.403	
	Zirconium (98.25)		2.617E-3
	Tin (1.45)		2.968E-5
	Iron (0.135)		5.873E-6
	Chromium (0.1)		4.673E-6
	Nickel (0.055)		2.277E-6
	Hafnium (0.01)		1.361E-7

## C.4 SHIELDING EVALUATION

The shielding evaluation is performed by calculating the dose rates at the top and radial directions so that the GBC-32 package meets the 10 CFR Part 71 dose rates during normal conditions of transport, i.e., 2 mSv/h (200 mrem/h) at the package surface and 0.1 mSv (10 mrem/hr) at 2 m from the accessible surface of the conveyance. Top dose rates were conservatively modeled to bound those of the bottom. Dose rates under hypothetical accident conditions were calculated to meet the regulatory limits of 10 mSv/h (1000 mrem/h) at 1 m from the package surface. The accident models were the same as those under normal conditions but with the impact limiter and neutron shield removed.

The evaluation performed for the GBC-32 package utilized the 3-D Monte Carlo shielding sequence, SAS4. This code sequence operates under the SCALE code system with the MORSE-SGC/S code actually performing the Monte Carlo calculations. Under this system, the neutron source multiplication is accounted for automatically.

The dose rate profiles along the cask side surface and 2 m locations are shown in Figures C.4 and C.5. The location for the surface doses is the actual outside surface of the resin neutron shield. The 2-m doses correspond to 2 m from the conveyance or a distance of 358 cm for the cask centerline. The doses peak at the cask midplane with surface and 2 m total dose values corresponding to 0.35 and 0.078 mSv/h (35 and 7.8 mrem/h) as shown in Table C.7. Both locations have neutron doses that are nearly a factor of two higher than the gamma doses. The hardware region is of little consequence to the overall doses.

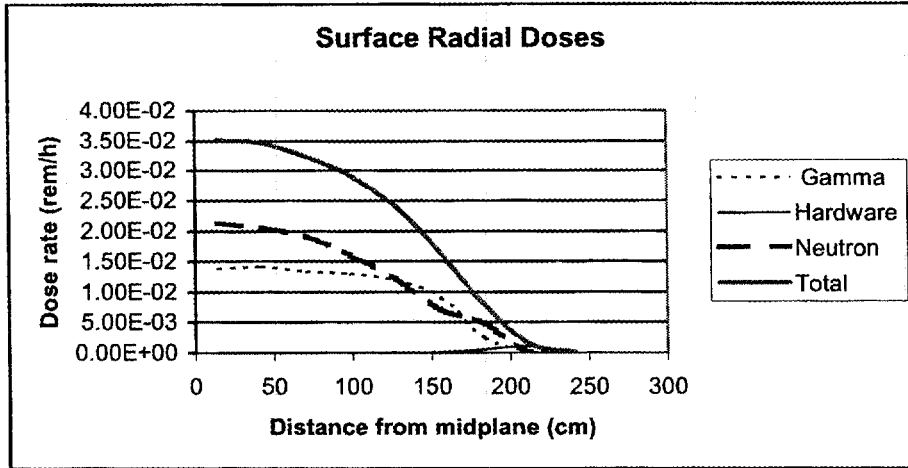


Figure C.4 Surface dose rate profiles along the side of GBC-32 cask

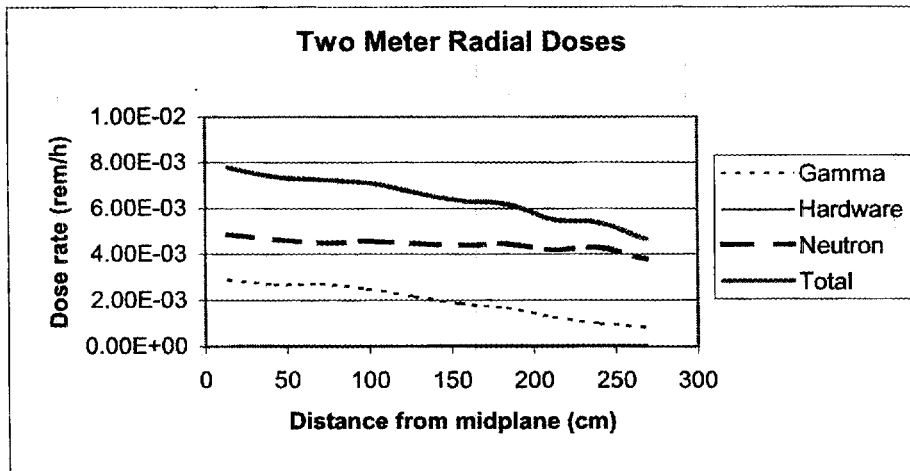


Figure C.5 Dose rate profile at 2 m from the conveyance surface for GBC-32 cask

Table C.7 SAS4 radial analysis results (in rem/h)

Radial dose rates on canister side surface					
Segment no.	Height <sup>a</sup> (cm)	Gamma (rem/h)	Hardware (rem/h)	Neutron (rem/h)	Total <sup>b</sup> (rem/h)
1	14.14	1.38E-02	0.00E+00	2.14E-02	3.52E-02
2	42.43	1.41E-02	0.00E+00	2.05E-02	3.47E-02
3	70.72	1.33E-02	1.18E-09	1.90E-02	3.24E-02
4	99.01	1.31E-02	5.31E-08	1.60E-02	2.91E-02
5	127.31	1.20E-02	2.57E-06	1.21E-02	2.41E-02
6	155.59	9.18E-03	7.54E-05	7.10E-03	1.64E-02
7	183.88	2.42E-03	6.03E-04	4.82E-03	7.85E-03
8	212.17	4.03E-04	1.06E-03	0.00E+00	1.47E-03
9	240.46	5.11E-05	1.43E-04	0.00E+00	1.94E-04
Radial dose rates at 2 meters from canister surface					
Segment no.	Height <sup>a</sup> (cm)	Gamma (rem/h)	Hardware (rem/h)	Neutron (rem/h)	Total <sup>b</sup> (rem/h)
1	14.14	2.91E-03	1.66E-05	4.86E-03	7.79E-03
2	42.43	2.67E-03	1.83E-05	4.67E-03	7.36E-03
3	70.72	2.71E-03	2.28E-05	4.51E-03	7.24E-03
4	99.01	2.51E-03	2.83E-05	4.58E-03	7.12E-03
5	127.31	2.17E-03	3.47E-05	4.48E-03	6.68E-03
6	155.59	1.87E-03	4.46E-05	4.41E-03	6.32E-03
7	183.88	1.65E-03	5.41E-05	4.46E-03	6.17E-03
8	212.17	1.27E-03	5.87E-05	4.20E-03	5.53E-03
9	240.46	1.00E-03	5.91E-05	4.29E-03	5.36E-03
10	268.76	8.26E-04	6.26E-05	3.77E-03	4.66E-03

<sup>a</sup> Height is from axial midplane.

<sup>b</sup> Peak value occurs at segment 1.

Along the top of the GBC-32 cask, the dose rates peak at the center of the cask, as can be seen in Figures C.6 and C.7. For the 2 m doses seen in Figure C.7, the peak appears to have moved slightly away from the centerline; however, this is due to the statistics, since the differences are of the same order as the Monte Carlo statistics (6–8% for the center doses, while the remaining values have statistics of 2–3%). The tabular results for these cases are given in Table C.8 indicate the dose rates near the center differ from the peak by only 5–8%. Along the cask top, the neutron doses clearly dominate those due to gamma rays since there is no neutron shield along the top of the cask. For these calculations, the materials in the impact limiter are ignored; however, the surface doses correspond to the position of the impact limiter surface. The 2 m dose rates correspond to a location 2 m from the impact limiter outer surface.

The dose rate profiles for the cask side and top under accident conditions at 1 m from the package surface are shown in Figures C.8 and C.9. The peak dose rate of 2.92 mSv/h (292 mrem/h) (see Table C.9) occurs along the case side at the midplane. These dose rate values are well below the regulatory limits and indicate the radiation levels under accident conditions are acceptable.

## C.5 SOURCE AND SHIELDING INPUTS

The sample inputs to the source term generation and gamma shielding for normal conditions are shown in Figures C.10 and C.11, respectively. The source calculations were performed using the SCALE code ORIGEN-ARP. The shielding calculations were performed with the SAS4 shielding sequence in SCALE.

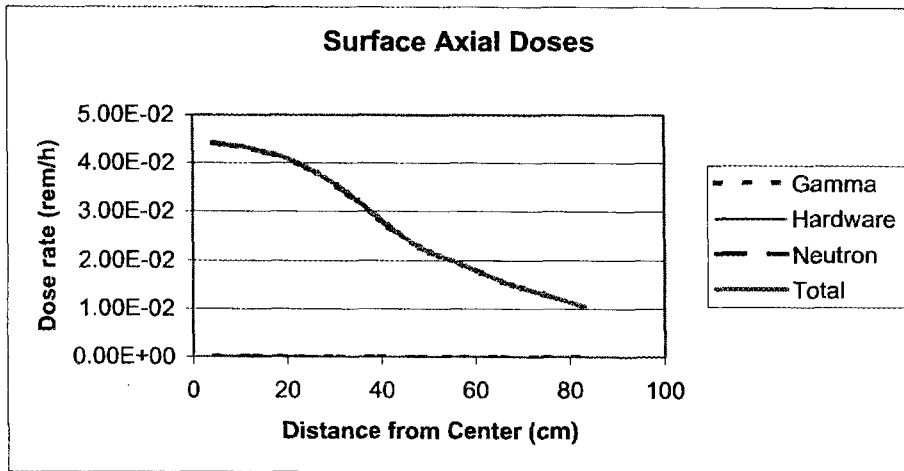


Figure C.6 Dose rate profile along top surface of GBC-32 cask (neutron dose is approximately equal to the total dose)

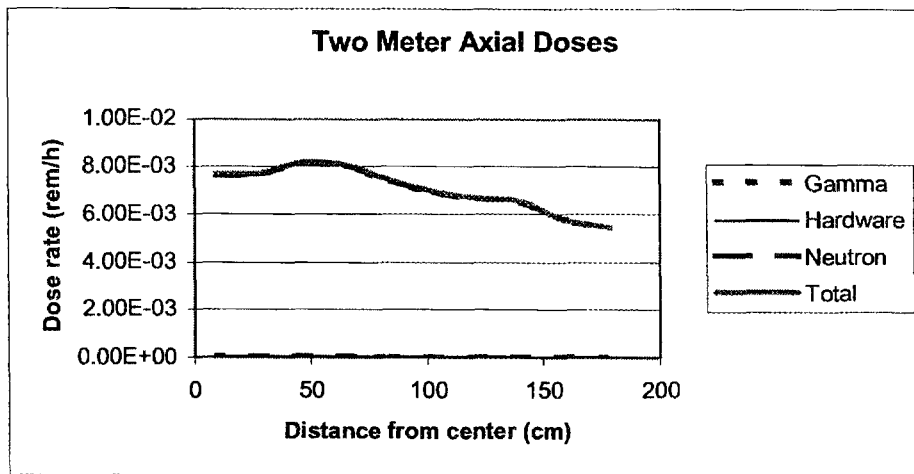


Figure C.7 Dose rate profile 2 m from top of GBC-32 cask (neutron dose is approximately equal to the total dose)

Table C.8 SAS4 axial analysis results (in rem/h)

Axial dose rates on canister top surface					
Segment no.	Segment radius (cm)	Gamma (rem/h)	Hardware (rem/h)	Neutron (rem/h)	Total <sup>a</sup> (rem/h)
1	4.38	7.56E-05	1.06E-04	4.42E-02	4.44E-02
2	13.12	6.58E-05	9.04E-05	4.28E-02	4.30E-02
3	21.88	5.25E-05	8.24E-05	4.01E-02	4.02E-02
4	30.62	3.72E-05	5.83E-05	3.54E-02	3.55E-02
5	39.38	3.31E-05	4.89E-05	2.88E-02	2.88E-02
6	48.12	2.09E-05	2.97E-05	2.28E-02	2.29E-02
7	56.88	1.75E-05	1.96E-05	1.94E-02	1.94E-02
8	65.62	9.22E-06	1.27E-05	1.58E-02	1.59E-02
9	74.38	6.10E-06	7.50E-06	1.32E-02	1.32E-02
	83.12	5.20E-06	5.29E-06	1.05E-02	1.05E-02
Axial dose rates at 2 meters from canister top surface					
Segment no.	Segment radius (cm)	Gamma (rem/h)	Hardware (rem/h)	Neutron (rem/h)	Total <sup>a</sup> (rem/h)
1	9.38	2.00E-05	2.06E-05	7.66E-03	7.70E-03
2	28.12	1.94E-05	2.19E-05	7.70E-03	7.74E-03
3	46.88	1.84E-05	2.27E-05	8.14E-03	8.18E-03
4	65.62	1.57E-05	2.32E-05	8.03E-03	8.07E-03
5	84.38	1.30E-05	1.88E-05	7.40E-03	7.43E-03
6	103.12	1.06E-05	1.63E-05	6.95E-03	6.97E-03
7	121.88	1.06E-05	1.52E-05	6.68E-03	6.71E-03
8	140.62	9.27E-06	1.14E-05	6.52E-03	6.54E-03
9	159.38	5.95E-06	1.04E-05	5.77E-03	5.79E-03
10	178.12	6.41E-06	9.73E-06	5.46E-03	5.47E-03

<sup>a</sup> Peak value occurs at segment 3.

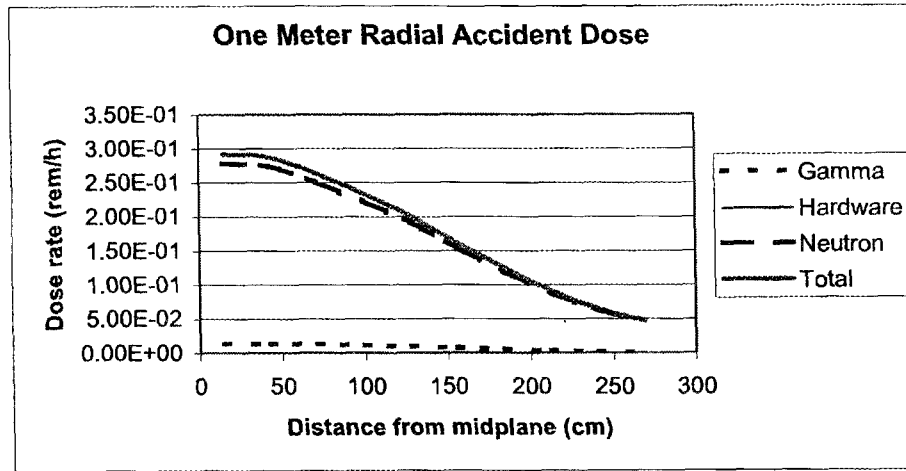


Figure C.8 Dose rate profiles at 1 m from side of GBC-32 cask under accident conditions (neutron dose is approximately equal to the total dose)

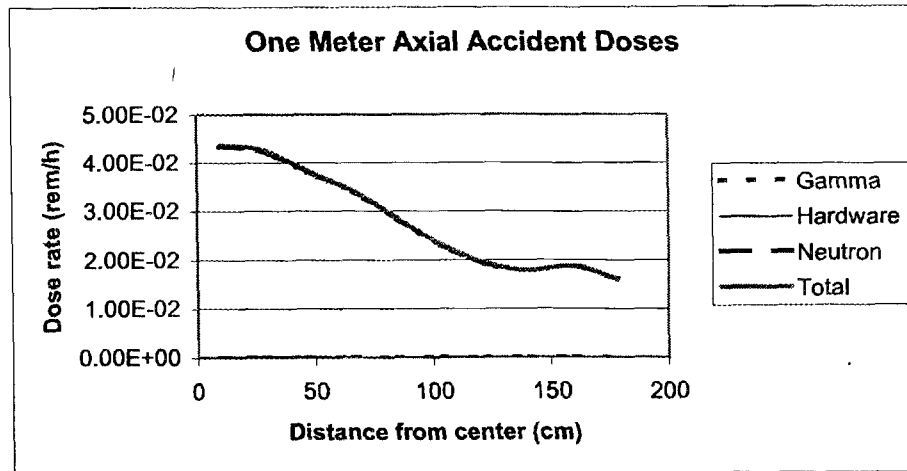


Figure C.9 Dose rate profiles for 1 m from top of GBC-32 cask under accident conditions (neutron dose is approximately equal to the total dose)

**Table C.9 SAS4 radial accident analysis results (in rem/h)**

<b>Radial dose rates on canister side surface</b>					
Segment no.	Height <sup>a</sup> (cm)	Gamma (rem/h)	Hardware (rem/h)	Neutron (rem/h)	Total <sup>b</sup> (rem/h)
1	14.14	1.39E-02	1.47E-05	2.79E-01	2.92E-01
2	42.43	1.30E-02	1.73E-05	2.75E-01	2.88E-01
3	70.72	1.34E-02	2.70E-05	2.51E-01	2.64E-01
4	99.01	1.18E-02	4.65E-05	2.23E-01	2.35E-01
5	127.31	9.77E-03	8.71E-05	1.92E-01	2.02E-01
6	155.59	7.52E-03	1.39E-04	1.55E-01	1.62E-01
7	183.88	5.37E-03	1.89E-04	1.21E-01	1.26E-01
8	212.17	3.09E-03	2.72E-04	8.87E-02	9.20E-02
9	240.46	1.95E-03	1.79E-04	6.30E-02	6.52E-02
	268.76	1.23E-03	1.08E-04	4.73E-02	4.87E-02

<sup>a</sup> Height is from axial midplane.

<sup>b</sup> Peak occurs at segment 1.

```
'This SCALE input file was generated by
'OrigenArp Version 2.00 1-18-2002
=arp
17x17
4
3
375
375
375
40
40
40
1
1
1
1
ft33f001
end
#origens
0$$$ a4 33 a11 71 e t
17x17 library, interpolated to 4.000000 wt% -- ft33f001
3$$$ 33 a3 1 27 a16 2 a33 18 e t
35$$$ 0 t
56$$$ 10 10 a10 0 a13 4 a15 3 a18 1 e
57** 0 a3 1e-05 0.3333333 e t
Cycle 1 -17x17 45 Gwd/MTU
1 MTU
58** 40 40 40 40 40 40 40 40 40 40
60** 37.5 75 112.5 150 187.5 225 262.5 300 337.5 375
66$$$ a1 2 a5 2 a9 2 e
73$$$ 922340 922350 922360 922380
74** 356 40000 184 959460
75$$$ 2 2 2 2
t
54$$$ a8 1 a11 0 e
56$$$ a2 9 a6 3 a10 10 a15 3 a17 4 e
57** 0 a3 1e-05 e t
Decay - 17x17 45 Gwd/MTU
1 MTU
60** 0.01 0.03 0.1 0.3 1 3 10 30 93.75
61** f0.05
65$$$
'Gram-Atoms Grams Curies Watts-All Watts-Gamma
3z 1 0 0 3z 3z 3z 6z
3z 1 0 0 3z 3z 3z 6z
3z 1 0 0 3z 3z 3z 6z
81$$$ a7 200 e
t
17x17 library, interpolated to 4.000000 wt% -- ft33f001
3$$$ 33 a3 2 27 a33 18 e t
35$$$ 0 t
56$$$ 10 10 a10 9 a15 3 a18 1 e
57** 0 a3 1e-05 0.3333333 e t
```

**Figure C.10 ORIGEN-ARP source generation sample input**

```

Cycle 2 -17x17 45 Gwd/MTU
1 MTU
58** 40 40 40 40 40 40 40 40 40 40
60** 37.5 75 112.5 150 187.5 225 262.5 300 337.5 375
66$$ a1 2 a5 2 a9 2 e t
54$$ a8 1 a11 0 e
56$$ a2 9 a6 3 a10 10 a15 3 a17 4 e
57** 0 a3 1e-05 e t
Decay - 17x17 45 Gwd/MTU
1 MTU
60** 0.01 0.03 0.1 0.3 1 3 10 30 93.75
61** f0.05
65$$
'Gram-Atoms Grams Curies Watts-All Watts-Gamma
3z 1 0 0 3z 3z 3z 6z
3z 1 0 0 3z 3z 3z 6z
3z 1 0 0 3z 3z 3z 6z
81$$ a7 200 e
t
17x17 library, interpolated to 4.000000 wt% -- ft33f001
3$$ 33 a3 3 27 a33 18 e t
35$$ 0 t
56$$ 10 10 a10 9 a15 3 a18 1 e
57** 0 a3 1e-05 0.3333333 e t
Cycle 3 -17x17 45 Gwd/MTU
1 MTU
58** 40 40 40 40 40 40 40 40 40 40
60** 37.5 75 112.5 150 187.5 225 262.5 300 337.5 375
66$$ a1 2 a5 2 a9 2 e t
54$$ a8 1 a11 0 e
56$$ a2 7 a6 1 a10 10 a14 5 a15 3 a17 2 e
57** 0 a3 1e-05 e t
Cycle 3 Down - 17x17 45 Gwd/MTU
1 MTU
60** 0.01 0.03 0.1 0.3 1 3 10
61** f0.05
65$$
'Gram-Atoms Grams Curies Watts-All Watts-Gamma
3z 1 0 0 3z 3z 3z 6z
3z 1 0 0 3z 3z 3z 6z
3z 1 0 0 3z 3z 3z 6z
81$$ 2 0 26 1 a7 200 e
82$$ 2 2 2 2 2 2 2 e
83**
1.E+7 8.E+6 6.5E+6 5.E+6 4.E+6 3.E+6
2.5E+6 2.E+6 1.66E+6 1.33E+6 1.E+6 8.E+5
6.E+5 4.E+5 3.E+5 2.E+5 1.E+5 5.E+4
1.E+4 e
84**
2.E+7 6.434E+6 3.E+6 1.85E+6 1.4E+6
9.E+5 4.E+5 1.E+5 1.7E+4 3.E+3 5.5E+2
1.E+2 3.E+1 1.E+1 3.04999E+0 1.77E+0
1.29999E+0 1.12999E+0 1.E+0 8.E-1 4.E-1
3.25E-1 2.25E-1 9.999985E-2 5.E-2 3.E-2

```

Figure C.10 (continued)

```
9.999998E-3 1.E-5 e
t
Cycle 3 Down - 17x17 45 Gwd/MTU Time Step 1
Cycle 3 Down - 17x17 45 Gwd/MTU Time Step 2
Cycle 3 Down - 17x17 45 Gwd/MTU Time Step 3
Cycle 3 Down - 17x17 45 Gwd/MTU Time Step 4
Cycle 3 Down - 17x17 45 Gwd/MTU Time Step 5
Cycle 3 Down - 17x17 45 Gwd/MTU Time Step 6
Cycle 3 Down - 17x17 45 Gwd/MTU Time Step 7
56$$$ 0 0 a10 1 e t
56$$$ 0 0 a10 2 e t
56$$$ 0 0 a10 3 e t
56$$$ 0 0 a10 4 e t
56$$$ 0 0 a10 5 e t
56$$$ 0 0 a10 6 e t
56$$$ 0 0 a10 7 e t
56$$$ f0 t
end
```

**Figure C.10 (continued)**

```

=sas4      parm=size=1000000
Generic 32-Assembly Burnup Credit Cask (GBC-32)
27n-18couple  infhommedium
'fuel
uo2      1  0.272 293 92235 4.0 92238 96.0 end
'
'      - Zr cladding
zirc2    1  0.0955 293  end
'
'      - Stainless Steel [Ref. LA-12827-M, page C-10]
cr       2  0  0.01743      293.0  end
mn       2  0  0.00174      293.0  end
fe       2  0  0.05936      293.0  end
ni       2  0  0.00772      293.0  end
'
'      - Boral Center - B-10 loading of 0.0225 g/sqcm
b-10    3  0  6.5795E-03  293.0  end
b-11    3  0  2.7260E-02  293.0  end
c       3  0  8.4547E-03  293.0  end
al      3  0  4.1795E-02  293.0  end
'
'      - Stainless Steel [Ref. LA-12827-M, page C-10]
cr       4  0  0.01743      293.0  end
mn       4  0  0.00174      293.0  end
fe       4  0  0.05936      293.0  end
ni       4  0  0.00772      293.0  end
'
'      - Aluminum [Ref. Duderstadt & Hamilton]
al      5  0  0.0602      293.0  end
'
' mixture 6, radial neutron shield
arbm:resin 1.58 6  1 0 1  5000 1.05 1001 5.05 6012 35.13 8016 41.73
13027 14.93 29000 2.11 6  1.0 293 5010 18.3022 5011 81.6978 end
' mixture 7, end plugs
zircalloy 7  0.42  end
' mixture 8, 25 guide tubes
zircalloy 8  0.008  end
' mixture 9, bottom nozzle
ss304    9  0.22  end
' mixture 10, top nozzle
ss304   10  0.33  end
inconel  10  0.034  end
' mixture 11, plenum
ss304   11  0.06  end
zircalloy 11  0.10  end
uo2     12  0.1751 293  end
zirc2   12  0.0615 293  end
end comp
ity=2  izm=3 frd=87.5 idr=0  end
87.5 114.5 124.5  end
12 2 6  end

```

Figure C.11 Sample SAS4 input for primary gamma calculation under normal conditions

```

xend
ttl='xy plot'
scr=yes
xul=-115 yul=115 zul=0
xlr=115 ylr=-115 zlr=0
udn=1.0 vax=-1.0 ndn=480 end
pend
ran=1a8456ead951 tim=120. nst=1000 nmt=2000 nit=400 sfa=1.119+17 igo=4
ipf=1 end
soe 8*0.0
' 1.170+7 1.238+8 1.368+8 7.294+7 9.109+7 9.112+7 4.178+7 6.158+6
19*0.0
3.40+05 1.60+06 8.16+06 2.03+07 8.30+08 6.63+09 1.07+11 2.70+11
1.36+13 1.00+14 1.80+14 3.79+15 3.41+14 8.00+13 1.23+14 4.17+14
5.72+14 2.05+15
end
sxy 1 -87.5 87.5 -87.5 87.5 0.0 182.9 87.5 182.9 124.5 247.88 end
sdr 0 282.9 0 282.9 0 282.9 0 282.9 end
sds 10 10 10 10 10 10 10 10 end
gend
GBC-32 cask, bottom geometry, 32 pwr assemblies
0 0 1 0
rcc 1 0.0 0.0 -212.88 0.0 0.0 425.76 87.5
rcc 2 0.0 0.0 -247.88 0.0 0.0 495.76 114.5
rcc 3 0.0 0.0 -188.0 0.0 0.0 376.0 124.5
rcc 4 0.0 0.0 -347.88 0.0 0.0 695.76 224.50
rcc 5 0.0 0.0 -447.88 0.0 0.0 895.76 322.00
rcc 6 0.0 0.0 -547.88 0.0 0.0 1095.76 358.00
rcc 7 0.0 0.0 -2000. 0.0 0.0 4000. 2000.
rcc 8 0.0 0.0 -2200. 0.0 0.0 4400. 2200.
rpp 9 -71.2698 71.2698 -47.5132 47.5132 -193.0 193.0
rpp 10 -47.5132 47.5132 -71.2698 -47.5132 -193.0 193.0
rpp 11 -47.5132 47.5132 47.5132 71.2698 -193.0 193.0
rpp 12 -11 11 -11 11 -182.88 182.88
rpp 13 -11 11 -11 11 -183.88 183.88
rpp 14 -11 11 -11 11 -186.0 186.0
rpp 15 -11 11 -11 11 -193.0 193.0
rpp 16 -11.75 11.75 -11.75 11.75 -193 193
rpp 17 -11.8783 11.8783 -11.8783 11.8783 -193.0 193.0
end
' zone description input
inn 1 -9 -10 -11
wtr 2 -1
jac 3 -2
de2 4 -3 -2
de3 5 -4
de4 6 -5
inv 7 -6
exv 8 -7
ar1 9
ar2 10
ar3 11
fue 12
plu 13 -12

```

Figure C.11 (continued)

```
gtb 14 -13
nzl 15 -14
can 16 -15
vol 17 -16
uvl 8 -17
end
3r1 2 1 2 12r1
11*0 7*1
1000 2 6 4*1000 0 -1 -2 -3 1 7 8 9 4 1000 -1000
6 4 1 4 1 1 4 1 1 0 0
32*1
0 0
end
```

**Figure C.11 (continued)**